2

Molecular Beams in Chemistry*

J. E. Jordan
Massachusetts Institute of Technology, Cambridge, Massachusetts

E. A. Mason
Brown University, Providence, Rhode Island

and
I. Amdur
Massachusetts Institute of Technology, Cambridge, Massachusetts

* This research was supported in part by the U.S. Office of Naval Research and by the National Science Foundation (M.I.T.) and in part by the U.S. National Aeronautics and Space Administration (Brown).

NGL-40-002-059

Table of Contents

I. Introduction

Molecular beams have been for many years a powerful tool for research into physical problems but have only fairly recently been applied to problems in chemistry. This is a rather curious situation because many of the pioneers in the development of molecular beams were physical chemists by training. Although this chapter emphasizes areas of interest primarily to chemists, the broader areas will be discussed briefly to place applications to chemistry in proper context. The phrase, molecular beam, is usually used to denote a beam of either atoms or molecules. It will be used in that general sense here; where discussion is limited to atoms the phrase atomic beam will be used.

The basic molecular beam technique was developed by Dunoyer[1] in 1911 to verify one of the fundamental postulates of the kinetic theory of gases, namely that molecules execute nearly rectilinear motions between collisions. He built an apparatus similar in principle to that shown in Fig. 1. The source chamber S was filled with vapor from heated metallic sodium and the other two chambers were evacuated to the point where intermolecular collisions were infrequent. The temperature of the sodium was controlled to insure that the mean free path in the vapor was large with respect to the aperture between the two chambers S and A. Under these conditions, the paths of the molecules became quite long and the molecules could be collimated into rays or beams by installing a coaxial aperture C. Since chambers A and B were evacuated the only intermolecular collisions which occurred were the relatively infrequent cases when faster molecules overtook slower ones moving along the same path. Thus the beam in chamber B was essentially unidirectional and collision-free. Dunoyer found that

the deposit of sodium on the cooled end of chamber B had the dimensions and form predicted by geometric optics and further that objects placed in the path of the beam produced well-defined shadows. In addition, he performed the first molecular beam scattering experiment by noting that the beam profile became diffuse when inert gas was introduced into chamber B.

In general, the molecular beam technique is a means for producing isolated atoms or molecules within a narrow range of speed and solid angle. The basic strength of the method lies in the fact that the atoms or molecules are isolated from their surroundings; when any experiment is performed with the beam it can be analyzed in terms of an unperturbed single particle interaction. It is difficult to generalize further because the degree of collimation, the range of particle velocities and the technique of observing interaction of the beam all depend on the particular experiment being performed. There are, however, three general kinds of phenomena that are studied with molecular beams; they can be classified on the basis of how the molecular beam is made to interact. The classifications are single particle interactions, many particle interactions, and two particle interactions. Examples of the types of experiments performed within these three categories are briefly indicated below.

A. Single particle interactions.

This area of molecular beam research is a class of experiments in which the isolated atoms or molecules in the beam are introduced into an electromagnetic field. Observation is then made of the interaction of the individual atoms or molecules with the field. The detailed manner in which the observation is made is determined by the particular experiment being performed. Ramsey[2] describes experiments of this type in detail.

Particles with resultant electric or magnetic moments can be deflected in inhomogeneous electric or magnetic fields. This fact has been used as the basis for a large number of extraordinary experiments, many of which were of great importance in the historical development of physics. One of the first of these was the Stern-Gerlach experiment[3] in which a beam of paramagnetic atoms, collimated from the effusive flow from a hot oven, was deflected in an inhomogeneous magnetic field into three distinct traces which could be correlated with the interaction of the field and the electron spins of the atoms. This experiment is an elegant proof of space quantization and of the need to include electron spin in accounting for the number of magnetic moments. Many similar experiments have been performed to determine atomic magnetic moments for a number of atoms and paramagnetic molecules. A molecule which is not paramagnetic, namely, which has no resultant electronic magnetic moment, can nonetheless be deflected in the inhomogeneous magnetic field if it has a nuclear magnetic moment, a rotational magnetic moment due to rotational angular velocity of the molecule, or a diamagnetic moment induced by an external magnetic field. All three of these magnetic moments have been determined in beam deflection experiments. Another large and important area of research in physics which has evolved from beam deflection experiments is referred to as radiofrequency spectroscopy. In the basic experimental arrangement a beam passes through three successive regions, the first and last of which are inhomogeneous magnetic fields which produce, in molecules with the same nuclear magnetic moment, equal but opposite deflections. Radiofrequency energy is coupled into the middle region. If the frequency of the applied field is resonant with a state transition in the molecule, it will leave the field in a different state, usually with a

change in effective nuclear magnetic moment. When the molecule traverses the second inhomogeneous field the deflection it now receives does not exactly compensate for the deflection in the first field, so it misses the detector. The method then consists of observing resonances, that is sharp intensity changes, as a function of the frequency of the exciting radiation. Thus spectra can be traced out which result from the coupling of nuclear moments with electronic motion in the molecule. Measurements of the structure of these spectra, called hyperfine structure, provide a wealth of information about nuclear properties, much of which has led to specific models of the nucleus.

Although the study of spectral fine structure is usually considered to be in the domain of optical spectroscopy, molecular beam methods have been applied here as well. One of the classic discoveries of modern physics was that of the Lamb shift[4], where a technique similar to the molecular beam method described above was the key to the experiment. Here resonant changes in intensity in a beam of metastable helium atoms were observed in a radiofrequency cavity when radiation of characteristic frequency induced intermultiplet transitions resulting in decay to the ground state. The observed multiplet splittings were in sharp disagreement with previous theory, which has now been modified to reflect the experimental observations.

Deflection of beams in inhomogeneous electric fields can also be induced[5], if the atoms or molecules in the beam have a permanent dipole moment. Electric deflection experiments have not as yet been exploited to the degree that magnetic deflection has, but the method has been used to measure atomic polarizabilities. An apparatus analogous to that used for magnetic resonance experiments can be used to study the interactions

of electron spins with rotational states of polar molecules.

Inhomogeneous electric and magnetic fields can also be used to focus atoms with selected quantum states. Such state-selected beams will be discussed at greater length below, but it can be mentioned here that this technique was instrumental in the development of the first maser[6]. The required population inversion (excess of atoms in the higher energy state of a transition) was achieved by passing a beam of ammonia molecules through an inhomogeneous electric field. Those molecules in an upper inversion state were focussed while those in lower states were defocussed; the beam then entered a resonant cavity where the downward transition was induced. This stimulated emission added power to the stimulating radiation and so the apparatus served as an amplifier at the resonant frequency.

B. Many particle interactions.

This classification includes experiments in which beams of ions or neutral particles, usually at rather high energy, are directed at dense targets, either gas phase or solid.

For many years investigations have been made of the range (that is, the depth of penetration) of fast particles in dense targets.[7,8] The particles, alpha particles for example, are slowed down by successive collision with atoms in the target and the range therefore represents a gross effect of many collisions. Total stopping power is defined as the sum over all possible inelastic processes of the product of the inelastic cross section and the energy lost for each inelastic process. Elastic scattering is not usually considered because the kinetic energy loss in elastic events is small. In order to calculate the total stopping power, all inelastic events must be considered. For beams of relatively low

mass, the interactions are principally those involving overlap of the orbital electron clouds, but for heavier and faster beams, nuclear collisions must also be considered. In calculations of ionic stopping power of dense gases, the possibility of electron capture and loss (charge exchange) must be accounted for because the ion can become a neutral particle during part of its trajectory[9]. A partial stopping power is that due to only one species in the beam; it is preferable, when possible, to investigate this rather than the total stopping power. It still is a dense target experiment; although only one kind of beam particle is monitored, the effects of multiple collisions are observed. The experimental procedure used in measuring the partial stopping power of a fast neutral beam is as follows.[10] The beam is passed through a long gas-filled cell placed in a magnetic field transverse to the axis of the beam. The field is strong enough to deflect any charged particles from the beam, so that the only particles which can emerge from the stopping chamber are those which have remained neutral throughout their trajectory. The emerging neutral particles are then ionized and their energy distribution determined with an electrostatic analyzer. Thus measurement of the average energy loss and the target thickness (the product of the density of the stopping gas and the path length) permits a calculation of the stopping power. Partial ionic stopping powers can be measured in a similar apparatus.[11] In this case the magnetic field confines the ions to an approximately circular path through the stopping chamber, and the entrance and exit slits are arranged so that only ions of a given charge are transmitted. Thus any ion suffering a charge transfer collision is excluded. The energy distribution of the transmitted beam is determined, as before, with an electrostatic analyzer. Essentially all the work being done in this field is at high

energy, upwards of at least ten kilovolts.

Another similar experiment is the measurement of the energy loss spectra of fast beams after they have passed through single crystals.[12-14] The ions tend to be channeled between crystal planes as they pass through the target and the energy loss spectra show structure which is attributed to transverse oscillation of the particles in the channels. With the aid of appropriate theory, the detailed structure of the spectra can be used to map out the stopping power in the channels, and to determine the interatomic potential of the beam particle with respect to the atoms in the channel. This work is also restricted to high energies.

Another area of research which can be included in the category of dense targets is the interaction of molecular beams with solid surfaces. The investigation of sputtering, the erosion of metal surfaces due to ion impact, has been carried out for more than a hundred years. A number of theories have been advanced[15] to account for the different sputtering yields observed for different materials, but the field is still largely an empirical one. This field has been rather inactive for some time, but in recent years renewed interest has developed.

Considerable work has been reported,[16] and much more is currently in progress, on molecular beam-surface interactions where the beam energy is too low to damage the surface. Much of the practical information which is sought in these experiments involves energy transfer from the beam to the surface, and measurement of the thermal accommodation coefficient has been a popular activity for some time. The accommodation coefficient for momentum transfer or for energy transfer is measured by directing a molecular beam at a surface and determining the momentum or energy transfer. The surface in question can be mounted on a torsion balance whose deflection is

a direct measure of the momentum transfer, or the kinetic energy of the beam can be determined (by time-of-flight methods) before and after striking the surface. The two extremes of energy transfer are permanent absorption with complete energy accommodation and completely elastic scattering. In the latter case, it is possible to arrange the conditions so that diffraction can be observed. The necessary conditions are that the substrate be a single crystal whose lattice spacing has the proper relationship to the de Broglie wavelength of the beam atom and to the angle of incidence. Diffraction of atomic beams from crystals provided an early verification of the concept of the de Broglie matter wave[17].

Energy transfer between the two extremes is more common, and many experiments have been performed in which a beam is directed at a surface and the reflected particles detected. Under some conditions, diffuse reflection is observed, suggesting that the beam has been adsorbed and re-emitted at a later time. In other systems the beam is reflected into distinct directions, and the results can often be related to the interaction potential of the beam-lattice system and to the lattice dynamics of the crystal.

A serious problem in this type of experiment is the difficulty of characterizing the surface, and in separating the effects of the lattice from those of surface adsorption. Gas-surface interaction is an area of research that has only recently attracted many workers; significant progress in this difficult field can be expected.

C. Two particle interactions.

This classification includes experiments where atomic or molecular beams are passed through thin gas targets or allowed to interact with another beam. When the experimental conditions are established correctly,

the experimental results can be interpreted in terms of two-body collision dynamics. In this sense, the experiments probe single molecular collisions.

General statements about two particle interaction experiments are not easy to make because they can be done in such a variety of ways and over such a wide range of energies. All such experiments require one or more sources which produce collimated beams of particles whose velocities are in a known range. Also required is a detector of some sort whose output response is a measure of the beam intensity or flux. The basic experiment (with many variations) is to establish single collisions of the particles in the beam with other particles and then to determine the changes in energy and momentum of both colliding partners. The dynamics of the collisions can be interpreted with this information and fundamental details of atomic and molecular interactions can be determined.

Two rather different kinds of experiment can be noted as representing the basic techniques. They can be called the crossed beam technique[18-20] and the attenuation technique[21,22]. In the crossed beam method, two independent collimated beams (usually one or both are velocity selected) are produced and permitted to intersect as shown in Fig. 2. Both beams are so dilute that the probability that a particle will make more than one collision in the region of intersection is very small and therefore any particles which are found to be scattered out of either beam result from single two particle interactions. This method is used when the changes in momentum and energy are relatively large so that the scattered particles are well separated from the primary beams; the beam energies employed are accordingly relatively small.

The key to the experiment is the detector. It must have good resolution in order to determine the energy and momentum changes accurately

and it must be able to discriminate between the various chemical species which are involved in the experiment. In addition it should be quantitative, at least ideally. The latter criterion is difficult to achieve and is frequently disregarded when only qualitative information is sought. The requirement, however, can be met in several ways; for example a mass spectrometer with a narrow input aperture has been used successfully. Other useful detectors are described in detail in a later section.

Providing that a suitable detector is selected, crossed beam experiments can be performed which provide much fundamental information. For example, if beams of two species are allowed to interact and a third species is found to have been produced, a chemical reaction has occurred. Careful investigation of the spatial distribution of the reaction product combined with the energy and momentum conservation laws permit estimates to be made of the energy transfer in the collision and shed some light on the mechanism of the reaction. Such studies can determine if a reaction occurs at large or at small separations of the reactants and whether some intermediate collision complex is formed. It is possible to produce beams with quite narrow distributions of velocity and to do an energy analysis (by a time-of-flight method, for example) of the reactive products. In addition, it is possible to produce beams in specific quantum states and with such detailed energy and spatial information the reactive collisions can be extensively characterized.

The crossed beam technique can also be employed to study non-reactive collisions. The basic technique is the same; the information sought is the energy and spatial analysis of the scattered beam particles. If the collisions are elastic, that is, where there is no transfer of translational energy into any internal states of the colliding system, the experi-

mental data may be analyzed to obtain information about the intermolecular potential. Where inelastic collisions occur, the data can be interpreted to find out if the excitation can be assigned to a particular internal state (or group of states) and how the excitation energy can be transferred to other internal states.

The crossed beam method is a powerful tool for the investigation of atomic and molecular collisions. Its particular strengths are flexibility and the lack of ambiguity in the interpretation of experiments. The only weakness of the method is the fact that at the intersection of two molecular beams the intensities are so low that only a few percent of the beam particles collide and the flux of scattered particles is therefore small and not easy to measure. It is difficult to devise a detector which gives a measure of absolute beam intensity but especially difficult when the detector must be extremely sensitive at the same time. Consequently many crossed beam experiments are performed with detectors without absolute calibrations. Nonetheless such experiments can be valuable, particularly in the study of reactive scattering. Even though it may be impossible to measure the absolute intensity of a particular reaction product, the fact that it is found to be scattered into a particular solid angle may provide much information about the details of the reactive collision.

The attenuation technique in molecular beam research has a longer history and is still in wide use. It is useful over a large range of beam energy; it can employ conventional effusive oven beams, ion beams accelerated from an ion source, or high velocity neutral beams produced by neutralizing fast ion beams. The interaction with the beam is achieved by allowing it to be attenuated as it passes through a thin layer of gas,

as shown in Fig. 3. Two particle interactions are assured by adjusting the gas pressure so that no beam particle is likely to make more than one collision in traversing the layer of gas. Such a condition is established when the attenuation of the beam is linear with pressure. Even though single collisions predominate, since the particle scattering density is much higher than it is in a crossed beam experiment many more collisions take place and the requirements on the detector are less severe.

Both elastic and inelastic scattering can be studied in the same apparatus with only slight modification. Figure 3 is a schematic drawing of a typical apparatus for investigating elastic scattering. The beam attenuation due to scattering gas at density n is given by

$$I = I_o \exp[-nS\Delta x(1+\alpha)] \qquad (1)$$

where I is the beam intensity after passage a distance Δx through the scattering gas, I_o is the initial intensity and S is the scattering cross section. The background term, $(1+\alpha)$, accounts for the fact that a small part of the scattering gas escapes through the entrance and exit apertures and can scatter the beam in the regions outside the scattering box. The scattering cross section, S, will be discussed in detail below, and it will be shown that measurements of S as a function of beam particle velocity can be analyzed to obtain values of V(r), the interaction potential for the colliding pair. Such an analysis is only possible when the scattering angle for each collision is known, so that a careful analysis of the geometry of the scattering region must be made. One possible experimental configuration is shown in Fig. 4. The cross section S is a function of the angle θ_L between the undeflected path of a particle and the deflected ray which causes that particle to strike an edge of the detector. As indicated in Fig. 4, every position within the scattering region is associated

with a different value of θ_L and therefore a different value of S. Since a beam particle can be scattered at any point in the scattering region it is clear that an experimental value of S actually represents an average over the finite dimensions of the beam, scattering region, and detector. The nature of the averaging process will be discussed below. It should be noted that the dimensions in Fig. 4 are distorted and that generally the average scattering angles are small, on the order of 10^{-2}-10^{-3} radians. This experiment makes selection of the detector relatively easy because Eq. (1) shows that only the intensity ratio is needed so that only a detector whose response is proportional to the beam intensity is satisfactory. Many such detectors are available.

As indicated above, inelastic scattering can be studied in a similar apparatus. For example, the cross section for ionization can be determined by measuring the initial beam intensity and the number of ionizing events. One arrangement involves collecting the slow ions with a transverse electric field and collection electrode. Other possibilities for detecting inelastic events, such as observing light of characteristic wavelength in the scattering region, are conceptually straightforward but can be extremely difficult in practice.

Sometimes hybrid experiments using features from both crossed beam and attenuation techniques are devised[23]. In these, the concept of a layer of scattering gas is employed, but the detector is moved to determine the intensity scattered out of the beam. These experiments are difficult to perform and to interpret, but when successful, they provide much more information than the simpler attenuation experiment.

The category of two particle interactions is only introduced here to provide a basis for the rest of this chapter. The first two categories

were included in the discussion to provide an idea of the scope of molecular beam research, but since they are generally of more interest to physicists or engineers than to chemists, they will not be discussed further. The third category is of interest to physicists and chemists but this chapter will include those topics that we feel would most appeal to chemists. The methods and techniques of molecular beam research are common to both chemical and physical problems, so that the description of experimental details might be applicable to experiments in any of the three categories above; it is in the theoretical development that differences develop. Accordingly, the next section introduces the theoretical concepts needed for understanding two particle experiments. The following sections describe some of the experimental methods used in molecular beam research and discuss some of the significant results obtained from these experiments.

II. Theoretical Background

The results of scattering experiments fall naturally into two categories: collisions which do not result in atomic rearrangements, and collisions which do. Since most chemistry involves rearrangement collisions, these are of greatest interest to the chemist. Unfortunately, they are also the most difficult to study, both experimentally and theoretically, and the bulk of our knowledge is presently limited to collisions which do not involve rearrangement. But even these collisions can supply considerable insight into chemical phenomena. In the first place, the study of simple elastic collisions supplies the conceptual basis for the description of more complicated collisions. Secondly, elastic collisions give information on the interactions between atoms and small groups

of atoms which can be applied to such chemically interesting phenomena as the conformation of large molecules and the degradation of the energy of "hot atoms". Thirdly, inelastic collisions which do not involve rearrangement but only changes in internal energy (rotational, vibrational, and electronic) can be considered prototypes of simple chemical reactions.

This section accordingly discusses elastic and inelastic collisions first, and then rearrangement collisions. All can be studied over a wide range of energies.

A. Elastic and Inelastic Collisions.

For reasons made clear in the next section, experimental molecular beam research can be divided into three energy regions. A similar division can also be made for theoretical reasons, depending on the relation of the de Broglie wavelength to molecular dimensions. When the wavelength is small compared to molecular dimensions, classical mechanics furnishes a good description of molecular collisions. This is the usual situation for high-energy beams. However, for thermal-energy beams the wavelength is often comparable to molecular dimensions, so that quantum effects are apparent. These take the form of wave interference effects, which contribute structure to the observed scattering cross sections. Classical mechanics no longer furnishes a good description, but semiclassical approximations may be satisfactory. For intermediate-energy beams the situation is less clear; sometimes quantum effects are important, sometimes not, depending on particular experimental circumstances.

The principal aim of elastic scattering measurements is the determination of the potential energy of interaction between the particles. First a brief account of the mathematical description of elastic scat-

tering is given, and then the scattering potential is related to other properties such as transport coefficients and the equation of state. Much of this carries over, in a general way, to the discussion of inelastic and rearrangement collisions. Each of the three energy regions is then discussed in turn, with special reference to the type of potential energy information obtainable, and some indication of the application of this information to other problems.

1. Formalism and Definitions

The discussion of scattering will be entirely in terms of the center-of-mass coordinate system, in which the collision is viewed as if an observer were located at the center of mass of the colliding system. The relation between the center-of-mass and the laboratory coordinate system depends only on conservation of momentum and energy, and is hence valid in both classical and quantum mechanics. Good accounts of the transformation between the coordinate systems are available in many books.[24]

The angular distribution of particles scattered from a beam is described both classically and quantum-mechanically by a differential cross section $\sigma(\omega)$, defined by the statement that the number of particles scattered into solid angle $d\omega$ per unit time is $I\sigma(\omega)d\omega$, where I is the flux density of the incident beam in particles per unit area per unit time, so that $\sigma(\omega)$ has the dimensions of area. In molecular beam scattering by gas targets there is usually axial symmetry of the beam and random orientation of target particles, in which case $\sigma(\omega)$ depends only on the polar deflection angle θ and not on the azimuth angle ϕ, and can be written as

$$\sigma(\omega)d\omega = \sigma(\theta)\ \sin\theta\ d\theta d\phi \quad . \tag{2}$$

Often the angular distribution of scattered particles is not measured directly, but only the fraction of the beam that is scattered into all angles greater than θ_o, the angular aperture of the apparatus. This may be called the integrated cross section $S(\theta_o)$, and is given by

$$S(\theta_o) = 2\pi \int_{\theta_o}^{\pi} \sigma(\theta) \sin\theta d\theta \quad . \tag{3}$$

The true total scattering cross section is obtained when $\theta_o = 0$.

The maximum amount of direct information from a scattering experiment is thus obtained from the differential cross section as a function of angle and initial relative kinetic energy. The extension of this description to inelastic and simple rearrangement collisions is straightforward. A species A in internal energy state $\underline{i}$ collides with species B in internal state $\underline{j}$ with kinetic energy of relative motion ε; the collision produces species C in state $\underline{k}$ and D in state $\underline{\ell}$, with kinetic energy of relative motion ε' and at angles θ,ϕ:

$$A(i) + B(j) = C(k) + D(\ell) \quad . \tag{4}$$

This will be described by a differential cross section $\sigma(k,\ell,i,j,\varepsilon,\theta,\phi)$, just as for elastic collisions; the essential difference is that more quantities must be specified to describe the collision than were needed for the elastic case. If C and D are different from A and B, then there is said to be a chemical reaction if the speaker is a chemist, or a rearrangement collision if the speaker is a physicist. If C and D are the same as A and B, but states $\underline{k}$ and $\underline{\ell}$ are different from states $\underline{i}$ and $\underline{j}$, then an inelastic collision is said to have occurred.

We record here for future reference the relation between the differential cross section $\sigma(\theta)$ and the potential $V(r)$, and defer comments on

the extraction of $V(r)$ from $\sigma(\theta)$ (the inversion problem) to the discussions of scattering in the three different energy ranges.

In a classical description of the scattering of two particles with reduced mass μ and relative velocity $\vec{v}$ the collision trajectories are well defined, and for a given kinetic energy of relative motion each value of the impact parameter b results in a definite value of the scattering angle, as shown in Fig. 5. Thus all the particles falling on the target area between b and b + db will be scattered into angles between θ and $\theta + d\theta$; conservation of particles and the definition of $\sigma(\theta)$ then allows us to write $2\pi b|db| = 2\pi\sigma(\theta)\sin\theta|d\theta|$, from which the expression for $\sigma(\theta)$ is obtained

$$\sigma(\theta) = \frac{b}{\sin\theta|d\theta/db|} \quad . \tag{5}$$

The integrated cross section is then

$$S(\theta_o) = 2\pi \int_{b(\pi)}^{b(\theta_o)} bdb = \pi b^2(\theta_o) \quad , \tag{6}$$

since $b(\pi) = 0$ (head-on collision). The dependence of the cross section on $V(r)$ is implicitly contained in the relation between θ and b appearing in Eqs. (5) and (6),[24]

$$\theta(b,\varepsilon) = \pi - 2b \int_{r_c}^{\infty} \left[1 - \left(\frac{b}{r}\right)^2 - \frac{V(r)}{\varepsilon}\right]^{-1/2} \frac{dr}{r^2} \, , \tag{7}$$

where r_c is the distance of closest approach, given by

$$1 - \left(\frac{b}{r_c}\right)^2 - \frac{V(r_c)}{\varepsilon} = 0. \tag{8}$$

If the potential is not purely repulsive or attractive, several values of b may lead to scattering into the same θ. In such cases the expression for

$\sigma(\theta)$ becomes a sum over the several values of b, but the expression for $S(\theta_o)$ involves both sums and differences.[25]

Precise collision trajectories cannot be specified in quantum mechanics, and a wave-like description of scattering is necessary.[24] The total wave function consists of an incident wave plus a scattered wave; at distances far removed from the collision region, the incident wave is a plane wave and the scattered wave a spherical wave. The asymptotic form of the wave function is thus

$$\psi = \psi_{in} + \psi_{scatt} \sim e^{i\kappa z} + \frac{e^{i\kappa r}}{r} f(\theta) \quad , \tag{9}$$

where $\kappa = \mu v/\hbar$ is the wave number of relative motion and $f(\theta)$ is the scattering amplitude. The differential cross section is given by

$$\sigma(\theta) = |f(\theta)|^2 \quad . \tag{10}$$

In principle, $f(\theta)$ must be found by solution of the Schrödinger equation. The usual procedure for elastic scattering is to expand the wave function into a series of partial waves, one for each value of the angular momentum quantum number, ℓ. The incident and scattered partial waves then differ only in phase, and the problem is reduced to evaluation of the phase shift for each partial wave. The scattering amplitude is found to be

$$f(\theta) = (2i\kappa)^{-1} \sum_{\ell=0}^{\infty} (2\ell+1)(e^{2i\delta_\ell}-1) P_\ell(\cos\theta) \quad , \tag{11}$$

where δ_ℓ is the phase shift of the ℓ-th partial wave and $P_\ell(\cos\theta)$ is a Legendre polynomial. The δ_ℓ must usually be found by numerical integration of the radial Schrödinger equation, although useful approximations are sometimes available. The expression given in Eq. (3) for the integrated cross section still holds if the lower limit is permitted to extend to $\theta_o = 0$, but it yields a simple result only for the total cross section,

$$S(0) = (4\pi/\kappa^2) \sum_{\ell=0}^{\infty} (2\ell+1)\sin^2 \delta_\ell \ . \qquad (12)$$

A semiclassical approximation is often useful for atomic and molecular scattering, in which the summations over phase shifts are replaced by integrations and the phase shifts are calculated by the Jeffreys-Wentzel-Kramers-Brillouin-Langer (JWKBL) approximation,

$$\delta_\ell \approx \delta(b) = \kappa \int_{r_c}^{\infty} \left[1 - \left(\frac{b}{r}\right)^2 - \frac{V(r)}{\epsilon}\right]^{1/2} dr - \kappa \int_{b}^{\infty} \left[1 - \left(\frac{b}{r}\right)^2\right]^{1/2} dr, \qquad (13)$$

where the impact parameter is

$$b = (\ell + 1/2)/\kappa \ . \qquad (14)$$

The relation between the phase shifts and the classical deflection angle in this approximation is

$$\theta(b) = 2 \frac{d\delta_\ell}{d\ell} = \frac{2}{\kappa} \frac{d\delta(b)}{db} \ . \qquad (15)$$

Fairly extensive studies of the semiclassical approximation in atomic and molecular scattering are available.[22,26-28]

2. Relation to Other Phenomena

The complete differential cross section, if measured over a complete range of θ and a wide range of ϵ, contains a great deal of information. However, it is almost never fully measured. In practice only partial information on the differential cross section is available -- the ranges of angles and energies are limited by experimental difficulties. From such partial scattering information therefore only partial information on the potential can be extracted. In fact, to obtain any sensible answer at all, it is usually necessary to inject some independent information on the potential, such as whether or not it is monotonic, and if so, whether it is attractive or repulsive, or indeed whether the scattering is caused

by a single potential rather than by two or more potentials. Although in practice only partial information on $\sigma(\theta)$ is known, it is interesting to ask what phenomena other than scattering could be calculated if $\sigma(\theta)$ were known completely.

In the first place, only binary collision phenomena could be calculated rigorously, since the scattering under discussion here involves collisions of only two molecules at a time. If only elastic collisions are possible, this means that only the two-body properties contained in the dilute-gas transport coefficients and equation of state -- viscosity, thermal conductivity, diffusion, thermal diffusion, and the second virial coefficient can be obtained. If inelastic collisions are also possible, the absorption and dispersion of sound waves in gases, and similar related phenomena can be calculated. Information on rearrangement collisions extends the range to include calculations of bimolecular chemical rate coefficients in the gas phase. But strictly speaking, phenomena in dense gases, liquids, and solids would remain out of reach, as would chemical reactions that required three or more molecules to interact simultaneously. Of course, one always tries to make approximations that will extend the range of usefulness of strictly two-body information. Such approximations usually aim to build up many-body phenomena as collections of two-body phenomena: for example, the assumption of pairwise additive interatomic particles, of effective potentials such as appear in optical models, or the representation of a ternary collision as a transient orbiting binary pair struck by a third particle. Many of these approximations are astonishingly successful and are discussed in subsequent sections, but it is well to remember that they are approximations and subject to failures.

This brings up a second limitation. A well-founded theory is required that connects the observable phenomena to $\sigma(\theta)$, and such a theory may not be simple. It is at this point that it is necessary to include the realm of general statistical mechanics, with its great fascination and many unsolved fundamental problems. For instance, if only elastic collisions occur, there is an excellent theory available from which the viscosity, thermal conductivity, diffusion, and thermal diffusion coefficients of a gas can be calculated to any desired accuracy, once the differential cross section is given. But the calculation of the second virial coefficient from $\sigma(\theta)$ alone is a much more difficult task, for it requires knowledge of the bound two-body states. Moreover, if inelastic collisions can occur, the basic connecting theory for the transport coefficients becomes much more complex, and involves some intractable features that are still not completely resolved. Finally, if rearrangement collisions can occur, then the theory is very complicated indeed, and only parts of it are as yet worked out.

As an illustration of these remarks, consider the viscosity of a dilute gas in which only elastic collisions occur. The Chapman-Enskog kinetic theory of gases gives the viscosity in terms of some integrations over the differential cross section,[29,30]

$$\frac{1}{\eta} = \frac{16}{5}\left(\frac{\pi}{mkT}\right)^{1/2} \int_0^\infty \gamma^7 e^{-\gamma^2} \left[\int_0^\pi (1-\cos^2\theta)\sigma(\theta,\varepsilon)\sin\theta d\theta\right] d\gamma \quad , \qquad (16)$$

where η is the viscosity, m the molecular mass, k the Boltzmann constant, and $\gamma^2 = \varepsilon/kT$. Thus if $\sigma(\theta,\varepsilon)$ is known for all values of θ and ε, η can be calculated for all temperatures. However, if $\sigma(\theta,\varepsilon)$ is known only over a limited range of ε, η is reliably determined only over a limited range of

T, corresponding roughly to the region of the maximum in the weighting function $\gamma^7 e^{-\gamma^2} d\gamma$ (that is, to $kT \approx \frac{1}{3} \varepsilon$). Similar remarks apply to the other transport coefficients.

There are two interesting features about Eq. (16) and similar equations. The first is that there seems to be no need to determine the potential energy V(r), for the desired property can be calculated directly from $\sigma(\theta,\varepsilon)$. This appears to contradict the earlier remark about the principal aim of elastic scattering being the determination of V(r). The second feature is that the calculation throws away most of the hard-won information contained in $\sigma(\theta,\varepsilon)$ by integrating over all angles and all values of γ. This feature is aggravated if inelastic collisions are possible, for then the calculation further involves summation over all internal energy states.[31] Thus it appears that attempts to measure $\sigma(\theta,\varepsilon)$ involve unnecessary complexity.

The rationalization of these features lies in the fact that scattering is studied in the hope of understanding enough about collisions and interactions to be able to make predictions and calculations on the basis of incomplete information. Furthermore, only fragmentary information on $\sigma(\theta,\varepsilon)$ ever exists. Thus the aim is to proceed from partial information on $\sigma(\theta,\varepsilon)$ to something deeper -- the potential -- from which useful calculations can be made. Such a program requires a well-founded theory and careful analysis.

As an example, consider the calculation of transport properties from scattering experiments in which only small-angle scattering is studied. The weighting factor of $(1-\cos^2\theta)$ in Eq. (16) effectively discards small-angle deflections as far as any influence on the viscosity (as well as the

other transport coefficients) is concerned. Thus one may get a superficial impression that small-angle scattering measurements are useless for determining transport coefficients, and this is true as far as only $\sigma(\theta,\varepsilon)$ is concerned. The picture is quite different in terms of an analysis through the potential. In terms of internuclear separations small-angle scattering probes only the outer fringes of the potential for a given collision energy. However, at a lower energy even a head-on collision can penetrate only that far. Therefore the small-angle scattering at high energies probes that part of the potential that controls the large-angle scattering at much lower energies and this is precisely what is needed to calculate the viscosity at temperatures corresponding to those low energies. For example, study of scattering at about 10^{-3} radian with a beam having kinetic energies in the range of 10^{3} eV probes that part of the potential having a magnitude of about 1 eV. This in turn determines a property such as viscosity at temperatures of a few thousand degrees Kelvin.

In short, by analyzing scattering in terms of something more fundamental than the differential cross section the ability to correlate and predict can be greatly expanded. In the case of elastic scattering the potential is the more fundamental quantity, and such prediction ability is highly developed. For reactive scattering, on the other hand, as yet mostly only correlation theories or phenomenological theories similar to and modeled on those in nuclear physics are available -- stripping reactions, complex formation, R-matrix theory, optical models, and so on.

The reader who wishes a comprehensive treatment of the relation of the intermolecular potential to transport properties and virial coefficients

should refer to specialized monographs.[29,30,32]

B. Rearrangement Collisions

1. Formalism and Definitions

The formalism used to describe elastic and inelastic two-body scattering may be used as a starting point for discussing rearrangement collisions. The general case is considered in which two isolated particles in given internal quantum states are converted by a single collision into two different isolated particles in specified internal quantum states. The treatment is therefore limited to reactions which are mechanistically bimolecular and kinetically second order. The origin of the limitation is the same as that previously discussed in connection with macroscopic transport and equilibrium properties of dilute gases.

The prototype reaction used earlier in connection with inelastic scattering is

$$A(i) + B(j) \rightleftharpoons C(k) + D(\ell). \tag{17}$$

C(k) and D(ℓ) are now products of different chemical species than the reactants A(i) and B(j), and i, j, k, and ℓ are the specified internal quantum states. The rate of reaction in the forward direction, Z_R, may be written as

$$Z_R = k_f c_{A(i)} c_{B(j)} , \tag{18}$$

where k_f is the rate constant and $c_{A(i)}$ and $c_{B(j)}$ are the volume concentrations of the reactants. On a molecular basis the reaction rate, which is simply the number of reactive collisions per unit time and unit volume, is proportional to the product of the number densities of the reactants and the average velocity with which they approach one another and, in addition, to the differential cross section for reaction $\sigma_R(k,\ell,i,j,p,\omega)$ which, as

indicated, is dependent on the internal states of the four species as well as the initial relative momentum $\vec{p}$ and the solid angle ω of scattering. The reaction rate may therefore be written

$$Z_R = \int_0^{4\pi}\int_{-\infty}^{+\infty}\int_{-\infty}^{+\infty} c_{A(i)} c_{B(j)} |\vec{p}/\mu| \sigma_R(k,\ell,i,j,p,\omega)\, F(\vec{p}_{A(i)}) d\vec{p}_{A(i)}\, F(\vec{p}_{B(j)}) d\vec{p}_{B(j)} d\omega \qquad (19)$$

where the initial relative momentum corresponds to the initial kinetic energy of relative motion ε or initial relative velocity $\vec{v}$, μ is the reduced mass of A(i) and B(j), and $F(\vec{p}_{A(i)})$ and $F(\vec{p}_{B(j)})$ are the momentum distribution functions of the reactants. The differential cross section per unit solid angle for chemical reaction is similar in character to the differential cross section $\sigma(k,\ell,i,j,\varepsilon,\theta,\phi)$ referred to earlier in connection with inelastic scattering.

An alternative and in some ways more useful method of deriving an expression for the reaction rate is through the impact parameter b defined earlier and shown in Fig. 5. The function $P(k,\ell,i,j,p,b,\phi)$ can be defined as the probability that a collision will result in reaction. Of those collisions involving impact parameters between b and b + db, the number per unit time and unit volume which result in reaction is the product of the density of reactants having specified differential ranges of momentum, their initial relative velocity and the reaction probability. Thus the total reactive collision frequency is

$$Z_R = \int_0^{c_{B(j)}} \int_0^{c_{A(i)}} \int_0^{2\pi}\int_0^{\infty} P(k,\ell,i,j,p,b,\phi) |p/\mu| b\,db\, d\phi\, dc_{A(i)} dc_{B(j)} \qquad (20)$$

Comparison of Eqs. (19) and (20) establishes the following relationships:

$$P(k,\ell,i,j,p,b,\phi)\ b\,db\,d\phi = \sigma_R(k,\ell,i,j,p,\omega)\ d\omega$$

$$dc_{A(i)}\ dc_{B(j)} = c_{A(i)}\ F(\vec{p}_{A(i)})d\vec{p}_{A(i)}\ c_{B(j)}\ F(\vec{p}_{B(j)})\ d\vec{p}_{B(j)}\ . \tag{21}$$

In order to perform the integrations in Eq. (20) it is clear from Eq. (21) that the momentum distribution functions $F(\vec{p})$ must be known. It has been shown[33] that the equilibrium, or Maxwellian, distribution is a satisfactory approximation in almost all cases. Some additional transformations are required to relate the components of the momenta in Eq. (21) to components of the center-of-mass momenta and the relative momenta and to reduce the integrations to a single one over the relative velocity v. Details of these transformation procedures, in which it is customary to use velocities rather than the corresponding momenta, are found in texts on kinetic theory of gases or kinetics of chemical reactions.[34,35] The results of this treatment of Eq. (20) leads to

$$Z_R = (\mu/kT)^{3/2}(2/\pi)^{1/2}\ c_{A(i)}c_{B(j)} \int_0^\infty \int_0^{2\pi} \int_0^\infty P(k,\ell,i,j,v,b,\phi)\ v^3 \times \exp(-\mu v^2/2kT)\ b\ db\ d\phi\ dv\ . \tag{22}$$

In analogy with the relations established above between the total scattering cross section and the differential cross section we express the total cross section for chemical reaction as

$$S_R(k,\ell,i,j,p) = \int_0^{4\pi} \sigma_R(k,\ell,i,j,p,\omega)\ d\omega = \int_0^\infty \int_0^{2\pi} P(k,\ell,i,j,p,b,\phi)\ b\ db\ d\phi. \tag{23}$$

It follows from Eqs. (18) - (23) that the temperature dependent rate constant for the forward reaction between isolated A(i) and B(j) molecules is a weighted average, over all initial relative momenta, of

the product of the total cross section for chemical reaction and the initial relative velocity. Thus,

$$k_f(k,\ell,i,j,T) = (\mu/kT)^{3/2}(2/\pi)^{1/2} \int_0^\infty \left[S_R(k,\ell,i,j,v)\ v\right] \times v^2 \exp(-\mu v^2/2kT)\ dv. \tag{24}$$

Since the initial kinetic energy of relative motion, $\varepsilon = p^2/2\mu = \mu v^2/2$, is also a convenient and frequently used variable, a useful third relation is

$$k_f(k,\ell,i,j,T) = (2/kT)^{3/2}(1/2\pi)^{1/2} \int_0^\infty \left[S_R(k,\ell,i,j,\varepsilon)\ (2\varepsilon/\mu)^{1/2}\right] \times \varepsilon^{1/2} \exp(-\varepsilon/kT)\ d\varepsilon. \tag{25}$$

Since any function of p may also be written as a function of v or ε, the designations of the functional dependence of P and S_R in Eqs. (22), (24) and (25) have been changed, when necessary, to be consistent with the selected variables of integration.

Although there has been significant recent progress in inelastic and reactive scattering in selecting beam particles in specific internal quantum states,[22,36-42] most beam studies of rearrangement collisions have involved reactants and products in a variety of quantum states. The difficulties of state selection are such, however, that much future work will almost certainly involve reactants and products in a wide variety of internal states. The formal procedure for removing the restriction that A(i), B(j), C(k), and D(ℓ) represent isolated molecules each in a single quantum state is therefore of interest. When this restriction is removed, Eq. (17) is applicable to a mixture of reactants and products in all possible quantum states and the relation for the rate constant for the forward direction becomes

$$k_f(T) = (2/kT)^{3/2}(1/2\pi)^{1/2} \int_0^\infty \left[S_R(\varepsilon)\ (2\varepsilon/\mu)^{1/2}\right] \varepsilon^{1/2} \exp(-\varepsilon/kT)\ d\varepsilon \qquad (26)$$

where

$$S_R(\varepsilon) = \sum_{i,j} x_{A(i)}\ x_{B(j)} \left[\sum_{k,\ell} S_R(k,\ell,i,j,p)\right]. \qquad (27)$$

The fractions of A(i) and B(j) in given quantum states have been designated as $x_{A(i)}$ and $x_{B(j)}$. If these fractions are assumed to be equilibrium fractions at all times with respect to $x_{C(k)}$ and $x_{D(\ell)}$, then $k_f(T)$ in Eq. (26) is time independent.

In general, the energy dependence of the total cross section for chemical reaction which appears in Eq. (26) will be determined by the dynamical motions of the reactants and products on a multidimensional surface which represents the variation in potential energy of the reacting system as its components change their internuclear separations and spatial orientations. For molecular interactions which are physically realistic the problem of determining the energy dependence of $S_R(\varepsilon)$ is formidable and the likelihood of obtaining an analytical expression for $k_f(T)$ is very small. However, with a sufficiently simple model a qualitatively correct picture of the usual behavior of $S_R(\varepsilon)$ and $k_f(T)$ can be obtained.

The model assumes that the reactants are structureless, repelling hard spheres which change into products when the kinetic energy of relative motion along the line of centers exceeds a threshold value ε_a. For this model, whose potential energy varies with internuclear separation as shown in Fig. 6, it has been shown[43] that

$$\begin{aligned} S_R(\varepsilon) &= \pi d_{AB}^2\ (1 - \varepsilon_a/\varepsilon) \qquad \text{for } \varepsilon > \varepsilon_a \\ S_R(\varepsilon) &= 0 \qquad\qquad\qquad\ \ \text{for } \varepsilon < \varepsilon_a\ . \end{aligned} \qquad (28)$$

The quantity πd_{AB}^2 is the cross sectional area of the sphere which envelops

the centers of the reacting spheres when they are in contact. Integration of Eq. (26) with $S_R(\varepsilon)$ given by Eq. (28) leads to

$$k_f(T) = \pi d_{AB}^2 \, (8kT/\pi\mu)^{1/2} \exp(-\varepsilon_a/kT). \tag{29}$$

Since ε_a is usually much greater than kT the temperature dependence of $k_f(T)$ is largely determined by the exponential term in Eq. (29) and a differentiation produces the approximate relation

$$d \ln k_f(T) dT \cong \varepsilon_a/kT^2. \tag{30}$$

Equation (30) describes the temperature dependence of the rate constant for a large number of bimolecular reactions for which a plot of $\ln k_f(T)$ vs 1/T gives a straight line whose slope, multiplied by k, is the so-called Arrhenius activation energy.

An addition to the notation will be introduced here in order to conform to common usage. Most kineticists use molar energies rather than the molecular energies which have been used so far. The molar energy E is defined as $N\varepsilon$, where N is Avagadro's constant. Both energies will be used interchangeably.

2. Collision Dynamics

In understanding microscopic features of reactive scattering it is often helpful to supplement the preceding theoretical treatment with a discussion of the conservation laws of energy and momentum.[44-47] If E is the initial kinetic energy of relative motion of the reactants, Z the associated internal energy (rotational, vibrational, or electronic), and ΔD_o° the difference in dissociation energy of products measured from zero-point levels, as shown in Fig. 6(b), then the final kinetic energy of relative motion of the products E' and the corresponding internal energy

Z' are given by

$$E' + Z' = E + Z - \Delta D_o^o. \tag{31}$$

In view of the fact that in most reactive scattering experiments neither reactants or products are likely to be in specifically selected internal quantum states, the simplified designations A, B, C, and D will be used rather than A(i), B(j), C(k), and D(ℓ) for reactants and products. Thus, the center-of-mass velocity vector $\vec{v}_c$, also known as the centroid, is defined in terms of the masses and initial velocity vectors of the reactants by the relation

$$\vec{v}_c = (m_A\vec{v}_A + m_B\vec{v}_B)/m \tag{32}$$

where m represents the total mass of the reactants, (m_A+m_B), which, is of course, also equal to that of the products. The total kinetic energy of the system is the sum of the kinetic energy of the reactants which can be shown to be

$$\frac{1}{2}m_A v_A^2 + \frac{1}{2}m_B v_B^2 = \frac{1}{2}(m_A + m_B)\, v_c^2 + \frac{1}{2}\,\mu v^2 \,. \tag{33}$$

The first term on the right in Eq. (33) is the kinetic energy of the total mass moving at the velocity of the center of mass. This energy can be shown to be constant and has therefore been omitted from both sides of Eq. (31). If $\vec{v}_A$ and $\vec{v}_B$ are plotted with a common origin, as shown in Fig. 7, the initial relative velocity, $\vec{v} = \vec{v}_A - \vec{v}_B$ intersects $\vec{v}_c$ at a point determined by the relations

$$\vec{v}_A - \vec{v}_c = m_B\vec{v}/m \tag{34}$$

and

$$\vec{v}_B - \vec{v}_c = -m_A\vec{v}/m. \tag{35}$$

Equations (34) and (35) state that at large internuclear separations

an observer stationed on the moving center of mass sees the reactants approach with velocities which are inversely proportional to their total mass and parallel to the initial relative velocity. Similarly, the recoil velocities with which the products recede from the moving center of mass are given by the relations

$$\vec{v}_C - \vec{v}_c = m_D\vec{v}'/m \tag{36}$$

and

$$\vec{v}_D - \vec{v}_c = -m_C\vec{v}'/m \tag{37}$$

where the final relative velocity $\vec{v}' = \vec{v}_C - \vec{v}_D$ may take any direction in space and therefore may be considered as pivoting around the end of $\vec{v}_c$. The vector diagram in Fig. 7 is a graphical representation of the relations of Eqs. (34) - (37) for a binary collision involving mutually perpendicular initial velocity vectors. For the case illustrated, θ_L is the angle in the laboratory system, measured from $\vec{v}_A$ and in the plane of $\vec{v}_A$ and $\vec{v}_B$, into which the product D is scattered with velocity $\vec{v}_D$. When the collision between A and B is elastic Z' and Z are equal, ΔD_o^o is zero, and E and E' are identical, or equivalently, $|\vec{v}'| = |\vec{v}|$. For a reactive collision, however, $|\vec{v}'|$ is restricted to $(2E'/\mu')^{1/2}$ where μ' is m_Cm_D/m and E' is subject to the condition specified by Eq. (31) in which neither Z' - Z nor ΔD_o^o will in general be equal to zero.

It is interesting to see how the conservation relations of Eqs. (33) - (37) and the vector diagram in Fig. 7 can be used to correlate or even to predict certain experimental features of reactive scattering. For example, a special case can be considered where $m_C \ll m_D$ so that $m_C/m \ll 1$ and also where E' is not much larger than E so that $|\vec{v}'|$ is approximately equal to $|\vec{v}|$. Equation (37) then states that the velocity vector $\vec{v}_D$ may be confined to a small cone around $\vec{v}_c$ so that the product D of mass m_D will be found

near the centroid. The imposed special conditions therefore result in an increased flux or intensity of D around a small range of θ near the centroid. However, because the intensity of D is so sharply peaked, it will be difficult to secure adequate angular resolution for accurate measurement of the differential scattering cross sections in this angular region. At the other extreme, if $|m_C\vec{v}'/m|$ is sufficiently larger than $|\vec{v}_c|$ the product D with velocity $\vec{v}_D$ may be found at any laboratory angle. Herschbach and co-workers[45,46] have given a detailed analysis of the collision dynamics on which the conclusions for these special cases are based.

The discussion of collision dynamics thus far has illustrated the type of microscopic information that may be obtained by invoking the conservation laws for total energy and linear momentum. In general the total angular momentum is also a collisional invariant and additional microscopic information can be obtained by requiring that this particular quantity also be conserved. The initial angular momentum of the system is a vector sum of the orbital angular momentum $\vec{L} = \mu\vec{v}b$ and the rotational angular momenta $\vec{J}_A$ and $\vec{J}_B$ of the reactants. If $\vec{J} = \vec{J}_A + \vec{J}_B$ and $\vec{J}' = \vec{J}_C + \vec{J}_D$ the conservation law for total angular momentum may be written as

$$\vec{L}' + \vec{J}' = \vec{L} + \vec{J} \tag{38}$$

where $\vec{L}' = \mu'\vec{v}'b'$. For the special case of elastic scattering in a central potential $\vec{J}' = \vec{J}$ so that $\vec{L}' = \vec{L}$. Although the initial orbital angular momentum $\vec{L}$ must be perpendicular to the initial relative velocity $\vec{v}$, the initial rotational angular momentum $\vec{J}$ may have any spatial orientation as shown in Fig. 8a which also shows the possible spatial orientation of the initial total angular momentum vector. Frequently $\vec{L} >> \vec{J}$ and $\vec{L}' >> \vec{J}'$ and

under these conditions the final velocity vector $\vec{v}'$, which must be perpendicular to $\vec{L}'$, will also be almost perpendicular to $\vec{L}$. However, even if the final relative velocity vectors are assumed to be uniformly distributed about the initial orbital angular momentum, an anisotropy in the spatial distribution of the product D can be expected. This conclusion can be visualized by referring to Fig. 8b in which the final relative velocity vectors, for a particular $\vec{v}$ and $\vec{L}$, are represented as uniformly spaced radii in the circle perpendicular to $\vec{L}$. For a selected value of $\vec{v}$, it is possible to have all values of $\vec{L}$ which are uniformly distributed in directions perpendicular to $\vec{v}$, so that the spatial distribution of $\vec{v}'$ vectors is obtained by rotating Fig. 8b about $\vec{v}$ as shown. In the sphere generated by the rotation of the circle containing the final relative velocity vectors, these vectors will be denser along the $\vec{v}$ axis than near the plane produced by the rotation of L.[45]

If μ/μ' is greatly different from unity a marked change may occur in the orbital angular momentum and, according to Eq. (38), a corresponding change in the rotational angular momentum. For example, if $\mu/\mu' \gg 1$ and if $\vec{L}$ is large, the products must be in highly excited rotational states since $\vec{J}' \gg \vec{L}'$, and the orientation of the final rotational angular momentum vectors will be approximately parallel to the initial total angular momentum.[45,48]

The discussion of the dynamics of collisions has shown some of the microscopic features of reactive scattering which are applicable, in certain special cases, to any bimolecular reaction which can be experimentally investigated by the method of crossed molecular beams. By combining the material in this section with the theoretical background for rearrangement

collisions in the preceding section and with the theoretical background for elastic and inelastic collisions, we may proceed to analyze many of the microscopic features of specific bimolecular reactions. Limitations of space prevent a discussion of all the experiments which are relevant to this chapter. A selected group of reactions will be used to illustrate those features of rearrangement collisions which are of particular interest and significance.

III. Experimental Methods

Molecular beam experiments involve a large variety of types of apparatus and techniques. These reflect both the numerous experiments which have been performed as well as the extensive ingenuity of the experimenters. A complete description of experimental methods must of necessity be long and detailed. In this section, no effort will be made to attain such completeness; instead some typical examples of the various experimental methods will be given. The basic configurations of beam experiments were discussed in the Introduction and will not be repeated here. All experiments, however, require three basic elements; one or more sources to produce a collimated beam (or beams) with a known energy distribution, a detector to measure the beam intensity, and a region where two-body interactions can occur. These elements of beam experiment are discussed separately in this section. The experimental techniques also separate naturally into three categories according to the energy range of the beam particles. Methods of production, collimation, and detection are generally different in the three regimes, here rather arbitrarily defined as low energy (less than about 0.5 eV), high energy (above about 25 eV) and intermediate energy (between 0.5 and 25 eV). The

following discussion will briefly describe some of the general techniques useful in each range.

A. Low Energy Beams.

1. Production

Modern apparatus employed in research with thermal energy beams utilize sources operating on the same principle as that used in the very early experiments described in the Introduction. Most apparatus consist of several individually pumped chambers, the first of which contains an apertured, temperature-controlled oven filled with permanent gas, or vapor from condensed material. Succeeding chambers provide additional collimating apertures and space for various operations with the beam. The design of an oven source, particularly one which is to operate at a high temperature, depends strongly on the material which is to constitute the beam. Other than an obvious criterion with respect to melting point, the principal requirement considered when selecting the material to fabricate the oven is that it be chemically inert. Some means to prevent spattering and condensation at the exit slit must be provided; either the slit can be heated separately or an interior baffle can be installed. Operation at very high temperatures may require the use of radiation shields to protect nearby elements of the apparatus. Some commonly used substances which constitute the beam, for example the alkali metals, present handling problems. They are usually sealed into glass ampoules and some means is provided for opening the ampoules under vacuum and loading the ovens. Ovens for producing beams of permanent gases provide fewer design problems, but the demands placed upon the pumping system are usually much greater because all the gas emerging from the oven must be pumped away since there is no

condensation on the walls to add to the effective pumping speed.

Various methods have been adopted to make beams emerging from the oven more directional. These procedures all take the form of constructing the oven exit as a canal[49] rather than a thin aperture; in order to increase beam intensity without loss of directionality many parallel canals are often used. Stacks of hypodermic needles,[50] glass capillaries,[51] and stacks of alternate flat and corrugated metal foils[51] have all been used successfully. Recently Laval nozzles have been used as exit slits;[18] as will be discussed later, these nozzles provide large intensities and, in addition, considerably narrower velocity distributions than conventional source apertures.

Many other special thermal beam sources have been constructed. It is often necessary to form a beam of atoms from species which are stable only as molecules. In such cases, some form of electrical discharge is produced in the oven, the most common type being the microwave arc. Beams of hydrogen atoms[52] and the halogens[53] have been obtained this way. Use of a Wood's tube discharge to produce atomic hydrogen has also been extensively reported.[54] Hydrogen atoms have also been obtained from a thermal dissociater,[55] the most usual form of which is a tungsten tube with an exit slit which can be electrically heated to about 2500°K. Such thermal dissociaters have been used mostly for hydrogen. Many experiments require beams of atoms or molecules in excited states.[56] Sometimes this is achieved with state selectors, to be described below, other times excitation is provided by electron impact or by optical excitation to a higher state which decays into a metastable state.

The molecules emerging from an effusive oven will have a velocity distribution which can be written in terms of the Maxwellian distribution

at the temperature of the oven. The energy of the particles in the beam can be varied to some extent therefore by adjusting the temperature of the oven. Only a limited temperature range is available, however; at low temperatures the vapor pressure of the material forming the beam becomes too low to provide a beam of useful intensity, and at high temperatures the beam atoms may be internally excited, usually to an unknown degree. A more useful method of varying the beam energy is to select from the beam only those particles in a narrow range of velocity. Not only does this permit the selection of a range of velocity any place within the distribution, but it always simplifies the interpretation of an experiment when the velocity spread is small. The first velocity selector was that of Lammert[57] who used it to verify that the density distribution of an effusive beam is indeed Maxwellian as had been predicted. He passed a beam through slots in two successive disks which rotated at a speed such that only those atoms in a chosen range could pass. This fundamental concept has been used in the design of a number of velocity selectors.

The first basic design to receive widespread use was that of a rotating cylinder containing helical grooves[58-60]. This selector has high transmission and completely eliminates the velocity sidebands which are transmitted by the simpler selector containing two slotted disks. The cylinders are, however, difficult to fabricate and in general have a relatively large mass which poses problems in achieving high angular speeds. A more recent development has been the design of selectors employing multiple slotted disks[61-65]. These selectors are easier to make than grooved cylinders and can be made with a low moment of inertia. By adjusting the inter-disk spacing and the relative displacement of the slots,

the selector can be made to pass a beam of selected velocity range free of sidebands. An additional advantage of the slotted disk configuration is that it can be used with beams of condensable vapors as well as with permanent gases because most of those atoms not transmitted are removed by collision with the face of a disk rather than with the sidewall of a groove.

At least three published discussions[63-65] deal with the optimum relative position and angular displacement of the slotted disks in order to eliminate sidebands completely while minimizing the total rotating mass. The details will not be repeated here because, in general, they involve specific features of each selector, for example whether or not the disks have varying thickness.

The various velocity selectors now provide, in fairly routine manner, beams of adequate intensity with energy spreads of a few percent. A recent innovation has been the development of techniques for selecting beams with atoms in specified quantum states. The basic techniques of quantum state selection are those which have long been used in molecular-beam high-frequency resonance experiments such as those described by Ramsey.[2] If a molecule has a permanent magnetic or electric moment, interaction with an external inhomogeneous magnetic or electric field is possible and the amount of deflection of the beam and its direction in the external field is a function of the angular momentum quantum number and its projection on the local field direction. Pauly and Toennies[22,66] discuss a number of experimental arrangements for such deflections and alignments, from the traditional Stern-Gerlach arrangement which deflects the beam particles without focusing, to multi-pole electrode assemblies which can be used to focus molecules in different (j,m) states. The

application of state selection to specific experiments will be discussed later.

2. Detection.

Methods of detecting molecular beams have been the subject of extensive research. The original method, that of condensation, is clearly inefficient and awkward because it requires a relatively long time to condense enough material to observe, and obviously provides difficulties for permanent gases and materials with low melting points. The search for a faster, more sensitive detector for thermal beams has been under way for many years and has produced a number of successful devices. An early example is the chemical detector[67,68], which detects chemically active species whose chemical reaction with the target material at impact causes a color change. A more recent development[69] is a variation of the condensation detector in which the beam contains a radioactive species. Modern counting techniques are such that a measurable deposit is obtained much faster than by the simple condensation method. Quite recently two more investigations have been reported in the continuing search for useful beam detectors. Brooks and Herschbach[70] have applied modern electronic techniques to the Kingdon gauge[71] first proposed in 1923. This gauge is a diode operating with space charge limited electron emission. A beam particle entering the diode is ionized by electron impact and the resulting positive ion partially neutralizes the space charge producing a large increase in plate current. Johnston and King[72] report the use of field ionization in the construction of a beam detector. Here, the large electric fields near the point of a field emitter tip can quantitatively ionize atoms; the ions are then measured routinely.

Although many ingenious devices have been developed for use as detectors for thermal beams, only three are extensively used at present. These are the Pirani, surface ionization, and electron bombardment detectors. The Pirani gauge[51] is generally used to detect beams of the permanent gases. The beam passes into an enclosure through a long narrow orifice where it scatters at the walls, equilibrates and eventually effuses back through the orifice. The steady-state pressure rise measured with a Wheatstone bridge, as with a conventional hot-wire pressure gauge, is proportional to the beam intensity. The pressure rise is small and for satisfactory performance it is necessary to measure the difference in response between two identical cells, one of which can respond to fluctuations in the background pressure but which is not exposed to the beam. It is possible to increase the sensitivity of the detector by making the entrance orifice longer and narrower, but only at a cost of increasing the equilibration time.

The Pirani gauge cannot be used where the material constituting the beam will condense on the walls. For many of such materials, surface ionization[73-75] can be used to produce an effective detector. In this method, the beam particles are directed onto a heated wire from which they quickly evaporate. In general, if the work function of the wire substrate is greater than the ionization potential of the beam particle, the probability is large that the particles will leave as positive ions. The ion current is therefore proportional to the beam intensity. The surface ionizer is effective for detecting only atoms with low ionization potentials but is nonetheless an extremely useful device. It has the advantages of short time constant, high ionization efficiency, and simplicity. The

most common wire used in surface ionizers is tungsten; the tungsten must be oxidized to increase its work function in order to use it to detect the two lightest alkali metals, sodium and lithium. The alkali halides dissociate at the hot wire and also may be detected. Of critical importance to the study of reactive scattering, to be discussed below, was the discovery that both K and KBr (for example) are surface ionized with a tungsten wire while platinum wire ionizes only K. Simultaneous use of both wires therefore permits the determination of K and KBr in a mixed beam.

A number of species, notably the halogen atoms, may be detected by the formation of negative atoms at a hot wire.[51] In this case it is the relationship of the electron affinity and the metal work function that determines whether or not an atom can be surface ionized.

The third type of detector which is commonly employed is the electron bombardment detector, sometimes called the universal detector. In essence, it consists of a means for ionizing some fraction of the incident beam, discriminating between these ions and those due to the inevitable background gas, and collecting the primary ions. In principle, such detectors could be used with beams of any material and considerable effort in various laboratories[76-86] has been devoted to their development.

The large variety of successful designs reflects the different constraints put on the detection system by various experiments. In some cases the ionizer is followed by a mass spectrometer so that the intensity of a particular species can be monitored in the presence of other material. In other cases the technique of phase sensitive detection can be employed,[87] as when an ion current must be observed in the presence of a much larger

background current arising from the ambient gas. In this technique, the signal which is to be extracted from the extraneous background is modulated, mechanically or otherwise, at a fixed frequency. An amplifier tuned to this frequency will reject all signals except the desired one.

Beams of metastable atoms are relatively easy to detect because they will eject an electron from a metal surface if the excitation energy of the metastable is greater than the work function of the metal.[56] This energy criterion is met by metastables of the rare gases and mercury which eject electrons from surfaces such as gold with efficiencies of about 0.2. In order to make absolute intensity measurements, the ejection efficiency must of course be accurately determined. Detection of metastables other than those of the rare gases and mercury is usually done by an absorption method[88] in which light of a characteristic wavelength is absorbed, exciting the metastable to a higher level from which it can decay by emission of light.

3. Scattering.

The final aspect of a molecular beam experiment is the design of the interaction region, which can take many forms depending on the specific experiment being performed. As indicated in the Introduction, one method of permitting particles in a beam to interact with other particles is to pass the beam through a thin layer of gas. The gas is contained in a small differentially pumped vessel and the pressure adjusted until the molecules in the beam are likely, on the average, to suffer no more than one collision in traversing the gas layer. Such conditions are established when the beam attenuation is linear with pressure. The presence of apertures in the vessel for beam entrance and exit means that there is a steady flow of gas out of the chamber and that there will be some scattering of the

beam outside the chamber and in the finite length of the beam apertures. It is possible to account for this background scattering; the calculation is relatively simple if the mean thermal velocity of the scattering gas is less than the beam velocity, but is more difficult if the two velocities are comparable. Recently an experimental determination was made of the background scattering of the thermal beam[89]. A scattering chamber with adjustable scattering path length was designed. Two measurements of a scattering cross section were made with different, known, scattering path lengths. The two measurements were compared by a difference method such that the background correction was eliminated. In most cases it is not necessary to resort to such methods because it is usually possible to design a scattering chamber so that less than ten percent of the scattering occurs outside the chamber.

The measurement of the scattering gas density in a chamber is a matter of considerable importance. The elastic scattering cross section of atoms with thermal velocities is large (relative to fast atoms) so that the layer of scattering gas must be relatively dilute. The pressures which must be used fall generally into a region around 0.1 mTorr, where accurate measurements are difficult. The McLeod gauge is in common use, but for this pressure it tends to be large and bulky and therefore to some extent fragile. The pumping effect of the cold trap recently discovered[90] also can contribute serious error in this pressure range unless it is accounted for or suppressed.[91-93] Another gauge which has recently been widely employed is the diaphragm gauge. This gauge is composed of two chambers, one at a known pressure (usually zero), separated from the other by a thin diaphragm. As pressure moves the diaphragm, its displacement is picked up with a capacitative sensor. These gauges require no cold trap, are rela-

tively free of contaminants, can be readily calibrated, and the calibration is independent of gas species. Ionization gauges are sometimes used to measure the scattering gas pressure but their use is fraught with difficulties. They tend to be unstable, are difficult to calibrate, and must be calibrated individually for each gas used. Increasing the required scattering gas pressure by shortening the length of the chamber has only limited effectiveness since the decrease in path length only increases the importance of the background corrections.

The geometry of the scattering region must be tractable in order to interpret a scattering experiment. Tractability implies not only that the dimensions and locations of the apertures defining the beam and target be accurately known but that the exact dimensions of the region in which the interaction takes place also be known. The shape and dimensions of this region, here called the scattering volume, are necessary for interpreting a scattering experiment because those particles in a beam scattered into any arbitrary element of solid angle can originate from any point within the scattering volume, and any experiment involves an average over the finite dimensions of the beam.[94] Definition of the scattering volume for an attenuation experiment with fixed axial detector is usually straightforward. If, however, the experiment measures the differential cross section at varying relative angle, the scattering volume can not only become rather complicated geometrically, it must be differently defined for each scattering angle. Many ingenious scattering chambers have been designed to reduce the difficulties which arise from this problem.[23, 95,96]

The other common arrangement for scattering a beam is to cross it with another beam or jet of molecules. The density of scattering centers

in the crossed beam is determined by measurement of beam intensity in the same way as is done with the primary beam so that no pressure gauge is necessary. If a crossed beam experiment is performed at various relative orientations, the definition of the scattering volume becomes complicated, just as for the measurement of the differential cross section discussed above. In a few crossed beam experiments it is unnecessary to make quantitative intensity measurements so that variation of the scattering volume with angle is of no real consequence.

B. High-Energy Beams.

High-energy beams are formed by accelerating ions to the desired energy and collimating either mechanically as with thermal beams or with electric or magnetic focussing fields. Fast neutral beams are produced by neutralizing the accelerated ion beam in a gas-filled region where charge transfer can occur. Most of the following discussion concerns the details of ion beam experiments because clearly it is necessary to form an ion beam for both ion and neutral beam experiments. The few special features of neutral beam experiments are presented after the discussion of ion beams.

1. Production.

The development of ion sources has a history dating back more than fifty years. Most sources used in molecular beam research produce the ions in a discharge, usually either DC or radio frequency. A large number of different designs has been reported[97] which reflect the different requirements of various experiments. The two principal input considerations are power and gas flow efficiency; the output performance criteria are beam divergence, energy spread, total current, and internal

state of the ions. It is generally not possible to optimize all these parameters and a given experiment usually indicates which conditions are most important.

Collimation and focussing of the ion beam usually must be considered as parts of the design of the ion source. The principal problem involved in focussing intense ion beams is that of space charge dispersion; the usual solution is a combination of keeping the source-to-detector distance short and of using some form of focussing electrodes. The theory of ion optics in the presence of space charge[98,99] is only partially developed, so that most ion lenses which are used are operated with parameters chosen experimentally by performance tests. The difficulty of lens design is increased by the fact that the lenses must function in the presence of fringe fields (electric or magnetic) of the source which are difficult to estimate in advance, and that the ions are usually extracted from a plasma boundary whose shape and position are not stable.

Energy determination and selection are also considerations in the design of beam collimators. The energy distribution of ions extracted from most sources is not broad, as in thermal beam ovens. Generally speaking, there will be three species in the flux issuing from an ion source; thermal atoms, high-energy neutral particles, and high-energy ions, each of which will have different energy distributions. The thermal-energy atoms appear because the ion source is a gas-filled chamber with an exit slit and therefore acts as a thermal beam oven. Since the energy distribution of these atoms is nearly Maxwellian and peaked at an energy much lower than the high-energy particles or ions, the effect of this thermal beam can be eliminated by energy discrimination. The high-energy neutral

component of the beam flux arises from charge transfer collisions of the ion beam with atoms of the source gas during extraction of the beam. Since it is never certain where, in the acceleration history of the ion, the charge transfer event occurred, the energy distribution of this neutral beam is never known, and can be expected to depend strongly on the detailed design of each source. This neutral beam can be removed when desired, by a slight deflection of the ion beam with an electric or magnetic field. The energy distribution of the ion beam can be quite narrow, although the energy resolution achieved in electron guns[95] can never be reached. The ions are extracted from a plasma, a region where the pressure is high enough to ensure that collisions take place; and in addition, the ions are extracted from a finite region of the plasma where the potential distribution may be nonisotropic. A typical energy spread is a few electron volts in a source producing a beam of a few hundred eV and upwards.

The determination of the energy distribution of high-energy beams must be performed on the ion beam rather than the neutral component. Rotating disk selectors are usually of little use at high energies because the rotor speeds required are much too high to be practicable. However, measuring the ion current transmitted as a function of an applied retarding potential will determine the energy spread of the beam. Although conceptually straightforward, retarding potential analysis involves a number of difficult experimental problems.[100] It is common to use electric or magnetic fields, separately or in combination, as velocity selectors.[101,102] Since an electric field can be used to select an almost arbitrarily small range of energies, and magnetic fields can be used for selection of momentum, selection of both energy and momentum automatically selects a specific mass.

Magnetic selection involves use of a sector field deflector with entrance and exit slits. The size of the slits controls the resolution and clearly high resolution is obtained only at the expense of decreased intensity. Energy analysis with electric fields can be accomplished in a variety of ways. In the cylindrical electrostatic analyzer[103], a radial, inverse first-power electric field is established in the annulus between two cylindrical electrodes. In such a field, charged particles follow circular paths. If two particles with the same energy enter the analyzer with divergent angles, they will recross the axis at a point 127° with respect to the entrance point. A similar device is the spherical analyzer where the electrostatic field is established between concentric spheres, a configuration which provides focussing in two dimensions. The spherical analyzer,[104,105] especially the 180° deflection version, has been extensively used for energy analysis of electrons[106] but is only slowly being applied to the analysis of ions. An electric field applied between parallel plates can also be employed as an energy selector.[107] A beam of charged particles can be injected at 45° through a slit in the lower plate; the particles will follow parabolic trajectories between the plates, and those of a given energy will pass through exit slits some distance down from the entrance. A large variety of devices are available, many commercially, which perform velocity selection by a time-of-flight method.[102,108] The most commonly used technique is to accelerate a group of ions to a given energy and then observe a short pulse of these ions as it propagates down a drift tube. Ions with different velocities (which in this context means ions with different mass) arrive at the end of the drift tube at different times, and a measurement of current as a function of time will show a spectrum of velocities present in the ion

pulse. This technique is more useful for measuring a distribution of velocities than for selecting ions of a given velocity. Other time-of-flight methods are used regularly for velocity selection, however, such as radio-frequency spectrometers which can take many forms. One example is the Bennett[109,110] spectrometer in which two sets of fine mesh grids normal to the axis of ionic motion are alternately spaced. Radio-frequency accelerating voltages of opposite polarity are applied to each set of electrodes. If an ion with the proper velocity enters the system with the proper phase with respect to the radio-frequency field it will be accelerated during its flight between each electrode, while all other ions will lose synchronization with the field. A retarding potential grid placed as the last electrode can permit the passage only of those resonant ions which have received the maximum acceleration.

There is clearly a wide variety of techniques available for velocity selection or analysis of high-energy ion beams. Which method is used in a given experiment is frequently determined by intensity considerations. High resolution magnetic mass spectrometers require long path lengths and narrow slits and so inevitably provide low intensities. The radio-frequency spectrometer described above has quite a short length and no slits at all, but the fact that it does not transmit those ions with the resonant velocity whose entrance phase is wrong again results in poor beam intensities. For this reason the energy analysis is sometimes combined with beam detection, by using some form of mass spectrometer directly as a beam detector.[84] This is particularly attractive for experiments with neutral beams because it permits the neutralization of the beam at a short distance from the ion source, thereby minimizing losses in intensity due to space-charge effects. Although this advantage is partly offset by the

inefficiency of re-ionization in the spectrometer source, the method is still attractive. The method essentially amounts to performing an experiment in the presence of species which are unwanted or which have a wide variety of velocities by observing only the particles of interest. Frequently this is possible but in some cases the presence of unwanted species affects the interpretation of the experiment; in such cases the only recourse is to place the selector before the scattering chamber. Finally, it might be noted that some mass spectrometers, notably the radio-frequency quadrupole spectrometers,[111,112] perform their role well but completely destroy the beam collimation in the process of mass analysis. Such spectrometers are only useful as part of the detection system.

As indicated earlier, beams of neutral particles can readily be formed by passing the ion beam through a layer of the parent gas where a substantial fraction of the ion beam can be neutralized by resonant charge exchange.[113] The neutralization can be made to occur in a differentially-pumped chamber with beam entrance and exit slits or in a jet of gas which crosses the ion beam. If the density of the charge-exchange gas is large, the ion beam can be almost entirely neutralized; at such high densities, however, the neutral beam which is formed is significantly attenuated by scattering. The usual procedure therefore is to adjust the charge-exchange gas density until the neutral beam flux is optimized; the density so selected is such that the neutral beam intensity is about half the ion beam intensity.[114] The energy exchange in resonant charge transfer is very small, on the order of the ratio of the mass of the electron to that of the ion, so that velocity selection performed on the ion beam is essentially unchanged for the neutral beam which passes through the usual arrangement of axial collimating slits. The charge transfer process

also acts somewhat as a filter for impurities in the beam. The impurities will in general have different ionization potentials than the charge exchange gas; in that case, the non-resonant charge exchange cross sections are not only small, but the energy defect requires that the neutral particle in a non-resonant collision be deflected. It has been experimentally verified that passing an ion beam through a non-resonant medium results in low intensities and if the energy difference is large enough (for example, Ar^+ into He) no axial neutral beam is produced even though a substantial part of the ion beam is neutralized.[114] Another experimental verification of this phenomenon was obtained when a beam of helium ions, mass analyzed to show several impurity peaks, was neutralized in helium gas. The resulting He beam was mass analyzed and no impurity peaks were found.[115]

2. Detection.

The detection of fast ion beams is straightforward and usually provides no problems. Either the ion current is measured in a Faraday cup assembly or the ions are counted. The latter procedure has become more common recently as the elaborate electronic equipment developed in nuclear physics has become available. Direct measurement of ion currents is usually made only when the current levels are relatively high. Noise levels in electrometers are higher than in multipliers, and the electrometer time constant is longer so that it is difficult to follow transient phenomena. If either method is used it is necessary to assure that secondary electrons emitted at the collector electrode are not permitted to escape since this would result in a false measurement. The collecting electrode can be made long and deep, or fitted with internal

fins to assure that the secondary electrons do not escape, or a grid system can be placed in front of the collector to repel the secondaries back into the collector.[95]

The detection of neutral particles is more difficult but a number of techniques have been developed over the years. One powerful technique is the calorimetric measurement of the total beam energy.[21] Thus if the energy of the individual particles is known, the flux can be calculated. Calorimetric detectors have taken many forms; they usually consist of a mask, slightly larger than the beam, which is attached to a thermocouple, thermopile, or bolometer. In order to have high sensitivity they are constructed with very fine wires and are therefore rather fragile and tend to have long time constants. At least two types of thermal detector which are mechanically sturdy but still have reasonably high responsivity and short time constant have been reported. The Harris thermopile[116] has the disadvantage, for some experiments, that the detector sensitivity is not uniform over its surface. The thermistor bolometer[117] can be built with a time constant of only a few milliseconds, and is customarily operated in an AC mode by modulating the beam with a chopper wheel. This is done primarily to take advantage of the simplification of AC electronics rather than to distinguish the beam from the background gas. One of the greatest advantages of calorimetric detectors is that they automatically discriminate against the background gas. Interfering signals due to the presence of background gas are usually negligible because, although the background gas is present in concentrations much greater than that of the beam, the detector does not respond to it because its energy is so much lower than the beam energy.

Calorimetric detectors are also used to detect beams of atoms which

were formed from diatomic molecules.[118] Energies of several electron volts are released at the detector surface when the atoms recombine and this energy can be detected since its effect is to heat the detector. Since the atomic recombination energy is known, measurement of the detector signal can be converted into a value of the flux.

Other neutral beam detectors which have been devised provide a means for producing a number of charged particles proportional to the beam flux. The universal detector described in connection with thermal energy beams can be used for detection of fast beams but its efficiency decreases with increasing beam energy because the ionization probability is proportional to the transit time in the ionizer. Its use for fast beams is therefore rare. More common is the use of electron multipliers[51] in which secondary electrons, released on impact of the fast beam on the cathode, are caused to strike a series of subsequent electrodes where each impact produces more secondary electrons. It is possible to obtain gains in such instruments of 10^6-10^7; that is, that many electrons are produced at the anode for each electron released at the cathode. The most popular instrument currently in use is the Bendix magnetic multiplier[119] which is less sensitive than most multipliers to surface contaminants. A recent development, also due to Bendix,[120] is the channeltron which takes the form of a narrow tube whose inner surface is a high resistance, high secondary-emission material. A potential is applied along the axis of the tube and the fast beam is directed obliquely into the end of the tube. Secondary electrons released on impact propagate down the tube making zig-zag paths and releasing more electrons at each wall collision. This simple device produces very high gains and can be made extremely compact. Arrays of channeltrons can be assembled to probe the beam intensity.

Multipliers can be operated either as current measuring devices or as particle counters. In the current mode the multiplier can be used only for measurements of the relative beam intensity; determination of the absolute intensity from the measured current requires that both the overall gain and the secondary emission coefficient of the cathode be known, and neither of these can be obtained with accuracy. Operation in the counting mode is therefore more common because each incoming particle generates a pulse which can be counted accurately, so long as the secondary emission coefficient is greater than unity. Operation in either mode is affected at high intensities by saturation effects; for example in the current mode when the current carried by the multiplied electrons becomes comparable to the current in the dynode strip, the final stages of amplification are in effect shorted out. Discrimination against background gas signal is usually done by maintaining the multiplier in a separate, differentially pumped chamber where the pressure can be reduced to as low as 10^{-9} torr. Mounting the multiplier in such a separate low pressure chamber also reduces dynode contamination and subsequent gain deterioration. Discrimination against background gas can also be achieved by the traditional method of modulating the beam and switching the multiplier output into two scaling channels in phase with the beam modulation.[121] When operating in the counting mode, background discrimination can be accomplished by pulse height analysis. The low-energy background particles in general create much lower pulse heights than those associated with the faster beam particles and a discriminator can be placed before the scaler to reject all pulses below a certain height. It should be pointed out that multipliers are most useful at the higher beam

energies where they have high gains and relatively good background discrimination.

Other secondary electron detectors have also been built which employ a positively biassed electrode to collect the secondary electrons.[122] This detector has all the disadvantages of the multiplier without the advantage of producing high gains and so has not been widely used. Other, similar, detectors have been devised[122] in which the beam particles, or secondary electrons produced by the beam, are directed onto a phosphor in order to release photons which are detected with a photomultiplier. These devices have only been used to detect beams with very large energy.

3. Scattering.

The design of scattering chambers and the measurement of the pressure of the scattering gas are in general simpler for fast molecular beams than for thermal energy beams. The principal reason for this is the fact that the scattering cross sections for fast atoms are relatively small. Thus the gas pressure needed in typical fast beam attenuation experiments is of the order of 10 mTorr, whereas for a thermal beam experiment it might be a factor of a hundred or more lower. In fast beam experiments a variety of well-understood pressure gauges are available, such as null-diaphragm, Pirani, and McLeod gauges. At these higher pressures the error in McLeod gauge measurements caused by pumping of the cold trap is frequently negligible. McLeod gauges are usually the standard to which other gauges are referred, but such a calibration can in turn be checked against an accurate expansion system so that possible errors in the measurement of the pressure can be reduced to negligible levels. The smaller scattering cross sections for fast beams also result in less beam attenua-

tion in the ambient gas in the apparatus, and so experiments with fast beams present less severe constraints on the pumping system. As noted earlier, the correction which must be applied to account for the attenuation of the beam in the background gas is much simpler to calculate for fast beams than slow beams because it can be assumed that the scattering molecules are stationary, thereby eliminating the complex problem of including a velocity distribution of the target atoms.

C. Intermediate Energy Beams

Research with beams of intermediate energy, those with kinetic energies between about 0.5 and 25 eV, have been less fully developed than either the high energy or the low energy beams. For the most part, this is due to the much greater difficulty of producing beams in this energy range which are sufficiently stable (or reproducible), sufficiently monoenergetic to be useful for quantitative studies, and which in addition have adequate intensity. In large measure, the underdevelopment of intermediate energy beams must be attributed to the lack of interest in the past on the part of research workers in this energy range. Many methods of producing beams in this energy range have been investigated but at this time the experimental situation is far from satisfactory when compared to that for high or low energy beams.

1. Production.

The greatest expenditure of effort has gone into the development of nozzle beams. These beams have high intensities and can be manipulated to produce particles with energies between about 0.1 to 10 eV. The method substitutes for the Knudsen effusive source of thermal beams a supersonic jet produced by hydrodynamic expansion of a gas or suitable

gas mixture through an appropriately designed nozzle. The technical difficulties are many and great, but the prospect of producing beams of high intensity in a hitherto inaccessible energy range has spurred a large number of investigators to enter this field and to continue in it. One group of the many avid workers in this field has been Anderson, Andres, and Fenn, whose review articles[124,125] give a very detailed picture of the present state of the development of nozzle beams.

A recent approach[126,127] to the study of two-body collisions of heavy particles in the energy range from a few tenths of an eV to about 100 eV involves the simultaneous use of two fast beams traveling in the same direction along a common axis. The technique is referred to as the use of merging beams, superimposed beams, overtaking beams, or confluent beams. The method has several advantages. Two fast beams, each with laboratory energy of the order of one or two keV and a modest energy spread, say 1.5 eV, can be merged to produce interaction energies as small as 0.25 eV, or less, with a spread in the interaction energy of the order of 0.01 eV. The high energy of the fast beams minimizes loss of beam intensity associated with space charge divergence of ions extracted from sources. The detection problem is also comparatively easy since, in addition to detectors which can be used for both slow and fast beams, other detectors which are uniquely suited to fast beams can also be used. These include thermal detectors and secondary electron emission detectors with or without particle multiplier features. Particle counting detection may also be used. It is worth mentioning that if a single source is used, only ion-neutral interactions can be studied by the merging beam technique. This is achieved by partial charge transfer of the original ion beam to produce a mixed ion-neutral beam and then retarding the ion beam component

to achieve the desired difference in energy and accordingly, the desired small interaction energy. If two sources are used, the ions from each source can be used to obtain neutral beams by charge transfer and, after removal of ions which have not been neutralized, interactions between the two neutral beams may be investigated. A review of the rather small amount of research completed thus far with merging beams of heavy particles has been published.[128] That article describes the method, explains the theory, indicates the type of collision processes for which the technique is suitable, and cites references to published results.

Recently a new method was described for producing beams of potassium with energies in the approximate range of 0.25 to 50 eV.[129] This method, which had also been independently investigated at Freiburg[130], uses an ion source such as a uno-plasmatron to focus a beam of ions, usually Ar^+ or Xe^+ with energies of 5 to 30 keV, on a potassium surface. Neutral potassium atoms are sputtered from the bombarded mass of potassium metal to form a beam which has an approximate cosine-squared distribution and is peaked in a forward direction which is determined by the angle at which the ions impinge upon the potassium surface. By use of velocity selectors, collimated beams of small energy spread and good intensity are obtained. The method has reached the point where it can be used to obtain total scattering cross sections which appear to be of the right magnitude and energy dependence. It appears, therefore, that the technique is well on its way to becoming a useful tool for producing beams in the intermediate energy range. It is interesting to observe that in principle, and probably in practice, the sputtering source can be used to produce beams of intermediate energy from a wide variety of materials, conductors as well as

non-conductors. In the case of non-conductors the charge that would build up as the ions impinge on the substrate (and which, if not eliminated, would eventually repel the fast ions from the plasmatron source) could be prevented from forming simply by having a source of electrons close to the substrate. Although these electrons could be swept across the surface of the non-conductor, it appears that all that is required is that they be close to the surface that would otherwise build up a charge. Additional experimental details of this cathode sputtering method have been recently published.[131]

The use of a shock tube as a high temperature thermal source for the production of a molecular beam has been under investigation for some time[132]. Since it is possible to raise the temperature of a shocked gas to several thousand degrees, a source of this type usually produces a beam with an energy of a few tenths of an electron volt. Although it is possible to increase this energy by producing stronger shocks, this procedure introduces difficulties which are associated with production of a mixed beam which may contain one or more of the following species: ground state particles; dissociated atoms or free radicals; excited and metastable atoms or molecules of the original gas or its dissociation products; and ions. However, an interesting application of shock tubes has been made which produces beams with an energy or about 1 eV and minimizes the difficulties introduced by extremely strong shocks.[133-135] The method uses a conventional shock tube source whose shocked gas, heated only to several thousand degrees or less, is then hydrodynamically expanded to produce a nozzle beam similar to that described above.

The use of a shock tube as a primary source or as a source for a nozzle

beam has an inherent disadvantage in that it is a pulsed experiment. This disadvantage not only restricts the time available for actual useful experiments, but also greatly increases the difficulty of obtaining reproducible results. Nevertheless, the inclusion in this review of the technique of using shock tube sources for producing molecular beams is an interesting example of the ingenuity that has gone into the development of sources for molecular beams in the intermediate range of energy.

It was pointed out earlier that multi-pole fields can be used for state selection and focusing of molecules with permanent magnetic or electric moments. However, this method is applicable only for molecules in states that gain energy with applied external field. Another apparatus has been designed and built[136] which is applicable to situations where there is either a gain or loss in energy. The apparatus, which may be regarded as a linear accelerator for neutral molecules, operates as follows.

In its present form it uses 700 stages of dipole accelerators, and for molecules with a large dipole moment such as LiF there is a gain of about 3 meV at each stage so that at the completion of the acceleration a beam with a kinetic energy of about 2 eV is obtained. At one end of the apparatus dipolar molecules drift into an electric field produced by a pair of carefully aligned electrodes and are accelerated into the gap between the electrodes. At this moment the field is turned off and the dipoles drift toward the next pair of electrodes. The field is then turned on again and the dipolar molecules are further accelerated. The process is repeated until an intermediate energy neutral beam emerges from the last pair of electrodes. At this time the apparatus is complete

and the difficult task of aligning the 700 pairs of electrodes, which extend over a length of more than 30 feet, is in progress. A brief description of the apparatus is contained in a recent review article.[137]

Another example of the specialized apparatus developed for the intermediate-energy range is the scheme to form a pulsed beam of intermediate energy by mechanical acceleration. The procedure involves accelerating a gas sample contained in a hollow projectile by firing it from a rifle or light gas gun, and when it reaches the desired velocity, releasing the gas sample which expands downstream with a velocity which is the sum of its average thermal velocity and the projectile velocity. Calculations[138] indicate that the projectile can be accelerated without substantial heating of the gas inside, and, because the gas sample can be loaded at a very high pressure, very large intensities can be expected. Research performed thus far has not produced a molecular beam system, but it has been shown that it is possible to accelerate gas-loaded projectiles to high velocities, open them in flight, and observe the subsequent expanding gas cloud as it moves down range[139]. The problems which remain before this device can be developed into a useful molecular beam system are many and difficult. It is not yet certain that it will ultimately be a usable tool for molecular beam research.

It is apparent that the intermediate-energy range experiments present difficulties primarily in the matter of formation of the beam. Procedures for collimation, detection, and provision for scattering the beam can be taken directly from the techniques already established in high or low energy experiments. Because so much effort has been expended merely to develop new methods of beam formation, only a few experiments performed with intermediate-energy beams have been reported.

IV. Results

Molecular beam research has been carried out for over fifty years. In that time an immense number of experiments have been performed and the results reported. To give even a representative sampling of this work would be such a formidable task that in this section only a few examples are selected to illustrate the kind of information that can be obtained from elastic, inelastic, and reactive scattering. The elastic scattering section will be separated, as before, into three regimes on the basis of energy.

A. Elastic Scattering

1. High-Energy Scattering

The most important property of high-energy molecular beams is their ability to probe the intermolecular potential at close distances of molecular approach, thus supplying information that is almost unattainable by other means. The range of beam energies is roughly 25 to 10^4 eV; at such energies the scattering is very strongly peaked in the forward direction, and the preferred procedure is therefore to measure the integrated cross section $S(\theta_o,\varepsilon)$ rather than $\sigma(\theta,\varepsilon)$, using a small value of θ_o.

Two detailed reviews of high-energy molecular scattering have appeared,[21,140] which pay particular attention to the technical problems involved in the inversion of the scattering data to obtain intermolecular potentials. In one respect the inversion problem is simple, because classical mechanics furnishes an adequate description of the scattering, and because the potentials are usually satisfactorily represented as single monotonic repulsions in the region probed by the scattering. For such a monotonic repulsion, all scattering angles are monotonic and Eq. (7) can be transformed to a power series in the energy

$$\theta(b,\varepsilon) = \sum_n a_n(b)\varepsilon^{-n} \quad . \tag{39}$$

For large energies and small angles, the series in Eq. (39) can be truncated after one or two terms for sufficient accuracy. If an algebraic form for the potential is assumed the coefficients $a_n(b)$ can be evaluated and the series inverted to obtain the impact parameter, and then through Eq. (6), the cross section $S(\theta_o,\varepsilon)$ corresponding to the angular aperture θ_o. As an example, for the inverse power potential, $V(r) = Kr^{-s}$, the first term in the series gives

$$S(\theta_o,\varepsilon) = \pi(KC/\varepsilon\theta_o)^{2/s} \tag{40}$$

where

$$C = \sqrt{\pi}\ \Gamma\left(\frac{s}{2} + \frac{1}{2}\right)\Big/\Gamma\left(\frac{s}{2}\right). \tag{41}$$

When necessary, higher terms in Eq. (39) can be evaluated resulting in additional terms of powers of θ_o in Eq. (40). Equation (39) has also been evaluated for the exponential and the screened coulomb potentials.[114] As indicated in the Introduction, the experimental value of $S(\theta_o,\varepsilon)$ represents an average over the dimensions of the beam and detector because an attenuation experiment involves scattering over a range of angles. Considerable care is needed to take account of such instrumental effects. When this has been done properly the potential parameters can be deduced by comparing Eq. (40) with the experimentally determined cross sections.

The two reviews[21,140] cover most of the work through 1964, which emanated largely from M.I.T.; several subsequent papers have by now appeared.[114,141-144] Recently Leonas and coworkers in Moscow have initiated a similar research program,[145-150] and their results provide valuable corroboration and extension of the M.I.T. work. Results published to date from both M.I.T. and Moscow include the five noble gases and their ten

possible unlike pairs, plus the systems He→(H_2,D_2, N_2, CH_4, CF_4), Ar→(H_2, N_2, O_2, CO, CH_4), H→(He, H_2, N_2, O_2), N→(N_2,O_2), O→(N_2, O_2), N_2→(N_2, O_2), H_2→H_2, and O_2→O_2. A number of other systems have been reported in conference proceedings[151,152] and reviews,[21] but not yet published in detail.

An impression of the general level of consistency and reliability of potentials obtained from high-energy elastic scattering can be gained from Figs. 9 and 10, where various results for He-He and Ar-Ar are compared.

The He-He system is probably the single system most thoroughly investigated, both experimentally and theoretically. The results of four separate high-energy scattering investigations[114,145,153,154] using four different apparatuses are shown in Fig. 9; the consistency is quite good. Perhaps more important is the agreement with potentials obtained by entirely different experimental methods. Figure 9 also shows potentials obtained from analysis of high-temperature thermal conductivity data[155] and from analysis of viscosity and second virial coefficient data.[156] Although these do not overlap the scattering potentials, they are close enough to show that there is a high degree of consistency. Also shown in the figure are the results of two accurate ab initio quantum-mechanical calculations.[157,158] The only empirical information used in these calculations are the numerical values of Planck's constant and the charge and mass of the electron. Here the agreement is a little poorer, but within the estimated uncertainties of the calculations and the experiments.

The Ar-Ar results are shown in Fig. 10. Again four different scattering investigations are shown.[143,145,159,160] The overall consistency is quite good, although the Moscow results seem high at their largest

separation distances. No accurate quantum-mechanical calculations are available for a system with such a large number of electrons, nor are enough accurate high-temperature gas data available for argon to permit the additional comparisons shown for helium. However, a potential valid at small separations has been deduced for argon from the results of shock compression of the liquid,[161,162] and this is shown in Fig. 10. The agreement is remarkably good.

The validation of the absolute accuracy of the high-energy scattering potentials is so important that it is worth mentioning comparisons with the few other available accurate quantum-mechanical calculations. The most accurate other calculation is probably the recent one on H-He by Fischer and Kemmey.[163] These are in excellent agreement with the M.I.T. scattering results[164] (but the Moscow results[150] are inexplicably low). Results of more difficult calculations are available for the more complicated systems He-H_2 [165] and He-Ar,[166] and the agreement with the experiments[142,143,145] is satisfactory.

Although a number of potentials have been determined by high-energy scattering, the amount of direct information available seems meager indeed in comparison with the variety and complexity of most chemical systems. It is therefore important to see whether it is possible to predict potentials for unknown complicated systems from those for simpler known systems. Only in this way is there any hope that molecular beam results will be of much chemical use in the near future.

The simplest type of prediction is the calculation of a third noble-gas potential, from two known noble-gas potentials. An example would be the prediction of the He-Ar potential from measured He-He and Ar-Ar potentials. It happens that a geometric mean combination rule works

surprisingly well,

$$V_{12} = (V_{11}V_{22})^{1/2}. \qquad (42)$$

The basis for such a relation is discussed in a recent review.[167] The theoretical reasons are not very strong, and the relation should be regarded as mainly empirical. It has been tested by direct experiment a number of times, however; the most extensive tests have been in fact for He-Ar, and these results are shown in Fig. 11. The dashed curve shows the combination-rule prediction based on the results for He-He and Ar-Ar shown in Figs. 9 and 10; the solid curves represent three direct scattering measurements[143,145,168] plus one potential based on high-temperature diffusion measurements.[169] The agreement is very good.

The prediction procedure for interatomic potentials becomes much more complicated if free atoms having incomplete electron shells are involved. Here one must deal not with a single potential for each pair of atoms, but with multiple potentials corresponding to all possible molecular states involved. For instance, two ground-state hydrogen atoms can interact in either of two ways, depending on whether their electron spins are parallel or antiparallel, and two ground-state nitrogen atoms can interact in four different ways. In such cases it is necessary to invoke more elaborate molecular quantum mechanics in order to generate combination rules. This has been done with fair success, but the results are not of much direct interest yet in chemical applications, where it is seldom necessary to consider the interaction between two free valence-unsaturated atoms. At any rate, a recent review is available.[167]

Of perhaps more chemical interest are interactions between an atom and a molecule, between two molecules, or between separate parts of large

molecules. The same theoretical ideas used in the treatment of free valence-unsaturated atoms lead to the idea that each atom can be considered a separate source of potential, and that the potential between two molecules can be approximated as the sum of all the atom-atom potentials acting between the two molecules.[167,170] Empirical evidence for this idea comes from some of the beam-scattering results. For instance, the interaction between an Ar atom and a CH_4 molecule was found to be better described as the interaction of the Ar with the peripheral H atoms than as the interaction with a single central potential.[141] Such an approximation opens up immense possibilities, for the geometric rule of Eq. (42) should apply to the effective atom-atom potentials if there is no correlation between their electron spins, as there is not if one or both of the atoms is bound as part of a molecule. Thus a few good beam measurements on relatively simple systems would be a sufficient basis for the calculation of interactions between rather complex molecules of chemical interest.

The subject has not yet progressed that far, but a promising beginning has been made. As an illustration, the Ar-O_2 and Ar-Ar measurements can be used to predict the Ar-O, O-O_2, and O_2-O_2 potentials, all of which have been measured independently. Details can be found elsewhere,[21,144] but the general procedure is as follows. The Ar-O_2 potential, averaged over all molecular orientations, is obtained from the scattering of a high-energy Ar beam in O_2 gas; from this the effective Ar-O potential is deduced. Combination of the Ar-O potential with the measured Ar-Ar potential according to Eq. (42) then yields an effective O$\cdots$O potential corresponding to no correlation of electron spins; this may be built up into O-O_2 and O_2-O_2 potentials, which can be averaged over all molecular orientations for comparison with directly-measured beam results. In Fig.

12 the predicted potentials[144] for Ar-O, $O-O_2$, and O_2-O_2 are compared with the measured[148,149,151] ones. The agreement is fair for $O-O_2$ and remarkably good for Ar-O and O_2-O_2.

Thus the prospects at present seem good for the application of high-energy beam potentials to problems of chemical interest. Five areas where information on short-range potentials would have direct application are as follows:

(1) High-temperature gas properties.

(2) Vibrational relaxation.

(3) Radiation damage.

(4) Hot-atom chemistry.

(5) Conformational analysis.

A few comments on each of these areas follow.

The previous discussion suggested that a direct and obvious application of potential-energy information is the calculation of gas properties at high temperatures. Such properties are needed for a full understanding of many phenomena in upper-atmosphere physics and chemistry, combustion, detonation, high-speed gas dynamics, and similar fields. The first application of beam potentials to such calculations was only in 1958.[171] Much work has been done since then, and reviews are available.[172]

The interchange of vibrational and translational energy requires energetic collisions, even at room temperatures, and potentials at close distances of approach are involved.[173] Such vibrational relaxation is important in determining the absorption and dispersion of sound in gases, as well as the fate of the energy stored in vibrationally "hot" molecules.

Radiation damage frequently causes the formation or deposition of gas

atoms in crystal lattices. The rate at which these atoms can escape is controlled in part by the short-range forces between them and the atoms of the lattice. A similar situation arises in connection with the problem of the behavior of solutions of gases in solids.[174,175]

Hot-atom chemistry obviously involves high-energy collisions in a direct way.[176,177] A central problem, for example, is the determination of the energy losses of hot atoms by collisions with inert moderator gas. The potential energies involved in such collisions are in the range where molecular-beam information would be appropriate.

The geometric conformation of a complicated molecule is of fundamental importance to its chemical and physical behavior.[178] The conformation is dependent on the potential energy of interaction of nearby nonbonded atoms, and in many cases the short range repulsions are important. Here information from molecular beam experiments would be most helpful, for the usual extrapolations of potentials into the short-range region are notoriously unreliable. The first attempt to use molecular-beam information in conformational studies was restricted to the calculation of barriers to internal rotation and energy differences of rotational isomers for small molecules.[179,180] For larger molecules, such as polymers, polypeptides, and proteins, many nonbonded interactions are involved and computers are necessary, but the basic potential energy information is still required. Conformation calculations have become an active research subject in recent years,[181,182] but little use has yet been made of relevant molecular beam results.

2. Low-Energy Scattering

Thermal energy scattering experiments probe the intermolecular potential at large distances of molecular approach, the beam energies being

generally much less than 0.5 eV. At these distances the potential energy has both attractive and repulsive components and is not monotonic as at close distances of approach; instead it is attractive at long range and repulsive at shorter range, with an attractive well in between. The measured cross sections for such potentials do not show the smooth behavior in energy or angle that occurs with high-energy beams, but tend to have more structure. Such structure may also depend strongly on the fact that the de Broglie wavelength of the relative motion is not negligible compared to molecular size. Of course a measured curve with structural features contains more information than a smoothly varying one, and so rather detailed potential information is often obtainable from thermal energy scattering measurements.

Two excellent reviews on the determination of intermolecular potentials from thermal energy molecular beams have recently appeared,[22,183] and the discussion will therefore be confined to some remarks about the major features of the observed cross sections, the type of information on the potential that is obtained from those features, and some applications of the results.

Because the peaking of the scattered intensity in the forward direction is much less pronounced at low energies than at high, it is possible to make measurements of the total scattering cross section S(0). It is possible to construct an apparatus with aperture θ_o near enough to zero so that most measurements of integrated cross sections are therefore essentially equal to total cross sections. Total cross sections probe the outermost fringes of the potential field, and always require quantum mechanics for their interpretation. The reason is that a long range force that nominally extends to infinity always gives an infinite S(0) in a

classical description, for a slight deflection is produced by any encounter, no matter how distant. The uncertainty principle of quantum mechanics limits the size of an observable deflection and leads to a finite value of S(0) when the proper quantum treatment is carried out.

A convenient criterion for determining when quantum mechanics must be used can be written in terms of the scattering angle. When this angle is smaller than a critical angle which may be written as[140]

$$\theta_{crit} \sim h/2\mu v r_c \tag{43}$$

the scattering must be analyzed with quantum mechanical methods.

For a potential of the form

$$V(r) = -C_s/r^s \ , \tag{44}$$

in which C_s is a constant, the total cross section is

$$S(0) = p(s)(C_s/\hbar v)^{2/(s-1)} \ , \tag{45}$$

where p(s) is a constant whose value depends on s. For many systems the longest range component of the potential is the London dispersion energy corresponding to s = 6. A large number of London C_6 constants have been measured in this way; Bernstein and Muckerman[183] give a comprehensive tabulation. Measurements of $\sigma(\theta,\varepsilon)$ at small angles also give essentially the same information.

The total cross section is determined by the distance r_c at which a grazing collision occurs which just produces "zero" direction within the meaning of the uncertainty principle. Another class of collisions also produces zero deflection. In these collisions the distances of closest approach are less than r_c. The trajectory is warped from a straight line by both attractive and repulsive forces, but their effects compensate each

other and no net deflection is suffered. Such trajectories are called glory trajectories after an analogous optical phenomenon.[26,184] Waves following the glory trajectories have different phase shifts than those following the grazing trajectories; the resulting wave interference produces undulations of S(0) vs. v about a smooth curve. These undulations have been analyzed in considerable detail.[183] Their spacing essentially gives the area of the attractive well of the potential, and their total number gives the number of bound states that the well can accommodate; information from these glory undulations of S(0) thus complements the information from the absolute magnitude of the average S(0). Most of the important features of this type of scattering can be understood without detailed mathematical analysis through the use of optical analogies.[185]

If the beam energy is somewhat larger than the depth of the potential-energy well, a large intensity of scattered particles will appear near some angle θ_r.[25,26] This is called rainbow scattering by analogy with the well-known optical phenomenon. It occurs whenever there is a minimum in the deflection angle as a function of impact parameter, since trajectories from many different impact parameters around the minimum all emerge at nearly the same angle. In classical terms, $\sigma(\theta,\varepsilon)$ becomes infinite whenever $d\theta/db = 0$, as Eq. (5) clearly shows, but the rainbow scattering is always substantially modified by wave interference (quantum) effects. These not only modify the shape of the rainbow, but cause it to break up into an interference pattern consisting of the primary rainbow plus a set of weaker peaks known as supernumerary rainbows.[186] An example of rainbow scattering is given in the next section.

The angle θ_r at which the primary rainbow occurs depends primarily on

the well depth and the kinetic energy, and only secondarily on the detailed shape of the potential well. The spacing of the supernumerary rainbows depends primarily on the ratio of the de Broglie wavelength to the distance at which the potential well has its minimum, and only secondarily on the shape of the well.

Other interference phenomena also occur in thermal energy scattering, and are discussed in various reviews.[22,26,28,167,183] The important point is that thermal-energy beam scattering gives information on the part of the potential around the attractive well, and outwards. In some ways this is less useful information from a chemical point of view than information on the short-range potential, for most of the interesting chemistry involves rather energetic collisions. Direct applications would probably include only gas properties and conformational analysis. Nevertheless, much of our chemical intuition about molecular interactions is based to some extent on what we know about the potential energy near the attractive well, so the indirect contribution is not to be slighted, even though much of this knowledge in the past came from studies of bulk properties, before the emergence of thermal-beam scattering as a research tool.

3. Intermediate-Energy Scattering

The energy range from about 0.5 to 25 eV involves extreme experimental difficulty, and what little knowledge we have comes mainly from interpolation between high energy and thermal energy results. This is most unfortunate from a chemical point of view, for much interesting chemistry occurs in this energy range. Most of the experimental effort to date has gone into the development of nozzle beams, merging beams, or sputtered beams, all of which are discussed in the section on Experimental Methods. So far almost no results of chemical interest have

emerged, for the experimental techniques are still under development. No great theoretical surprises are anticipated even if the techniques are eventually successful, and the major contribution is expected to be in the form of quantitative information.

B. Inelastic Scattering

The performance and interpretation of inelastic scattering measurements are more difficult and less highly developed than in the case of elastic scattering. This is unfortunate, although understandable, because inelastic collisions would be expected to be more characteristic of chemical reactions than of elastic collisions. At present only a few comments will be offered on the available studies of rotational, vibrational, and electronic excitation by molecular beams. The nature of the discussion will be different than that for elastic scattering because there is no particular aspect of inelastic scattering that is generally applicable to all experiments. Furthermore, there has not as yet been any significant effort to extend the results to chemical problems.

Experimentally, the inelastic process which is most readily detected is ionization. Although ionization of neutrals by neutrals has been studied over a long period, the center-of-mass energy in such studies has generally been in the kilovolt range. The result of these high energy ionization experiments has been reviewed in a number of articles and books[113,187]. A few years ago, however, some careful measurements were reported in which parallel plate collectors were used for slow charge collection, which showed that neutral beams of N_2 or O_2 could ionize N_2 or O_2 at center-of-mass energies not far removed from their ionization energies.[188,189] In fact, extrapolation of these measurements indicates that the threshold for the ionization process is the same as that for

ionization of these molecules by electrons. A similar result has been obtained more recently for the Ar-Ar system by using a cylindrical ion collector with appropriate grids for suppressing secondary electron emission.[190] In this case the measurements indicate a threshold, in center-of-mass energy units, of about 15 eV which is very close to the ionization potential of argon. Similar results have been cited for other systems in recent conference reports and in private communications.

Inelastic scattering which produces changes in rotational and vibrational energy has also been reported recently. The use of an inhomogeneous electric or magnetic field for selecting and focusing polar molecules has been used to measure cross sections associated with changes in the (j,m) states of LiF.[191] By using time-of-flight analysis to determine energy losses of velocity selected beams of K atoms, the rotational de-excitation of ortho deuterium according to

$$K + o\text{-}D_2(j=2) \rightarrow K + o\text{-}D_2(j=0)$$

has been observed.[192] Larger changes in rotational energy have also been reported[193] wherein a K-CO_2 crossed-beam system was used and rotational excitation was detected corresponding to J changes between 8 and 24. These experiments also confirmed the presence of intermediate complexes produced by "sticky" collisions, as reported earlier[194] on the basis of a difference between the observed angular distribution of K atoms and that which would be expected for purely elastic scattering. By proper choice of the projectile and target and the range of energy, it was found possible to excite either rotation or vibration.[195] For example, Ar^+ ions scattered in H_2 produced only rotational excitation; O^+ ions in O_2, only vibrational excitation. The excitation was detected by careful retardation

measurements of the primary ions.

Observation of vibrational excitation in H_2, without evidence for rotational excitation, has also been observed in scattering experiments with Li^+ ions having energies between 10 and 50 eV.[196] Time-of-flight techniques were used to determine energy loss and excitation of several vibrational levels of H_2 was observed. Similar time-of-flight techniques are currently being used[197,198] in the scattering of beams of K^+, Na^+ and Cs^+ into several different target gases, H_2, D_2, He^4, and He^3 at center-of-mass energies as high as 35 eV. When helium was used as the target gas, no inelastic scattering was observed, but in the case of H_2 and D_2 vibrational excitation, dissociation, and electronic excitation of the dissociated atoms could be inferred from the energy-loss spectrum.

A rather different approach was used[199] to obtain indirect evidence of rotational excitation. In a study of the scattering of beams of He atoms with energies up to 2 keV by hydrogen isotopes, the total scattering cross sections for H_2 and D_2 were found to be identical and in good agreement with elastic cross sections computed from the theoretical He-H_2 potential.[165] The He-HD cross section was somewhat larger than expected, and application of perturbation theory[200] showed that the enhancement was consistent with rotational excitation of HD.

Finally, a particularly interesting example of the transfer of internal energy in molecular collisions is found in a chemiluminescence study.[201] Beams of potassium atoms and bromine were crossed to produce vibrationally excited $KBr^{\ddagger}$ according to the reaction

$$K + Br_2 \rightarrow KBr^{\ddagger} + Br.$$

The vibrationally excited $KBr^{\ddagger}$ was then reacted with sodium in a triple-beam arrangement to produce electronically excited K^* according to the

rearrangement reaction

$$KBr^{\ddagger} + Na \rightarrow K^* + NaBr.$$

As the electronically excited K* decayed to the ground state, radiation was emitted and detected by a photomultiplier.

C. Reactive Scattering

The results of reactive scattering need not be separated into energy regimes because most experiments are done at thermal energies or slightly higher. Many reactive scattering experiments have been performed since the original one of Taylor and Datz.[73] Several review articles which discuss such experiments are available.[18,19,202,203] In general, differential cross sections for reactive systems can be expected to show structure, both because a chemical reaction has occurred and because of the effects of scattering by a non-monotonic potential. Such structure is indeed observable experimentally under the right circumstances. For example, it was pointed out above that the discontinuity in the differential cross section at the rainbow angle as predicted on the basis of classical arguments is actually not a sharp discontinuity but a rather broadened peak. In addition, it was noted that the rainbow angle depends on the relative velocity, and therefore the effects of rainbow scattering are generally not discernible without velocity selection, since each initial relative velocity is associated with a different θ_r and the fine structure in the differential cross section will be washed out by the overlapping rainbow angles if the spread of initial relative velocities is too broad. This is just a sample of the rather specialized experimental conditions which must be met in order to obtain useful information concerning reactive scattering. Almost every experiment requires its own

specific arrangement, but such details will be mostly excluded in the following discussion. The results of four particular crossed beam experiments are discussed, primarily in terms of the interpretation of the measurements; the experimental details can be obtained from the original papers or from one of the indicated review articles. The first example is a rather special case which illustrates many of the essential features of interpreting reactive scattering experiments. The other three which will be discussed are specific reactions illustrating different types of mechanisms by which reactive scattering processes may occur. Although there are semantic differences in the characterization of these three types, there is general agreement concerning the features by which the mechanisms can be identified. The categories used here appear elsewhere under either identical or closely related designations.[19,204,205] The mechanisms will be discussed in terms of the prototype reaction

$$A + BC \rightarrow AB + C$$

with appropriate specific illustrative examples.

1. Special Example.

The first example is

$$K + HBr \rightarrow H + KBr.$$

This system has several of the special features previously discussed, such as a small value of ΔD_o^o and a ratio of μ/μ' which is much larger than unity. The reaction was the subject of the first significant experiment on reactive scattering with crossed thermal beams. It was originally studied by Taylor and Datz[73] and the results of these first measurements were later reinterpreted by Datz, Herschbach, and Taylor.[46] Collimated beams of K effusing from an oven at temperatures between 541° and 837°K intersected

at 90° non-collimated cones of HBr which effused from a source kept between 373° and 400°K. Surface ionization detectors were used to monitor the fluxes of K and KBr in a manner that made it possible to distinguish between them, since both K and KBr are surface ionized by tungsten whereas platinum surface ionizes K but is essentially insensitive to KBr.[73-75] By taking the difference between the positive ion currents produced by the two types of detectors, the flux of product KBr was measured as a function of angle with respect to the K beam in the laboratory plane, that is, the plane defined by the direction of the K beam and the normal to the source from which the HBr effused. Because $\mu/\mu' >> 1$ and ΔD_o^o is small (about 3.8 kcal/mole), the KBr product is expected to be distributed in a fairly small cone near the centroid. However, Eq. (32) shows that there will be a different centroid for each pair of velocities in the reactant beams. Neither beam was velocity-selected in this experiment, so that the product KBr was actually distributed over a range of centroids. The experiment could only be analyzed by an elaborate calculation of the distribution of KBr, which required the use of a number of relevant experimental details as well as an assumption about the energy dependence of the reaction cross section. The threshold energy for reaction, E_a, was carried as a parameter in this calculation and the best agreement between the experimental and calculated distributions of KBr was found for $E_a \cong 3$ kcal/mole.

Beck, Greene, and Ross,[48] in a reinvestigation of this reaction, used a velocity selector to obtain a very nearly monochromatic beam of potassium. The introduction of velocity selection has several advantages among which is the partial elimination of the spread of centroids and a more precise determination of the threshold for reaction. Further, a great

deal of additional microscopic information can be obtained that is inaccessible when velocity selection is not performed.

The velocity selection of the K beam was such that if v_A was the maximum in a narrow band of selected velocities, the spread in velocity at half height was $0.084v_A$. The HBr beam was not velocity selected but effused from a thermal source at T_B. The initial average kinetic energy of the system was taken as $\bar{\epsilon} = \mu(\bar{v}_A^2 + \bar{v}_B^2)/2$ where $\bar{v}_B = (8kT_B/\pi m_B)^{1/2}$. The distribution of the KBr product flux was measured and from this, after a rather involved analysis of the spatial distribution of the reactant HBr, the total cross section for reaction S_R was obtained. It was found that the threshold energy E_a was quite low, less than 0.4 kcal/mole, and that for values of $\bar{E}$ larger than this threshold the total cross section for reaction $S_R(E)$ was essentially independent of the initial kinetic energy of relative motion. The discrepancy between this low value of E_a and that reported in the earlier experiment simply reflects the improvement possible with velocity selection of the beam.

In the same study, it was possible to obtain information about the reaction probability. The reaction probability that was determined was a special case of $P(k,\ell,i,j,p,b,\phi)$ first introduced in Eq. (20). In this experiment, the probability was not completely specified since there was no state selection, no velocity selection of the HBr beam, and the flux was measured only as a function of θ. Accordingly, the reaction probability was designated as $P(\bar{E},\theta)$ and the method used to obtain it was as follows.

The differential elastic cross section $\sigma(\bar{E},\theta)$ was measured as a function of θ. Measurements were also made of $\sigma(\bar{E},\theta)$ as a function of θ for the non-reactive analog of K + HBr, namely, K + Kr.[206] The experimental

determination of $\sigma(\overline{E},\theta)$ as a function of angle for a given value of the initial average kinetic energy of relative motion is straightforward. It requires measurement of the initial axial intensity of the beams of K atoms and the scattered flux of K atoms at selected laboratory angles associated with corresponding values of θ. The ratio of the off-axis flux to the axial intensity is the differential cross section for a given value of $\overline{E}$ and θ. For K + Kr the results for three different values of $\overline{E}$ are shown in Fig. 13 and the results for K + HBr for five different values of $\overline{E}$ are shown in Fig. 14. Although the ordinates in both figures are in arbitrary units, it is apparent that the scattering patterns of the two systems show qualitative similarities in that each curve shows a sharp decrease at very small angles, and a well-defined peak. The peak is that due to rainbow scattering as discussed previously. It was pointed out earlier that structure in the differential cross section is generally not observable without velocity selection. That it is so clearly observable in these two systems in which only the potassium beam was velocity selected is in part the result of suppressing the spread in the initial relative velocity. This was accomplished by having the Kr and HBr, both of which are heavier than K, effuse from sources which were lower in temperature than the K source. Thus the value of $\overline{v}_B$ for Kr or HBr was lower than the rather well-defined selected velocity v_A for K. Furthermore, an intersection angle of 90° as opposed to a larger angle further reduced the spread in v, although this effect was of secondary importance. The influence of the angle of intersection on the spread in the initial relative velocity has been analyzed by Pauly and Toennies.[22]

It can be assumed in analyzing the results shown in the figures that

the molecular interactions were a combination of central finite repulsive and attractive forces for which the two dimensional trajectory could be represented as shown in Fig. 5. The potential energy function associated with the trajectory was the so-called exp-6 potential which can be written as

$$V(r/r_m) = \frac{\varepsilon_m}{1 - 6/\alpha} \left\{ \frac{6}{\alpha} \exp \left[\alpha(1 - r/r_m) \right] - (r_m/r)^6 \right\} \qquad (46)$$

where r_m is the position of the potential minimum and ε_m the magnitude of its depth. Inversion procedures have been developed which permit the parameters ε_m and r_m in Eq. (46) to be evaluated (at least for the non-reactive system). The procedures utilize the position of θ_r and the negative slope of $\sigma(\bar{E},\theta)\sin\theta$ vs θ; details have been described by a number of investigators.[22,202,207,208]

The two most striking qualitative features about the differential cross section for the reactive system in Fig. 14 are the similarity to the non-reactive system at angles smaller than θ_r, and the distinct difference at large θ where $\sigma(\bar{E},\theta)\sin\theta$ is seen to decrease much more rapidly than for K - Kr. The latter behavior can be attributed to the chemical reaction. In general scattering near the relatively small angles near θ_r is not affected by chemical reaction. Accordingly, potential parameters can be obtained from the differential cross sections in the region near θ_r by the same inversion procedure used for the non-reactive system. (The significance of the shift of the rainbow scattering to larger angles for the case of K - HBr only means that the potential well for this system is deeper than that for K - Kr.) The potential so determined can be used to calculate hypothetical elastic differential cross sections at larger angles where, in reality, reactive scattering has a large effect on the

scattered flux of K. Thus if $\left[\sigma(\bar{E},\theta)\right]_{el}$ is the elastic differential cross section calculated on the assumption that no reaction has occurred, $\sigma(\bar{E},\theta)$ will be smaller than $\left[\sigma(\bar{E},\theta)\right]_{el}$ since some of the K beam atoms are lost due to chemical reaction. The reaction probability $P(\bar{E},\theta)$ for a given value of $\bar{E}$ is therefore defined as

$$P(\bar{E},\theta) = \frac{\left[\sigma(\bar{E},\theta)\right]_{el} - \sigma(\bar{E},\theta)}{\left[\sigma(\bar{E},\theta)\right]_{el}} \quad . \tag{47}$$

Beck, Greene and Ross[48] have shown that it is possible to extrapolate these reaction probabilities to obtain a value of the threshold energy, that is, the value of $\bar{E}$ for which $P(\bar{E},\theta)$ is zero. Their procedure involves extrapolation with respect to $\bar{E}$ at a fixed value of the potential which corresponds to a constant value of the distance of closest approach r_c. Their extrapolation method yielded a value of 0.15 kcal/mole for E_a. As previously indicated, their direct measurements based on detecting the onset of an appearance of a KBr signal gave an upper limit of 0.4 kcal/mole.

For a given value of $\bar{E}$, a threshold angle, θ_t, can be determined by noting the angle where Eq. (47) indicates that $P(\bar{E},\theta)$ is zero. Although θ_t is found to vary with $\bar{E}$, the threshold impact parameter, b_t, associated with θ_t is essentially invariant.[48] Thus the total reaction cross section for a given value of $\bar{E}$ is simply given by the analog of the general relation in Eq. (23), namely,

$$S_R(\bar{E}) = 2\pi \int_0^{b_t} P(\bar{E},b)\, b\, db \quad . \tag{48}$$

The values of $S_R(E)$ calculated as described above were in reasonable agreement with those obtained by direct measurement.[202,209] Another independent

calculation of $S_R(\bar{E})$ has been reported,[210] in which a potential surface is constructed and formal scattering theory is applied to the calculation of $S_R(\bar{E})$. Again, reasonable agreement is obtained with the experimental value of $S_R(\bar{E})$.

The use of elastic scattering in reactive systems involves approximations and assumptions. Yet the procedure is of special interest since in principle, and to a large extent in practice, it provides a nearly independent method for obtaining $S_R(\bar{E})$ with very little recourse to direct measurement of the yield of reaction product.

In concluding the discussion of the reaction of K and HBr, it is appropriate to show the type of microscopic information that can be obtained by selecting a suitable type of system, using both elastic and reactive scattering results, and including velocity selection. The most significant results are summarized in Table I which is taken from the paper of Beck, Greene, and Ross.[48] In making their calculations they used a value of -4.2 kcal/mole for ΔD_o^o instead of the more recent value of -3.8 kcal/mole. This difference in ΔD_o^o will produce no important changes in the entries in the table, particularly in view of the assumptions and approximations which were involved. For the sake of clarity and for emphasis of the special features of the reaction of K and HBr these assumptions and approximations are repeated.

The rotational angular momentum $\vec{J}_B$ of HBr is so small that it may be neglected in comparison with the initial orbital angular momentum $\vec{L}$ of the system. The final orbital angular momentum $\vec{L}'$ of the system is also very small compared to $\vec{L}$. This follows from the fact that μ' is very much less than μ, that $\vec{v}'$ is not likely to be very much different

Table I. Distribution of Energy in the Products of the Reaction K + HBr

$\overline{E}$, kcal/mole	1.49			4.49		
Angular momentum of HBr, j = 2, g cm^2/mole sec	0.00155			0.00155		
Rotational energy of HBr, j = 2, kcal/mole	0.15			0.15		
Potential at distance of closest approach, kcal/mole	0.15	0.6	1.2	0.15	0.6	1.2
Impact parameter b, Å	3.72	2.92	1.67	3.84	3.53	3.21
μv b, nearly equal to angular momentum of KBr, g cm^2/mole sec	0.068	0.053	0.030	0.121	0.111	0.101
Rotational energy of KBr, kcal/mole	2.52	1.55	0.51	8.07	6.83	5.65
Rotational quantum number	104			186		
Sum of final relative kinetic energy and vibrational energy of KBr, kcal/mole	3.17	4.14	5.18	0.59	1.83	2.42
Maximum vibrational state of KBr	5	6	8	1	3	4

than $\vec{v}$ because of the small value of ΔD_o^o, and that b' and b would be expected to have approximately the same magnitudes.[18,48] Thus, since $\vec{L} >> \vec{J}$ and $\vec{L} >> \vec{L}'$, the total angular momentum conservation condition given by Eq. (38) reduces to

$$\vec{L} \simeq \vec{J}'. \tag{49}$$

The rotational angular momentum of the KBr is therefore very nearly equal to the initial orbital angular momentum of the system. In arriving at the entries in Table I, HBr and KBr were treated as rigid rotors and harmonic oscillators. The main conclusions to be drawn from the rather detailed discussion of the reaction of K and HBr are that in this particular type of reaction the products that are formed will be in highly excited internal states, generally rotational states, and that the laboratory scattering angles at which the products would be expected to appear may be closely predicted without detailed knowledge of the dynamics of the collision.[19]

The special case of K + HBr was discussed in detail because that system contains so many interesting features. In the next sections, three reaction mechanisms which have been investigated with molecular beam technique are discussed. The treatment will be less detailed than the present section and is intended to show the kinds of general conclusions which can be reached in chemical reaction studies with beams.

2. Rebound Reactions.

These reactions typically have relatively small total reaction cross sections, about 50Å^2 or less, and in the center-of-mass system have quite anisotropic angular distributions of products. Figure 15 is a schematic representation of the collision trajectories for rebound reactions

in the laboratory and in the center-of-mass systems for beams of A and BC which intersect at 90° as indicated in Fig. 15a. In the laboratory system AB should appear at an angle close to 90° with respect to the direction of the beam of A atoms. As shown in Fig. 15b an observer traveling with the center of mass would see the A and BC beams approaching from his left and right to collide at his point of observation. After the collision he would observe that the AB product would return roughly in the direction from which the A atoms approached.

A typical example of this type of reaction is

$$K + CH_3I \rightarrow KI + CH_3$$

which was first investigated by Herschbach and coworkers.[47,211] Although velocity selection was not used in their experiments, it was observed that the distribution of KI product was strongly peaked at an angle of 83° as measured from the direction of the beam of K atoms. The experimental data are shown in Fig. 16. It was originally concluded that the total reaction cross section was small, of the order of 10Å^2 and that most of the liberated energy, about 90 percent, appeared in the internal degrees of freedom of the products rather than in their average kinetic energy of relative motion. In a re-analysis of the experimental results it was later shown that the average kinetic energy of relative motion of the products was considerably larger than originally estimated and that the internal energy of the products was correspondingly smaller.[212] The reaction was later re-investigated by Ross and coworkers[213] with velocity selected beams of K and the total reaction cross section, although still rather small, was found to be about 30Å^2. Other recent investigations of this reaction using state selection of the CH_3I have shown that there is a small but definite steric factor associated with the spatial orientation

of the K atom relative to the CH_3I molecule as they approach each other prior to reaction.[36-38] It was possible to effect partial spatial orientation of the CH_3I molecules with strong inhomogeneous fields with several different multipole electrode arrangements. Both velocity selected and non-velocity selected beams of K atoms were crossed with oriented CH_3I molecules and with non-oriented molecules. The analysis of the results permits a comparison of the total reaction cross sections for the two cases where the K atoms approach the CH_3I from the I end or from the CH_3 end. The ratio was about 1.5 and as might have been anticipated on physical grounds, the larger cross section was found for the approach of K toward the I end of the CH_3I. The experimental results are in accord with a theoretical study of this steric effect.[38]

3. Stripping Reactions

Typically these reactions have large total reaction cross sections, of the order of 200$Å^2$. As in the case of the rebound reactions the angular distribution of products is anisotropic. However, in stripping reactions, instead of a backward peaking of the molecular product in the center-of-mass system, there is strong forward peaking. This is shown in the schematic trajectories in Fig. 17 for 90° intersection of beams of A atoms and BC molecules. It can be seen that in both the laboratory and center-of-mass systems the product AB continues to travel in much the same direction as the original A atoms.

Stripping reactions are often referred to as proceeding by a "harpooning" mechanism, a description first suggested by M. Polanyi[214] in connection with his classic studies of reactions between alkali atoms and halogen molecules in dilute flames. Harpooning was pictured in terms

of an atom of A "tossing out its valence electron to hook atom B which it hauls in with the coulomb force of attraction". The spectrum of stripping reactions is quite broad and is a function of the initial kinetic energy of relative motion of the reactants and the magnitude of the total reaction cross section. A somewhat extreme type is referred to as spectator-stripping which may occur when the kinetic energy of the relative motion of the reactants is high. In this case there is little interaction during the impulsive collision between A and the atom C in the BC molecule. Thus C plays the role of a "spectator" to the interaction of A and B, a situation which is likely to occur only if the impact parameter associated with the reaction is large. The products in this type of stripping reaction separate in a time so short that there is no time for transfer of much momentum to C.

The application of the concept of stripping in two body collisions resulting in chemical reaction was first applied[215-217] as a result of mass spectrometric studies of ion molecule reactions. The first experimental studies of stripping reactions in neutral systems were reported simultaneously by two independent groups, one of which used a velocity selected Cs beam which reacted with Br_2,[218] the other a non-velocity selected beam of K atoms also reacting with Br_2.[219]

For the present discussion the example chosen to illustate stripping reactions will be

$$K + Br_2 \rightarrow KBr + Br.$$

The results of the first study of this reaction[219] are shown in Fig. 18 where the spatial distribution, in laboratory coordinates, of KBr product is shown. This was determined as usual with two detectors and the points

shown in the figure were obtained by subtraction. It was clear immediately that the KBr distribution showed a strong maximum near 0° with respect to the direction of the beam of K atoms and that the reaction did indeed correspond to the scheme shown in Fig. 17. A total reaction cross section of about 200Å^2 was deduced. In a subsequent study[220] under more refined experimental conditions the first results were confirmed and it was concluded from the angular distribution of the products that most of the energy available from the reaction appeared as internal excitation of KBr. These conclusions had also been reached in similar experiments involving velocity selected K atom beams.[221] An important and interesting refinement was added to the reaction by direct examination of the KBr to determine the extent to which it was rich in internal energy. In one arrangement[222] velocity analysis of the KBr showed that most of the 46 kcal/mole of energy available to the products appeared in the form of internal excitation of the KBr. Another arrangement employed deflection analysis of the KBr molecules as they traversed a strong inhomogeneous electric field.[223] It was found that of the total angular momentum available to the products, approximately equal amounts were distributed between the rotational angular momentum of the KBr and the orbital angular momentum associated with the relative motion of the products KBr and Br.

Although rebound and stripping mechanisms have been illustrated by examples which have been chosen to best illustrate the special characteristics of these mechanisms, there exists a group of reactions whose features represent a transition between the two types of mechanisms. In general these reactions will have moderate total reaction cross sections, of the order of 100Å^2 or less, and the distribution of molecular product in the center-of-mass system will be in angular regions between the backward and

forward directions. Among the reactions which show these transition characteristics are K + SF_6, Cs + HBr, and Na + $SnCl_4$.

4. Collision Complexes.

Both rebound and stripping reactions are characterized by having extremely short collision times. This is a direct conclusion from the observed anisotropic peaking which implies that the incident particles "remember" their initial direction of approach. If the impact parameter associated with reaction is small, the molecular product immediately rebounds in the center-of-mass system; if the corresponding impact parameter is large the atomic reactant strips an atom from the reactant molecule and the product molecule immediately continues in the forward direction. In order that such directed motions of the product molecules occur, the reaction must proceed in a time which is short compared to the time of rotation of the molecular adduct formed by the reactants when they are sufficiently close to react. If there were a rotation of even half a cycle the directional selectivity of the products would not take place. For these reactions there is therefore an upper limit of less than 10^{-12} second on the reaction time and therefore the A-B-C system at the time of collision is not in any sense a reactive complex; its lifetime is not greater than a vibrational period.

There are, however, a group of reactions in which the reactants do form a long-lived complex which can exist for a number of rotational and vibrational periods before dissociating into products or, in the event reaction does not occur, back into reactants. Those systems which do react exhibit two interesting experimental features. First, two maxima, in the laboratory angle system, appear in the measured intensity of

molecular product. Of the two peaks one, the smaller, is observed near 0°, near the direction of the beam atoms while the other is found near 90° close to the direction of the reactant BC beam. In the center-of-mass system these product distributions correspond to approximately equal distributions near 0° and 180°. Secondly, the total reaction cross sections are quite large, of the order of 200Å^2.

For this discussion the reaction

$$Cs + RbCl \rightarrow CsCl + Rb$$

will be used. It was investigated along with others of the same type by Herschbach and coworkers.[224] A collimated, but non-velocity selected beam of Cs atoms from a source at 473°K intersected at 90° a similar but higher intensity beam of RbCl from a source at 950°K. In this experiment a Pt-W alloy which has been pretreated with oxygen serves as a surface ionization detector which ionizes both Cs and CsCl with almost 100% efficiency. After pretreatment of the same alloy with methane the detector ionizes essentially none of the incident alkali halide molecules. The detection system was therefore capable of the same kind of discrimination as that involved in the use of pure tungsten and platinum detectors in the investigation of the reaction of K and HBr.

The experimentally observed angular distribution of CsCl as a function of the laboratory angle θ_L is shown in Fig. 19. The two maxima, one near 0°, the other near 90° stand out clearly. In the center-of-mass coordinate system, the two maxima are of equal magnitude. As expected, the total reaction cross section was large, between 150Å^2 and 200Å^2.

There is a specific reason which determines whether a reaction will proceed by direct or impulsive mechanisms or by mechanisms which involve

long-lived complexes. With the exception of RbCl the molecular reactants AB in all the reactions discussed above have covalent bonds. RbCl and the other alkali halide molecules, however, are ion pairs[225] so that the schematic equation for reactions which proceed through long-lived complexes is more informative if written as showing the ion pairs present during the reaction

$$A + B^-C^+ \rightarrow A^+B^- + C.$$

The fact that the bond strengths of B^-C^+ and A^+B^- are nearly equal and that diatomic alkali molecule ions are relatively stable make it probable that a complex $(AC)^+B^-$ will be formed.[226,227] The likelihood of the existence of such complexes is also strengthened by an electronic structure calculation for the K-Na-Cl system[228] which shows a basin in the potential energy surface whose depth is about 13.5 kcal/mole lower than the energy of the products.

The symmetrical distribution of molecular products in angular regions in the center of mass which are concentrated close to 0° and 180° may be visualized in terms of Fig. 8 in the section on Dyanmics of Collisions. The main features of the explanation have been mentioned above but are repeated here. The total initial angular momentum will consist for the most part of orbital angular momentum $\vec{L}$ particularly since the large total reaction cross sections imply that these reactions involve initial impact parameters that are quite large. If a long-lived complex is formed this orbital angular momentum will be converted into rotational angular momentum of the three atom complex which is likely to be approximately linear. When, after random intervals, decomposition of the complex occurs, the products will fly off in directions perpendicular to $\vec{L}$ as illustrated in

Fig. 8(b). Each vector $\vec{L}$ can thus be associated with a plane containing these vectors $\vec{v}'$ uniformly distributed over 2π radians. Since the impact parameters are uniformly distributed about directions which are parallel to the initial relative velocity, all directions of $\vec{L}$ in a plane normal to $\vec{v}$ are possible and a plane of the vectors $\vec{v}'$ can be associated with each direction of $\vec{L}$. Thus the overall spatial distribution of $\vec{v}'$ can be visualized by rotating the disk containing the $\vec{v}'$ for a given direction of $\vec{L}$ around $\vec{v}$. In the sphere generated in this way, vectors of $\vec{v}'$ will be concentrated in both directions along the $\vec{v}$ axis. This concentration is precisely the 0° and 180° peaking which is characteristic of reactions which proceed by mechanisms involving long-lived complexes. A more detailed description of the dynamical features of reactions which proceed through long-lived complexes can be found in the original paper of Herschbach and coworkers[224] and in the review article of Toennies.[19]

The existence of long-lived complexes may also be observed in non-reactive systems. Kinsey and coworkers[229] have given a preliminary report of a number of such systems which were studied by using velocity selected beams of K with SO_2, CO_2, and NO, and velocity selected beams of Cs with SO_2, CO_2, and NO_2. The angular distributions of K and Cs in the laboratory system showed definite evidence of long-lived complexes which, except in the case of NO_2, decomposed back into reactants. The authors concluded that the cross section for the formation of the complex was very small for NO, intermediate for CO_2 and large, in excess of 100Å^2, for SO_2 and NO_2. A comprehensive paper has also been written.[230]

5. Ion-Molecule Reactions

Molecular beam techniques have also been used to investigate bi-molecular reactions in which one of the reactants is a charged particle,

a positive or a negative ion. These reactions fall into the same two broad experimental classes as those discussed earlier; attenuation[231-233] and crossed beam experiments.[20,234] The ion sources used are similar in many cases to mass spectrometer sources, and indeed many ion-molecule experiments have been performed in suitably modified commercial mass spectrometers. More recently, special apparatus types have been constructed which employ appropriate focussing and decelerating electrodes to produce reasonably large intensities of ionic reactants in the approximate energy range of 1 - 100 eV.[20]

As a class, ion-molecule reactions which are exothermic have no appreciable barrier to reaction. It is usually assumed that this is the result of the charge-induced dipole attraction which accelerates the ion and neutral reactants toward each other. This energy, $-\alpha e^2/2r^4$, where α is the polarizability of the neutral reactant, e, the electronic charge, and r the internuclear separation of the reactants, in the absence of repulsion due to electron cloud overlap, may be sufficient to overcome a barrier of several kcal/mole. There are several excellent review articles and a monograph in which the dynamics and detailed mechanisms of ion-molecule reactions are discussed at length and in which extensive bibliographies are included.[187,235-239]

The general characteristics of ion-molecule reactions are similar to those of neutral-neutral reactions. Many of the reactions proceed by direct or impulsive collisions, indicating that the ion and the neutral particle are within the reaction distance for a very short period, of the order of a vibrational period, and accordingly the reactions show rebound, stripping, and spectator stripping features discussed previously. Of par-

ticular interest is the fact that in a number of reactions the actual mechanism is a function of the kinetic energy of relative motion of the reactants. An example is the reaction of Ar^+ and D_2 where at sufficiently high energies the nature of the products changes. This particular reaction will be used to illustrate the salient features of ion-molecule reactions which proceed by impulsive collisions. At relatively low energies the reaction may be written as

$$Ar^+ + D_2 \rightarrow ArD^+ + D.$$

In the limit of very low energy, if the reactants start essentially at rest they will accelerate toward each other as the result of the attractive ion-induced dipole forces and will tend to collide in a head-on collision. The products will then rebound and the ArD^+ will go back in the direction from which the Ar^+ came. Under these conditions the reaction will have the characteristics associated with a rebound mechanism. As the initial kinetic energy of relative motion is increased somewhat and becomes comparable or slightly less than the interaction energy, the reactants will have a tendency to spiral with respect to each other and the products may come off in several directions depending on the angle of spiralling. As the energy continues to increase the spiralling will decrease and the products will acquire a tendency to appear in a narrow, forwardly directed cone as in spectator reactions. At still higher energies, the attractive ion-induced dipole interaction is unimportant and the mechanism becomes for the most part that of spectator stripping as originally proposed by Henglein and coworkers.[231] It has been shown that even in this high energy region there is also an important component of rebound reaction which may result from those Ar-D-D collisions which are essentially head on.

As the energy increases still further the total reaction cross section for ArD^+ formation becomes extremely small and as the internal energy in ArD^+ tends to exceed the dissociation limit fragmentation results so that a different set of products is observed[232] according to

$$Ar^+ + D_2 \rightarrow Ar^+ + 2D$$

or

$$Ar^+ + D_2 \rightarrow Ar + D^+ + D.$$

This brief description of the reaction between $Ar^+ + D_2$ is a summary of a comprehensive account given by Wolfgang and coworkers.[240]

The discussion of the reaction of $Ar^+ + D_2$ shows that the features of direct, impulsive neutral-neutral bimolecular reactions may also be seen in ion-molecule reactions. Although long-lived collision complexes in ion-molecule reactions have actually been detected in mass spectrometric studies,[241] complexes which exist for only a few rotational periods (about 10^{-10} second) are not detectable by this method. However, the techniques which have shown the existence of short-lived complexes in neutral-neutral reactions, have also shown that they may be present in ion-molecule systems. The most recent, and probably the best documented reaction[242] is

$$O_2^+ + D_2 \rightarrow DO_2^+ + D.$$

The authors concluded that the long-lived collision complex mechanism is dominant at lower kinetic energies of relative motion, but that the mechanism changes to one of direct, impulsive interaction as this energy increases. They conclude that there are two significant reasons why the reaction proceeds through the long-lived collision complex mechanism at the lower energies. First, the reaction is endothermic by 1.9 eV.

Second, the $D_2O_2^+$ intermediate lies in a potential well whose depth, excluding activation barriers, is 2.6 eV lower than that of the reactants. Since the threshold for dissociation from the complex into products is therefore 4.5 eV, the lifetime of the complex, at least for low values of the initial kinetic energy of relative motion, would be expected to be reasonably long.

6. Charge Transfer.

A type of rearrangement collision which is usually of more interest to physicists than to chemists involves a process known as charge transfer. It is convenient to distinguish between systems of like atoms which undergo symmetric resonant charge transfer according to

$$A^+ + A = A + A^+$$

and systems of unlike atoms which undergo asymmetric non-resonant charge transfer according to

$$A^+ + B = A + B^+ + \Delta E.$$

The quantity ΔE is referred to as the energy defect and when all particles are in their ground states ΔE is the difference in ionization potentials of A and B. When ΔE is small or zero the process is referred to as being near-resonant. Charge transfer was mentioned earlier in this chapter as a method for producing fast neutral beams, usually by symmetric resonant charge transfer of fast positive ions in neutral atoms of their own species. An example of this type of charge exchange is

$$He^+ + He = He + He^+.$$

When used to produce a fast neutral beam, the incident He^+ was a fast ion, the target He, a slow atom. After charge transfer the He was a fast neutral and the He^+ a slow ion. As an example of non-resonant charge

transfer which involves only atoms or atomic ions one might use

$$He^+ + Ar \rightarrow He + Ar^+ + 8.825 \text{ eV}$$

where 8.825 eV is the difference between the first ionization potentials of He and Ar, both in their ground states.

Since most of the detailed experimental and theoretical features of charge transfer are not within the scope of this chapter, only the most general features will be presented. For symmetrical resonant charge transfer the cross sections are large at low kinetic energies of relative motion and decrease with increasing energy. The cross sections for non-resonant charge transfer, on the other hand, increase with increasing initial kinetic energy of relative motion and usually have relatively small values at lower energies, particularly if ΔE is of the order of several eV or higher. A comprehensive discussion of both experimental and theoretical aspects of charge transfer may be found in a number of excellent reviews[113,243].

Other classes of charge transfer reactions which are of interest are those in which the transfer is accompanied by dissociation as in

$$A^+ + BC = A + B^+ + C.$$

Specific instances of dissociative charge transfer have been studied by many investigators among them Lindholm[244], Gustafson and Lindholm[245], and Giese and Maier[246] who have investigated the system

$$X^+ + CO = X + C^+ + O$$

where X^+ represents either He^+, Ne^+, or Ar^+. This type of charge transfer may be regarded as a special category of ion-molecule reactions.

Finally, a useful type of charge transfer has been reported,[247,248] which uses highly polyatomic molecules such as butane or benzene as charge transfer gases. The existence of a very large number of internal

electronic states makes it highly probable that the positive ion will find an energy level in the molecule which will permit efficient charge transfer under near-resonant conditions. This may be referred to as accidental resonance. This type of charge transfer, which is frequently accompanied by dissociation of the target molecule, has been used to neutralize positive ions under conditions where symmetrical resonant charge transfer would be difficult.[247]

V. Conclusion

In this chapter an attempt has been made to relate the broad field of molecular beam research to chemical problems. Although the treatment has been highly selective, topics have been treated in which the contributions or interest of chemists have been particularly significant.

Since there is no doubt that the contributions and interest will continue, it would seem relevant to try to predict the direction in which such molecular beam research will go. Advances over a broad front are expected. Potential energies for complex molecular systems will be determined and the anisotropies in such potentials will be studied in much more detail than at present. More studies of inelastic scattering can be expected, particularly rotational and vibrational excitation. These studies in which extensive use will be made of state selection should provide valuable information for a clearer understanding of the microscopic features of reactive scattering. In the area of reactive scattering, future studies will be less confined to reactions involving alkali atoms and will therefore probe reactions with threshold energies considerably larger than those encountered in the past. Finally it would appear that the relatively small amount of ion-molecule research by molecular beam

methods will be greatly increased.

If these predictions are reasonable, this chapter will require frequent revision.

VI. Acknowledgments

This research was supported in part by the U.S. Office of Naval Research and by the National Science Foundation (M.I.T.) and in part by the U.S. National Aeronautics and Space Administration (Brown).

References

1. L. Dunoyer, Compt. rend. 152, 592 (1911).

2. N. F. Ramsey, Molecular Beams (Oxford University Press, London and New York, 1956).

3. W. Gerlach and O. Stern, Ann. Physik 74, 673 (1924).

4. W. E. Lamb, Jr. and R. C. Retherford, Phys. Rev. 79, 549 (1950).

5. B. Bederson and E. J. Robinson, Adv. Chem. Phys. 10, 1 (1966).

6. J. P. Gordon, H. J. Zeiger, and C. H. Townes, Phys. Rev. 99, 1264 (1955).

7. H. Bethe and J. Ashkin, Experimental Nuclear Physics, E. Segre, ed. (John Wiley and Sons, New York, 1953), Chap. 2.

8. A. Dalgarno, Atomic and Molecular Processes, D. R. Bates, ed. (Academic Press, New York, 1962), Chapter 15.

9. A. Dalgarno and G. W. Griffing, Proc. Roy. Soc. 232A, 423 (1955).

10. S. K. Allison, J. Cuevas, and M. Garcia-Munoz, Phys. Rev. 127, 792 (1962).

11. M. N. Huberman, Phys. Rev. 127, 799 (1962).

12. S. Datz, T. S. Noggle and C. D. Moak, Phys. Rev. Letters 15, 254 (1965).

13. S. Datz, T. S. Noggle and C. D. Moak, Nuclear Inst. Methods 38, 221 (1965).

14. H. O. Lutz, S. Datz, C. D. Moak and T. S. Noggle, Phys. Rev. Letters 17, 285 (1966).

15. H.S.W. Massey and E.H.S. Burhop, Electronic and Ionic Impact Phenomena (Clarendon Press, Oxford, 1952).

16. Fundamentals of Gas-Surface Interactions, H. Saltsburg, J. N. Smith, Jr., and M. Rogers, eds. (Academic Press, New York, 1967).

17. I. Estermann, R. Frisch, and O. Stern, Z. Physik 73, 348 (1931).

18. D. Herschbach, Adv. Chem. Phys. 10, 319 (1966).

19. J. P. Toennies, Ber. Bunsenges. Phys. Chem., 72, 927 (1968).

20. Z. Herman, J. D. Kerstetter, T. L. Rose, and R. Wolfgang, Rev. Sci. Instr. 40, 538 (1969).

21. I. Amdur and J. E. Jordan, Adv. Chem. Phys., 10, 29 (1966).

22. H. Pauly and J. P. Toennies, Advances in Atomic and Molecular Physics, D. R. Bates and I. Estermann, eds. (Academic Press, New York, 1965).

23. D. C. Lorents and W. Aberth, Phys. Rev., 139, A1017 (1965).

24. E. W. McDaniel, Collision Phenomena in Ionized Gases (John Wiley and Sons, Inc., New York, 1964).

25. E. A. Mason, J. Chem. Phys. 26, 667 (1957).

26. K. W. Ford and J. A. Wheeler, Ann. Phys. (N.Y.) 7, 259, 287 (1959).

27. R. J. Munn, E. A. Mason, and F. J. Smith, J. Chem. Phys. 41, 3978 (1964).

28. R. B. Bernstein, Adv. Chem. Phys. 10, 75 (1966).

29. S. Chapman and T. G. Cowling, The Mathematical Theory of Non-Uniform Gases (Cambridge University Press, New York and London, 2nd ed., 1952).

30. J. O. Hirschfelder, C. F. Curtiss, and R. B. Bird, Molecular Theory of Gases and Liquids (John Wiley and Sons, Inc., New York, 2nd printing, 1964).

31. C. S. Wang Chang, G. E. Uhlenbeck, and J. de Boer, Studies Stat. Mech. 2, 243 (1964).

32. E. A. Mason and T. H. Spurling, The Virial Equation of State (Pergamon Press, London, 1969).

33. I. Prigogine and E. Xhrouet, Physica 15, 913 (1949).

34. R. D. Present, Kinetic Theory of Gases (McGraw-Hill Book Co., Inc., New York, 1958).

35. I. Amdur and G. G. Hammes, Chemical Kinetics (McGraw-Hill Book Co., Inc., 1966).

36. K. H. Kramer and R. B. Bernstein, J. Chem. Phys. 42, 767 (1965).

37. P. R. Brooks, E. M. Jones, J. Chem. Phys. 45, 3449 (1966).

38. R. J. Beuhler, Jr., R. B. Bernstein, and K. H. Kramer, J. Am. Chem. Soc. 88, 5331 (1966).

39. T. G. Waech, K. H. Kramer, and R. B. Bernstein, J. Chem. Phys. 48, 3978 (1968).

40. R. J. Beuhler, Jr., and R. B. Bernstein, Chem. Phys. Lett. 2, 166 (1968).

41. P. R. Brooks, J. Chem. Phys. 50, 5031 (1969).

42. P. R. Brooks, E. M. Jones, and K. Smith, J. Chem. Phys. 51, 3073 (1969).

43. R. D. Present, Proc. Nat. Acad. Sci. 41, 415 (1955).

44. D. R. Herschbach, J. Chem. Phys. 33, 1870 (1960).

45. D. R. Herschbach, Vortex (Calif. Sec.,ACS 22, No. 8, October, 1961).

46. S. Datz, D. R. Herschbach, and E. H. Taylor, J. Chem. Phys. 35, 1549 (1961).

47. D. R. Herschbach, Discussions Faraday Soc. 33, 149 (1962).

48. D. Beck, E. F. Greene, and J. Ross, J. Chem. Phys. 37, 2895 (1962).

49. L. Davis, Jr., D. E. Nagle, and J. R. Zacharias, Phys. Rev. 76, 1068 (1949).

50. H. H. Stroke, Ph.D. Thesis, Physics Dept., M.I.T., Cambridge, 1954 (unpublished).

51. J. G. King and J. R. Zacharias, Adv. Electronics Elect. Phys. 8, 1 (1956).

52. D. E. Nagle, R. E. Julian, and J. R. Zacharias, Phys. Rev. 72, 971 (1947).

53. J. G. King and V. Jaccarino, Phys. Rev. 94, 1610 (1954).

54. J.M.B. Kellogg, I. I. Rabi, and J. R. Zacharias, Phys. Rev. 50, 472 (1936).

55. W. L. Fite and R. T. Brackman, Phys. Rev. 112, 1141 (1958).

56. E. E. Muschlitz, Jr., Adv. Chem. Phys. 10, 171 (1966).

57. B. Lammert, Z. Physik 56, 244 (1929).

58. J. G. Dash and H. S. Sommers, Jr., Rev. Sci. Instr. 24, 91 (1953).

59. R. C. Miller and P. Kusch, Phys. Rev. 99, 1314 (1955).

60. E. F. Greene, R. W. Roberts, and J. Ross, J.Chem. Phys. 32, 940 (1960).

61. H. G. Bennewitz and W. Paul, Z. Physik 139, 489 (1954).

62. H. G. Bennewitz, W. Paul, and Ch. Schlier, Z. Physik 141, 6 (1955).

63. S. V. Hostettler and R. B. Bernstein, Rev. Sci. Instr. 31, 872 (1960).

64. S. M. Trujillo, P. K. Rol, and E. W. Rothe, Rev. Sci. Instr. 33, 841 (1962).

65. J. L. Kinsey, Rev. Sci. Instr. 37, 61 (1966).

66. H. Pauly and J. P. Toennies, Methods of Experimental Physics, Vol. 7A, B. Bederson and W. L. Fite, eds. (Academic Press, New York, 1968), Chap. 3.1.

67. T. H. Johnson, J. Franklin Inst. 207, 629 (1929).

68. O. E. Kurt and J. E. Phipps, Phys. Rev. 34, 1357 (1929).

69. A. Lemonuck and F. M. Pipkin, Phys. Rev. 95, 1356L (1954).

70. P. R. Brooks and D. R. Herschbach, Rev. Sci. Instr. 35, 1528 (1964).

71. K. H. Kingdon, Phys. Rev. 21, 408 (1923).

72. W. D. Johnston and J. G. King, Rev. Sci. Instr. 37, 475 (1966).

73. E. H. Taylor and S. Datz, J. Chem. Phys. 23, 1711 (1955).

74. S. Datz and E. H. Taylor, J. Chem. Phys. 25, 389 (1956).

75. S. Datz and E. H. Taylor, J. Chem. Phys. 25, 395 (1956).

76. G. Wessel and H. Lew, Phys. Rev. 92, 641 (1953).

77. G. Fricke, Z. Physik 141, 166 (1955).

78. F. Bernhard, Z. Angew. Phys. 9, 68 (1957).

79. H. Heil, Z. Physik 120, 212 (1943).

80. W. Paul, Z. Physik 124, 244 (1948).

81. H. Friedman, Z. Physik 156, 598 (1959).

82. M. Von Ardenne, Phys. Zeits. 43, 91 (1942).

83. W. E. Quinn, A. Pery, J. M. Baker, H. R. Lewis, N. F. Ramsey, and J. T. LaTourette, Rev. Sci. Instr. 29, 935 (1958).

84. R. Weiss, Rev. Sci. Instr. 32, 397 (1961).

85. G. O. Brink, Rev. Sci. Instr. 37, 857 (1966).

86. O. F. Hagena and A. K. Varma, Rev. Sci. Instr. 39, 47 (1968).

87. R. H. Dicke, Rev. Sci. Instr. 17, 268 (1946).

88. A. V. Phelps and J. L. Pack, Rev. Sci. Instr. 26, 45 (1955).

89. K. Kodera, I. Kusunoki, and A. Sakiyama, Sixth International Conference on the Physics of Electronic and Atomic Collisions, Book of Abstracts, p. 169 (1969).

90. H. Ishii and K. Nakayama, Trans. 8th Nat. Vac. Symp., Vol. I, Pergamon Press, Oxford, 519 (1962).

91. E. Rothe, J. Vac. Sci. and Tech. 1, 66 (1964).

92. C. Meinke and G. Reich, Vacuum 13, 579 (1963).

93. A. deVries and P. Rol, Vacuum 15, 135 (1965).

94. P. Kusch, J. Chem. Phys. 40, 1 (1964).

95. C. E. Kuyatt, Methods of Experimental Physics, Vol. 7A, B. Bederson and W. L. Fite, eds. (Academic Press, New York, 1968), Chap. 1.1.

96. M. E. Rudd and T. Jorgenson, Jr., Phys. Rev. 131, 666 (1963).

97. M. Hoyaux and I. Dujardin, Nucleonics 4, 12 (1949).

98. H. F. Ivey, Adv. Electronics Elect. Physics 6, 137 (1954).

99. J. R. Pierce, Theory and Design of Electron Beams, (van Nostrand, New York, 1954).

100. J. A. Simpson, Rev. Sci. Instr. 32, 1283 (1961).

101. K. T. Bainbridge, Experimental Nuclear Physics, E. Segre, ed. (John Wiley and Sons, New York, 1953), p. 559.

102. L. Kerwin, Adv. Electronics Elect. Phys. 8, 187 (1956).

103. P. Marmet and L. Kerwin, Canad. J. Phys. 38, 787 (1960).

104. E. M. Purcell, Phys. Rev. 54, 818 (1938).

105. F. R. Paolini and G. C. Theodoridis, Rev. Sci. Instr. 38, 579 (1967).

106. C. E. Kuyatt and J. A. Simpson, Rev. Sci. Instr. 38, 103 (1967).

107. G. A. Harrower, Rev. Sci. Instr. 26, 850 (1955).

108. J. A. Alcalay and E. L. Knuth, Rev. Sci. Instr. 40, 438 (1969).

109. W. H. Bennett, J. App. Phys. 21, 143 (1950).

110. R.L.F. Boyd and D. Morris, Proc. Phys. Soc. Lond., A68, 1 (1955).

111. W. Paul and M. Raether, Z. Physik 140, 262 (1955).

112. W. Paul, H. P. Reinhardt, and V. von Zahn, Z. Physik 152, 143 (1958).

113. J. B. Hasted, Physics of Atomic Collisions (Butterworths, London, 1964).

114. J. E. Jordan and I. Amdur, J. Chem. Phys. 46, 165 (1967).

115. N. Peterson, private communication, 1969.

116. L. Harris, J. Opt. Soc. Am. 36, 597 (1946).

117. Barnes Engineering Company, Stamford, Connecticut.

118. M.A.D. Fluendy, Rev. Sci. Instr. 35, 1606 (1964).

119. G. W. Goodrich and W. C. Wiley, Rev. Sci. Instr. 32, 846 (1961).

120. G. W. Goodrich and W. C. Wiley, Rev. Sci. Instr. 33, 761 (1962).

121. J. Draper, Methods of Experimental Physics, Vol. 4A, V. W. Hughes and H. L. Schultz, eds. (Academic Press, New York, 1967), Chap. 2.1.2.

122. H. W. Berry, Phys. Rev. 75, 913 (1962).

123. N. R. Daly, Rev. Sci. Instr. 31, 264 (1960).

124. J. B. Anderson, R. P. Andres and J. B. Fenn, Advances in Atomic and Molecular Physics, D. R. Bates and I. Esterman, eds. (Academic Press, New York, 1965).

125. J. B. Anderson, R. P. Andres and J. B. Fenn, Adv. Chem. Phys. 10, 275 (1966).

126. S. M. Trujillo, R. H. Neynaber and E. W. Rothe, Rev. Sci. Instr. 37, 1655 (1966).

127. V. A. Belyaev, B. G. Brezhnev and E. M. Erastov, Zh. Eksperim.: Teor. Fiz.-Pisma Redact. 3, 321 (1966). English Trans. JETP Letters 3, 207 (1966).

128. R. H. Neynaber, Methods of Experimental Physics, Vol. 7A, B. Bederson and W. L. Fite, eds. (Academic Press, New York, 1968), Chap. 4.3.

129. J. Politiek, J. Los, J.J.M. Schipper and A.P.M. Baede, Entropie 18, 82 (1967).

130. E. Hulpke and Ch. Schlier, Z. Physik 207, 294 (1967).

131. J. Politiek, P. K. Rol, J. Los and P. G. Ikelaar, Rev. Sci. Instr. 39, 1147 (1968).

132. G. T. Skinner, Phys. Fluids 4, 1172 (1961).

133. G. T. Skinner and B. H. Fetz, Rarefied Gas Dynamics, J. H. Leeuw, ed. (Academic Press, New York, 1965), p. 536.

134. G. T. Skinner and J. Moyzis, Phys. Fluids 8, 452 (1965).

135. R. A. Oman, A. Bogan, C. H. Weiser, C. H. Li and V. S. Calia, Grumman Res. Dept. Rept. RE-166 (1963).

136. D. Auerbach, E.E.A. Bromberg and L. Wharton, J. Chem. Phys. 45, 2160 (1966).

137. R. Wolfgang, Sci. Amer. 219, 44 (1968).

138. L. Sodickson, J. Carpenter and G. Davidson, Report No. AFCRL-65-337, American Science and Engineering, Inc., Cambridge, Massachusetts, 1965.

139. J. E. Jordan and O. Shepard, Report No. AFCRL-69-0095, American Science and Engineering, Inc., Cambridge, Massachusetts, 1969.

140. E. A. Mason and J. T. Vanderslice, Atomic and Molecular Processes, D. R. Bates, ed. (Academic Press, New York, 1962), Chapter 17.

141. E. A. Mason and I. Amdur, J. Chem. Phys. 41, 2695 (1964).

142. I. Amdur and A. L. Smith, J. Chem. Phys. 48, 565 (1968).

143. S. O. Colgate, J. E. Jordan, I. Amdur, and E. A. Mason, J. Chem. Phys. 51, 968 (1969).

144. J. E. Jordan, S. O. Colgate, I. Amdur, and E. A. Mason, J. Chem. Phys. 52, 1143 (1970).

145. A. B. Kamnev and V. B. Leonas, Dokl. Akad. Nauk SSSR 162, 798 (1965) [Soviet Phys.-Dokl. 10, 529 (1965)].

146. A. B. Kamnev and V. B. Leonas, Dokl. Akad. Nauk SSSR 165, 1273 (1965) [Soviet Phys.-Dokl. 10, 1202 (1966)].

147. Yu. N. Belyaev and V. B. Leonas, Zh. Tekh. Fiz. 36, 353 (1966) [Soviet Phys.-Tech. Phys. 11, 257 (1966)].

148. Yu. N. Belyaev and V. B. Leonas, Dokl. Akad. Nauk SSSR 170, 1039 (1966) [Soviet Phys.-Dokl. 11, 866 (1967)].

149. Yu. N. Belyaev and V. B. Leonas, Zh. Eksper. Teor. Fiz. Pis'ma 4, 134 (1966) [Soviet Phys.-JETP Letters 4, 92 (1966)].

150. Yu. N. Belyaev and V. B. Leonas, Dokl. Akad. Nauk SSSR 173, 306 (1967) [Soviet Phys.-Dokl. 12, 233 (1967)].

151. Yu. N. Belyaev, V. B. Leonas, and A. V. Sermyaguin, Abstracts of Papers, Fifth International Conference on the Physics of Electronic and Atomic Collisions (Publishing House "Nauka", Leningrad, USSR, 1967), p. 643.

152. Yu. N. Belyaev, N. V. Kamyshov, V. B. Leonas, and A. V. Sermyaguin, Entropie 30, 173 (1969).

153. I. Amdur and A. L. Harkness, J. Chem. Phys. 22, 664 (1954).

154. I. Amdur, J. E. Jordan, and S. O. Colgate, J. Chem. Phys. 34, 1525 (1961).

155. N. C. Blais and J. B. Mann, J. Chem. Phys. 32, 1459 (1960).

156. E. A. Mason and W. E. Rice, J. Chem. Phys. 22, 522 (1954).

157. P. E. Phillipson, Phys. Rev. 125, 1981 (1962).

158. G. M. Matsumoto, C. F. Bender, and E. R. Davidson, J. Chem. Phys. 46, 402 (1967).

159. I. Amdur and E. A. Mason, J. Chem. Phys. 22, 670 (1954).

160. I. Amdur, J. E. Jordan, and R. R. Bertrand, Atomic Collision Processes, M.R.C. McDowell, ed. (North-Holland Publ. Co., Amsterdam, 1964), p. 934.

161. R. N. Keeler, M. van Thiel, and B. J. Alder, Physica 31, 1437 (1965).

162. M. van Thiel and B. J. Alder, J. Chem. Phys. 44, 1056 (1966).

163. C. R. Fischer and P. J. Kemmey, Phys. Rev. (to be published).

164. I. Amdur and E. A. Mason, J. Chem. Phys. 25, 630 (1956).

165. M. Krauss and F. H. Mies, J. Chem. Phys. 42, 2703 (1965).

166. R. L. Matcha and R. K. Nesbet, Phys. Rev. 160, 72 (1967).

167. E. A. Mason and L. Monchick, Adv. Chem. Phys. 12, 329 (1967).

168. I. Amdur, E. A. Mason, and A. L. Harkness, J. Chem. Phys. 22, 1071 (1954).

169. R. E. Walker and A. A. Westenberg, J. Chem. Phys. 31, 519 (1959).

170. H. Margenau and N. R. Kestner, Theory of Intermolecular Forces (Pergamon Press, London, 1969), Chapter 7.

171. I. Amdur and E. A. Mason, Phys. Fluids 1, 370 (1958).

172. E. A. Mason, Kinetic Processes in Gases and Plasmas, A. R. Hochstim, ed. (Academic Press, New York, 1969), pp. 57-100.

173. K. F. Herzfeld and T. A. Litovitz, Absorption and Dispersion of Ultrasonic Waves (Academic Press, New York, 1959).

174. D. R. Olander, J. Chem. Phys. 43, 779 (1965).

175. D. R. Olander, J. Chem. Phys. 43, 785 (1965).

176. R. M. Martin and J. E. Willard, J. Chem. Phys. 40, 3007 (1964).

177. R. Wolfgang, Ann. Rev. Phys. Chem. 16, 15 (1965).

178. J. F. Williams, P. J. Stang, and P. v. R. Schleyer, Ann. Rev. Phys. Chem. 19, 531 (1968).

179. E. A. Mason and M. M. Kreevoy, J. Am. Chem. Soc. 77, 5808 (1955).

180. M. M. Kreevoy and E. A. Mason, J. Am. Chem. Soc. 79, 4851 (1957).

181. G. N. Ramachandran and V. Sasisekharan, Adv. Protein Chem. 23, 283 (1968).

182. P. J. Flory, Statistical Mechanics of Chain Molecules (Interscience Publishers, New York, 1969), Chap. 5.

183. R. B. Bernstein and J. T. Muckerman, Adv. Chem. Phys. 12, 389 (1967).

184. M. Minnaert, Light and Colour in the Open Air (Dover Publications, New York, 1954).

185. P. Kang, E. A. Mason, and R. J. Munn, Am. J. Phys. (to be published).

186. E. A. Mason and L. Monchick, J. Chem. Phys. 41, 2221 (1964).

187. C. F. Barnett and H. Gilbody, Methods of Experimental Physics, Vol. 7A, B. Bederson and W. L. Fite, eds. (Academic Press, New York, 1968), Chapter 4.2.

188. N. G. Utterback and G. H. Miller, Rev. Sci. Instr. 32, 1101 (1961).

189. N. G. Utterback and G. H. Miller, Phys. Rev. 124, 1477 (1961).

190. R. H. Hammond, J.M.S. Henis, E. F. Greene, and J. Ross, Sixth International Conference on the Physics of Electronic and Atomic Collisions, Book of Abstracts, 1969, p. 408.

191. J. P. Toennies, Z. Physik 182, 257 (1965).

192. A. R. Blythe, A. E. Grosser, and R. B. Bernstein, J. Chem. Phys. 41, 1917 (1964).

193. D. Beck and H. Förster, Sixth International Conference on the Physics of Electronic and Atomic Collisions, Book of Abstracts, 1969, p. 634.

194. D. O. Ham and J. L. Kinsey, J. Chem. Phys. 48, 939 (1968).

195. T. Moran, private communication.

196. J. Schlötter and J. P. Toennies, Z. Physik 214, 472 (1968).

197. P. F. Dittner and S. Datz, Sixth International Conference on the Physics of Electronic and Atomic Collisions, Book of Abstracts, 1969, p. 469.

198. P. F. Dittner and S. Datz, J. Chem. Phys. 49, 1969 (1968).

199. M. C. Fowler, J. E. Jordan, and I. Amdur, Sixth International Conference on the Physics of Electronic and Atomic Collisions, Book of Abstracts, 1969, p. 516.

200. R. J. Cross and R. G. Gordon, J. Chem. Phys. 45, 3571 (1966).

201. M. C. Moulton and D. R. Herschbach, J. Chem. Phys. 44, 3010 (1966).

202. E. F. Greene, A. L. Moursound, and J. Ross, Adv. Chem. Phys. 10, 135 (1966).

203. Molecular Dynamics of the Chemical Reactions of Gases, Discussions Faraday Soc. 44, 1967.

204. J. I. Steinfeld and J. L. Kinsey, Progress in Reaction Kinetics, Vol. 5 (Pergamon Press, 1969).

205. K. J. Laidler, Theories of Chemical Reaction (McGraw-Hill Book Company, New York, 1969), pp. 189-190.

206. D. Beck, J. Chem. Phys. 37, 2884 (1962).

207. J. R. Luoma and C. R. Mueller, J. Chem. Phys. 46, 680 (1967).

208. R. E. Olson and C. R. Mueller, J. Chem. Phys. 46, 3810 (1967).

209. J. R. Airey, E. F. Greene, K. Kodera, G. P. Reck, and J. Ross, J. Chem. Phys. 46, 3287 (1967).

210. R. J. Suplinskas and J. Ross, J. Chem. Phys. 47, 321 (1967).

211. D. R. Herschbach, G. H. Kwei, and J. A. Norris, J. Chem. Phys. 34, 1842 (1961).

212. E. A. Entemann and D. R. Herschbach, Discussions Faraday Soc. 44, 289 (1967).

213. J. R. Airey, E. F. Greene, G. P. Reck and J. Ross, J. Chem. Phys. 46, 3295 (1967).

214. M. Polanyi, Atomic Reactions (Williams and Nargate, London, 1932).

215. A. Henglein and G. A. Muccini, Z. Naturforsch. 17a, 452 (1962).

216. A. Henglein and G. A. Muccini, Z. Naturforsch. 18a, 753 (1963).

217. A. Henglein, K. Lacmann, and B. Knoll, J. Chem. Phys. 43, 1048 (1965).

218. S. Datz and R. E. Minturn, J. Chem. Phys. 41, 1153 (1964).

219. K. R. Wilson, G. H. Kwei, J. A. Norris, R. R. Herm, J. H. Birely, and D. R. Herschbach, J. Chem. Phys. 41, 1154 (1964).

220. J. H. Birely, R. R. Herm, K. R. Wilson, and D. R. Herschbach, J. Chem. Phys. 47, 993 (1967).

221. R. E. Minturn, S. Datz, and R. L. Becker, J. Chem. Phys. 44, 1149 (1966).

222. A. E. Grosser and R. B. Bernstein, J. Chem. Phys. 43, 1140 (1965).

223. R. R. Herm and D. R. Herschbach, J. Chem. Phys. 43, 2139 (1965).

224. W. R. Miller, S. A. Safron and D. R. Herschbach, Discussions Faraday Soc. 44, 108 (1967).

225. E. Rittner, J. Chem. Phys. 19, 1030 (1951).

226. R. F. Barrow and A. J. Merer, Ann. Reports Prog. Chem. 59, 121 (1962).

227. Y. T. Lee and B. H. Mahan, J. Chem. Phys. 42, 2893 (1965).

228. A. C. Roach and M. S. Childs, Mol. Phys. 14, 1 (1968).

229. D. O. Ham, J. L. Kinsey and F. S. Klein, Discussions Faraday Soc. 44, 174 (1967).

230. D. O. Ham and J. L. Kinsey, J. Chem. Phys. (in press).

231. A. Henglein, K. Lacmann, G. Jacobs, Ber Bunsenges. Phys. Chem. 69, 279 (1965).

232. R. L. Champion, L. D. Doverspike, and T. L. Bailey, J. Chem. Phys. 45, 4377 (1966).

233. W. R. Gentry, E. A. Gislason, B. H. Mahan and C. W. Tsao, J. Chem. Phys. 49, 3058 (1968).

234. B. R. Turner, M. A. Fineman, and R. F. Stebbings, J. Chem. Phys. 42, 4088 (1965).

235. B. H. Mahan, Acc. Chem. Res. 1, 217 (1968).

236. Richard Wolfgang, Acc. Chem. Res. 2, 248 (1969).

237. E. W. McDaniel, Ion-Molecule Reactions (John Wiley and Sons, Inc., New York, 1970).

238. W. R. Gentry, E. A. Gislason, Y. T. Lee, B. H. Mahan, and C. W. Tsao, Discussions Faraday Soc. 44, 137 (1967).

239. E. W. McDaniel, Methods of Experimental Physics, Vol. 7A, B. Bederson and W. L. Fite, eds. (Academic Press, New York, 1968), Chap. 4.1.

240. Z. Herman, J. Kerstetter, T. Rose and R. Wolfgang, Discussions Faraday Soc. 44, 123 (1967).

241. R. F. Pottie and W. H. Hamill, J. Phys. Chem. 63, 877 (1959).

242. E. A. Gislason, B. H. Mahan, C. W. Tsao and A. S. Werner, J. Chem. Phys. 50, 5418 (1969).

243. R. F. Stebbings, Adv. Chem. Phys. 10, 195 (1966).

244. E. Lindholm, Arkiv Fysik, 8, 433 (1954).

245. E. Gustafson and E. Lindholm, Arkiv Fysik, 18, 219 (1960).

246. C. F. Giese and W. B. Maier II, J. Chem. Phys. 39, 197 (1963).

247. V. L. Talroze, private communication.

248. W. A. Chupka and E. Lindholm, Arkiv Fysik, 25, 349 (1963).

Figure Captions

Fig. 1 Schematic apparatus for production of a molecular beam.

Fig. 2 Schematic crossed beam experiment.

Fig. 3 Schematic attenuation experiment.

Fig. 4 Detail of scattering region and detector geometry. The scattering gas is confined between two planes which establish the scattering region.

Fig. 5 Classical collision trajectory. All particles incident on the ring of area $2\pi bdb$ appear after scattering on the ring of area $2\pi \sin\theta d\theta$.

Fig. 6 (a) Variation of potential for repelling hard spheres which react when the energy of relative motion reaches a threshold value of ε_a.

(b) Energy level diagram showing the definition of E_a and ΔD_o^o.

Fig. 7 Vector diagram of initial and final velocities of a collision.

Fig. 8 (a) Orientation of initial angular momentum vectors.

(b) Distribution of recoil vectors.

Fig. 9 Helium-helium potential energy determined from four different high energy scattering experiments, from high temperature thermal conductivity, from viscosity and virial coefficients, and from two ab initio quantum mechanical calculations.

Fig. 10 Argon-argon potential energy determined from four different high energy scattering experiments, and from shock compression measurements on liquid argon. The dashed curve is a single exponential representation of the three M.I.T. results shown.

Fig. 11 Helium-argon potential energy predicted from the scattering potentials for He-He and Ar-Ar (Figs. 9 and 10) by geometric-mean combination rule, compared with direct measurements.

Fig. 12 Comparison of derived Ar-O, O-O_2, and O_2-O_2 potential energies with direct measurements.

Fig. 13 Elastic scattering of the system K + Kr.

Fig. 14 The differential cross section, in arbitrary units, multiplied by $\sin\theta$ vs. the relative scattering angle θ for the system K + HBr at five different values of the kinetic energy of relative motion.

Fig. 15 Idealized trajectories of reactants and products for a rebound mechanism (a) Laboratory system (b) Center-of-mass system.

Fig. 16 The scattering of K + CH_3I. The curves show the intensity measurements from two detectors. The solid circles indicate the intensity of K, and the open circles the intensity of K + KI. The main K beam, shown at angle 0°, is attenuated about seven percent by the CH_3I crossed beam.

Fig. 17 Idealized trajectories of reactants and products for a stripping mechanism. (a) Laboratory system (b) Center-of-mass system.

Fig. 18 The scattering of K + Br_2. The curve shows the distribution of KBr product in the laboratory system.

Fig. 19 The scattering of Cs + RbCl. The curve shows the distribution of CsCl in the laboratory system.

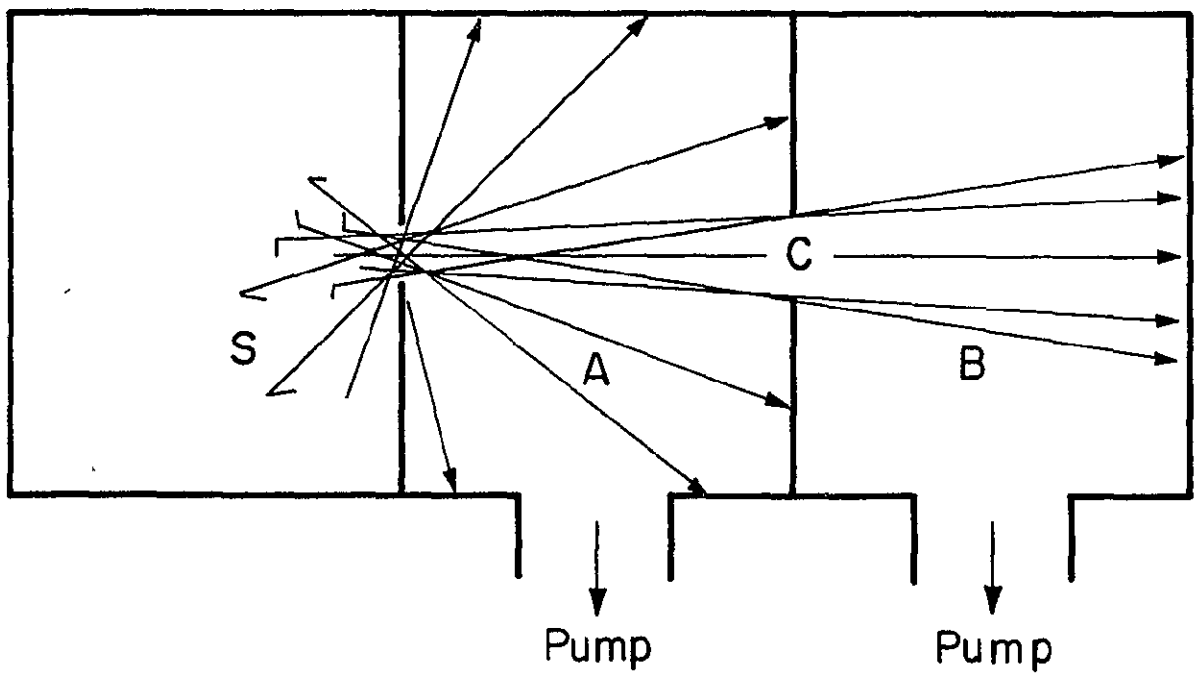

Figure 1

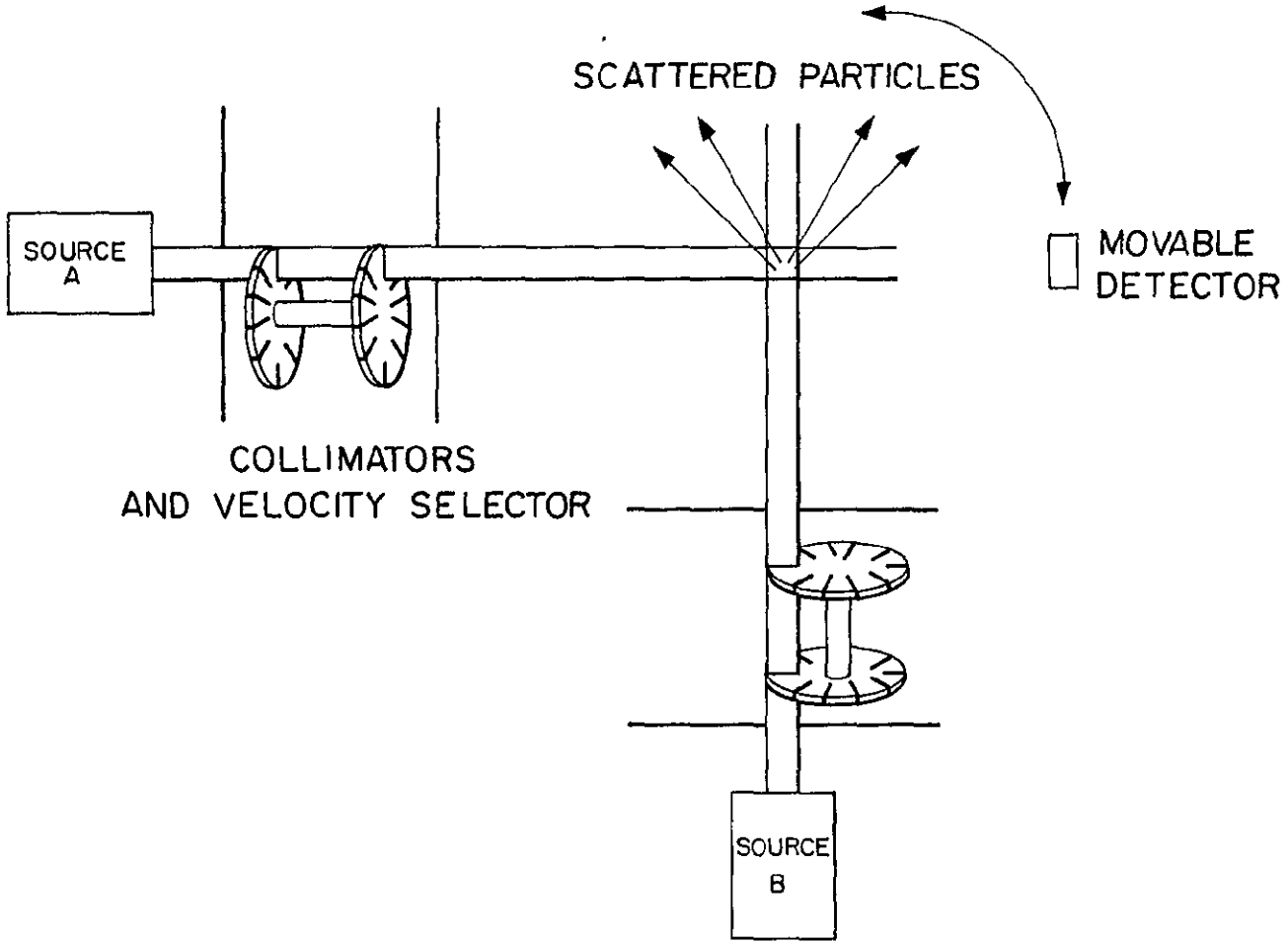
SCATTERED PARTICLES
SOURCE A
MOVABLE DETECTOR
COLLIMATORS AND VELOCITY SELECTOR
SOURCE B

Figure 2

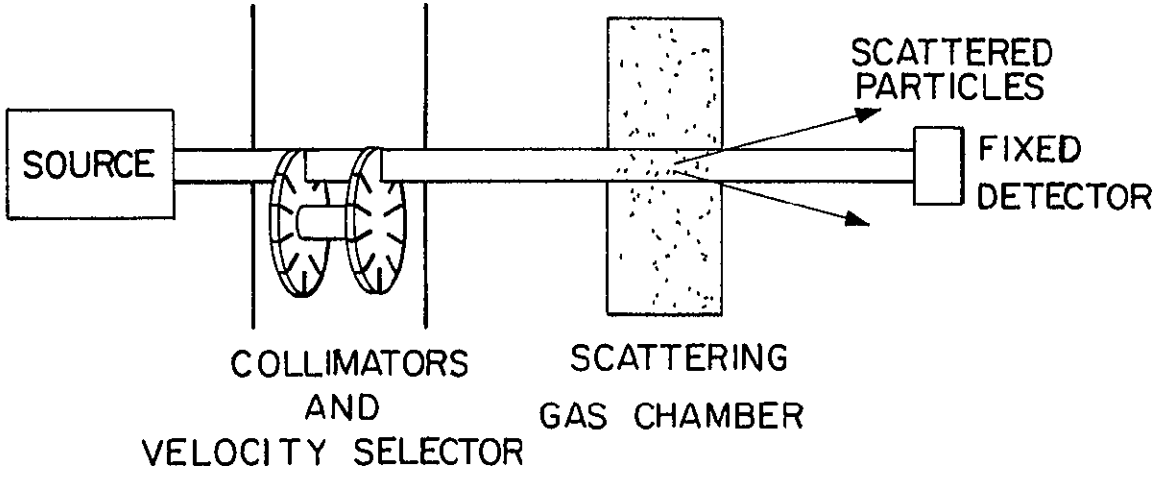
SCATTERED
PARTICLES
SOURCE
FIXED
DETECTOR
COLLIMATORS
AND
VELOCITY SELECTOR
SCATTERING
GAS CHAMBER

Figure 3

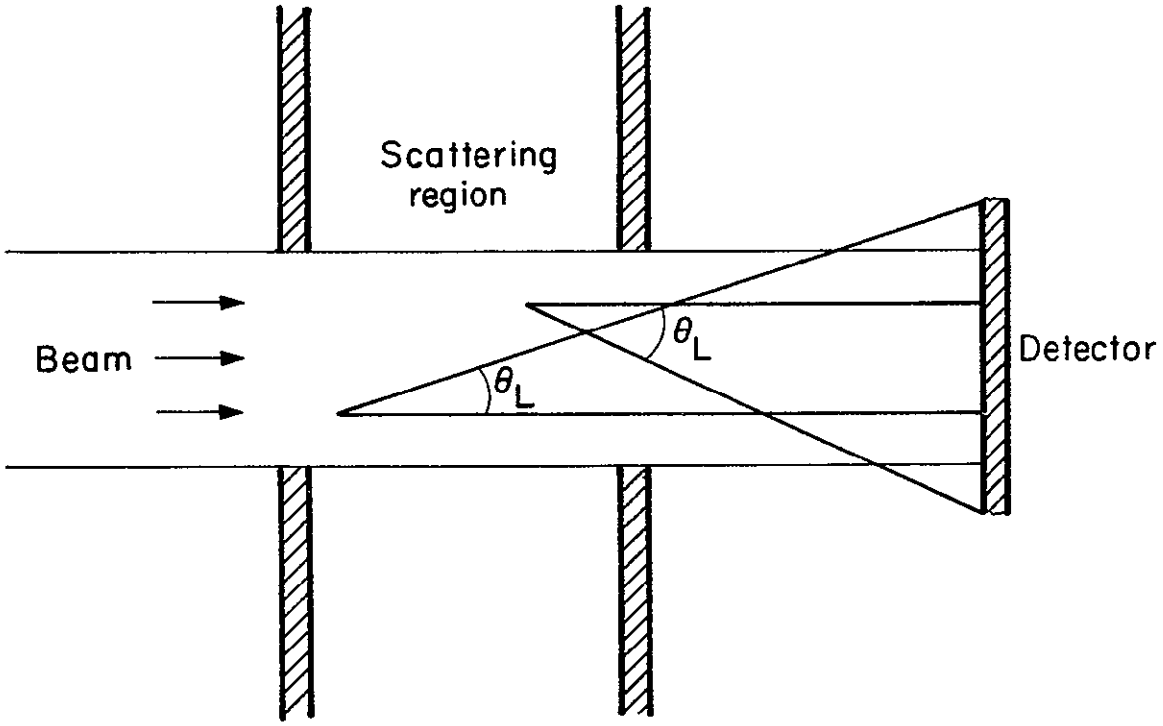

Figure 4

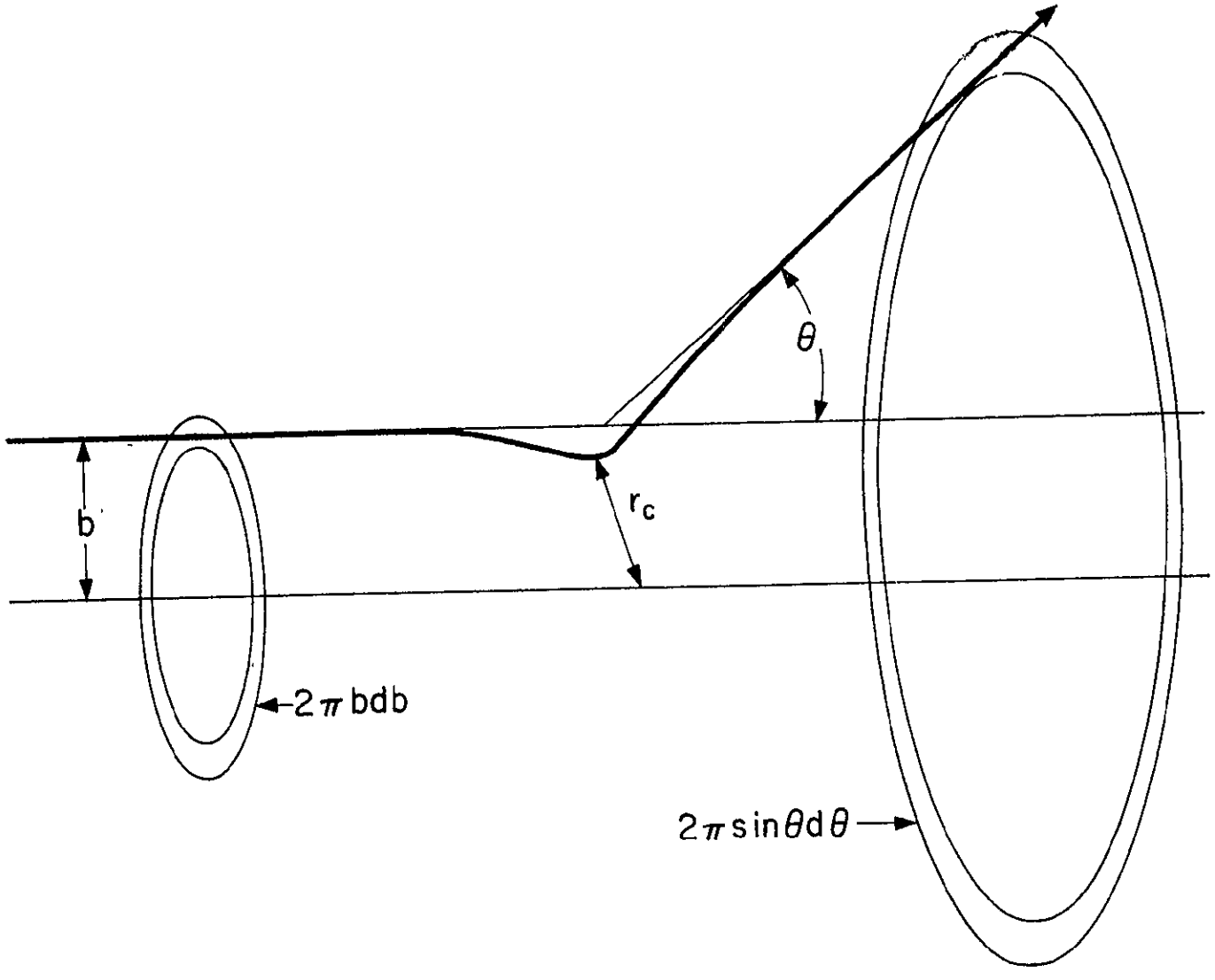

Figure 5

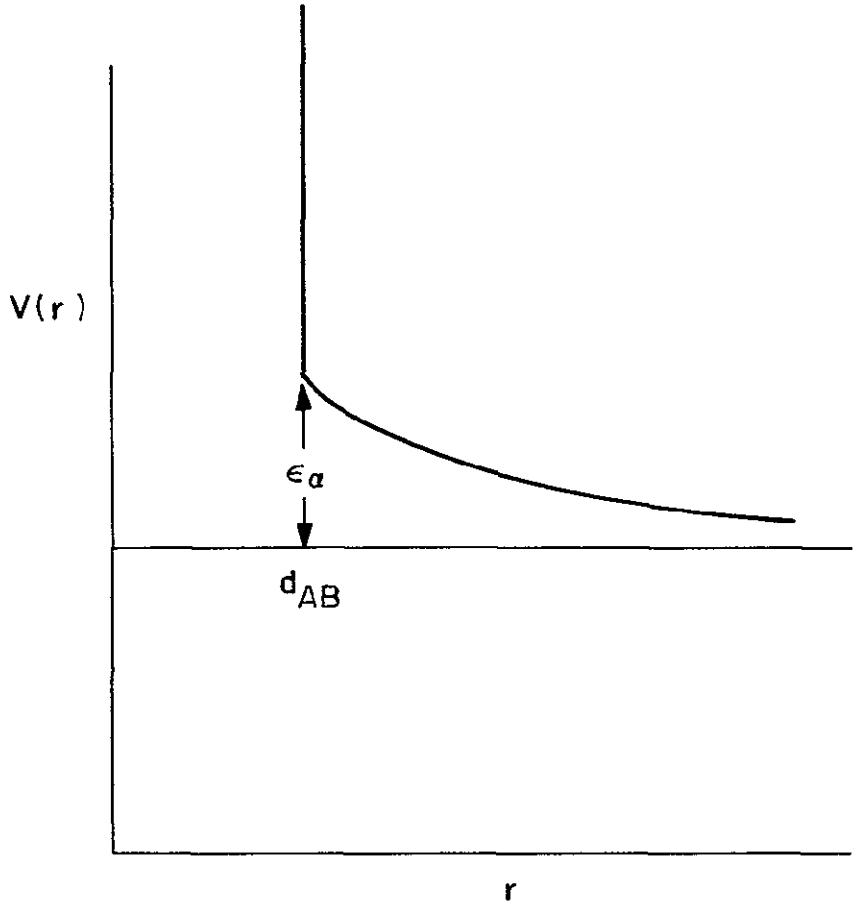
V(r)
ϵ_α
d_{AB}
r

(a)

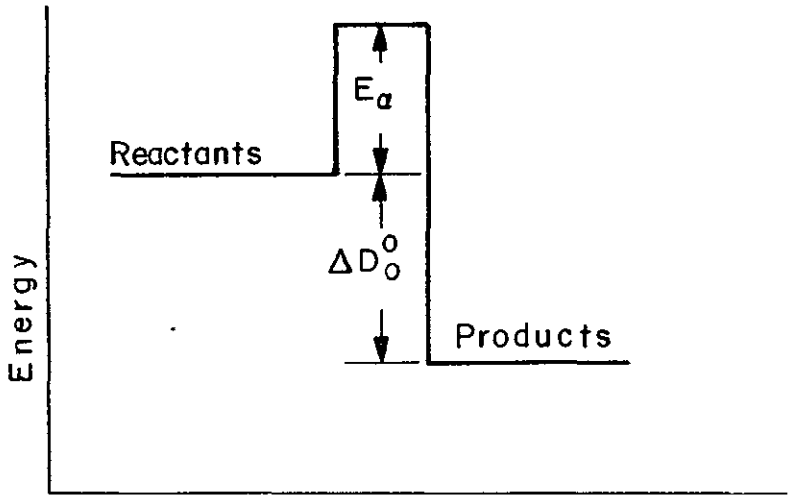
Energy
E_α
Reactants
ΔD_o^o
Products

(b)

Figure 6

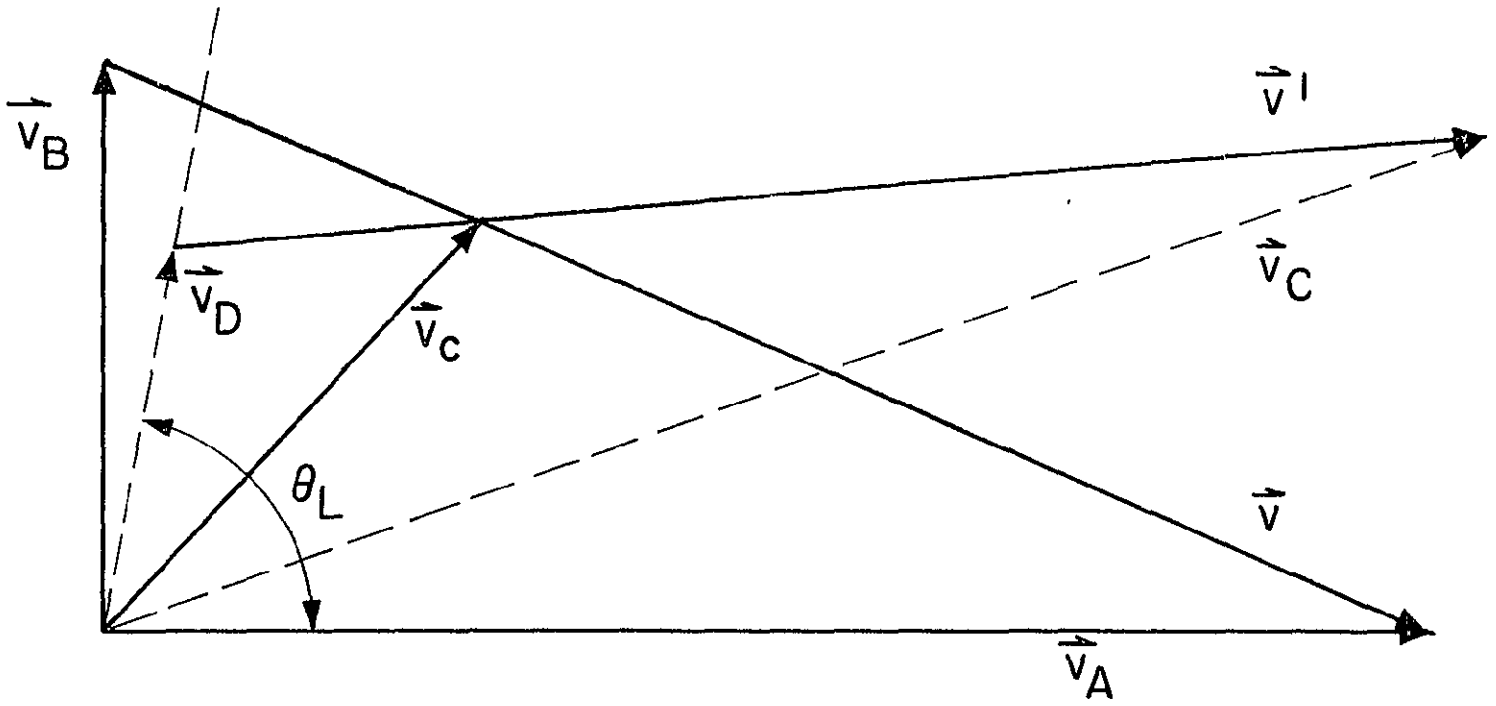

Figure 7

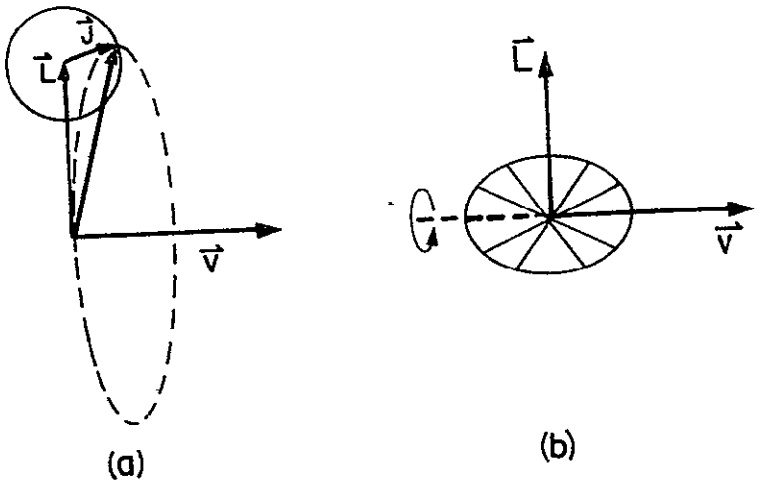

Figure 8

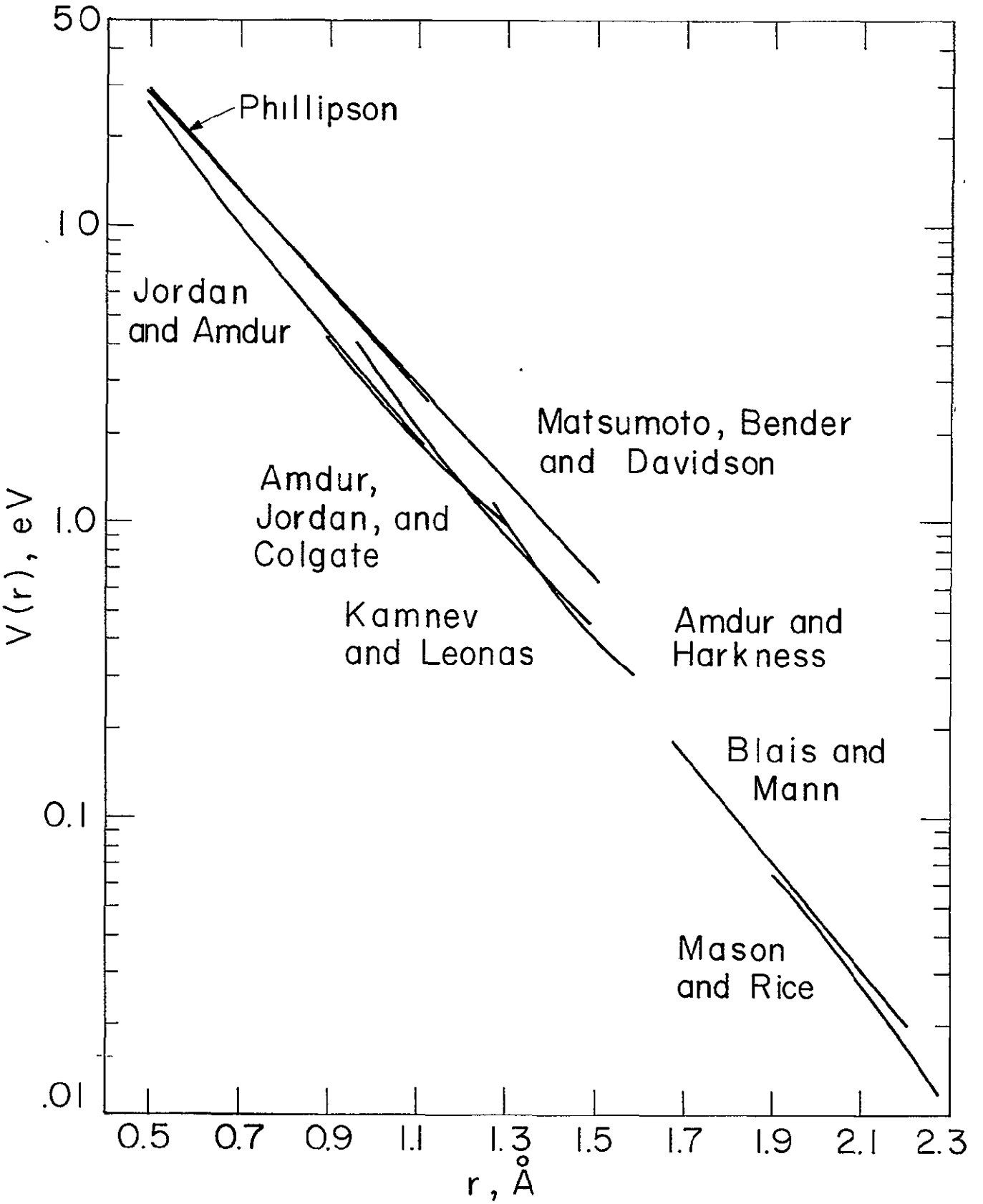
50
10
1.0
0.1
.01
V(r), eV
Phillipson
Jordan
and Amdur
Matsumoto, Bender
and Davidson
Amdur,
Jordan, and
Colgate
Kamnev
and Leonas
Amdur and
Harkness
Blais and
Mann
Mason
and Rice
0.5
0.7
0.9
1.1
1.3
1.5
1.7
1.9
2.1
2.3
r, Å

Figure 9

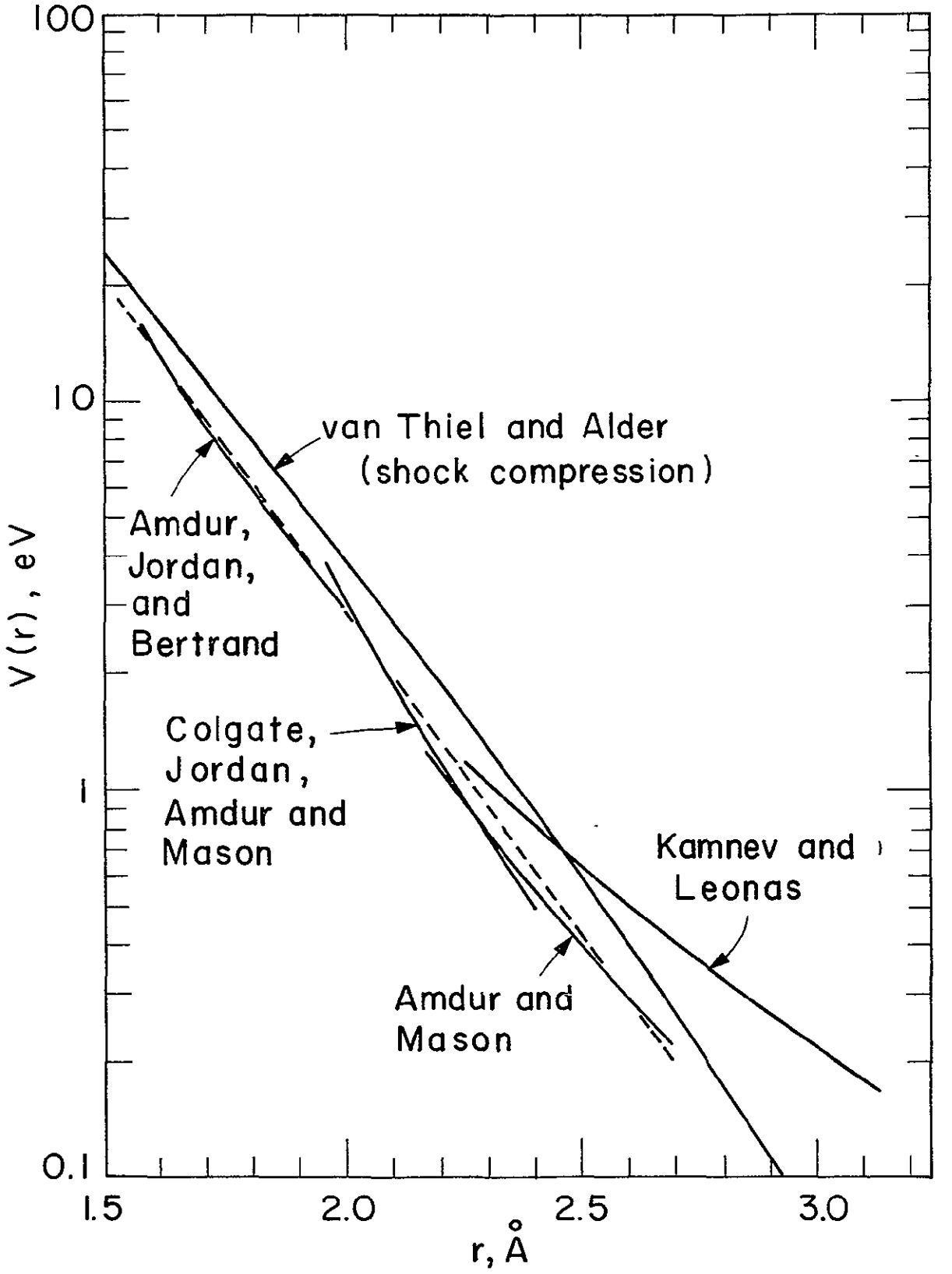
100
10
1
0.1
V(r), eV
1.5
2.0
2.5
3.0
r, Å
van Thiel and Alder
(shock compression)
Amdur,
Jordan,
and
Bertrand
Colgate,
Jordan,
Amdur and
Mason
Kamnev and
Leonas
Amdur and
Mason

Figure 10

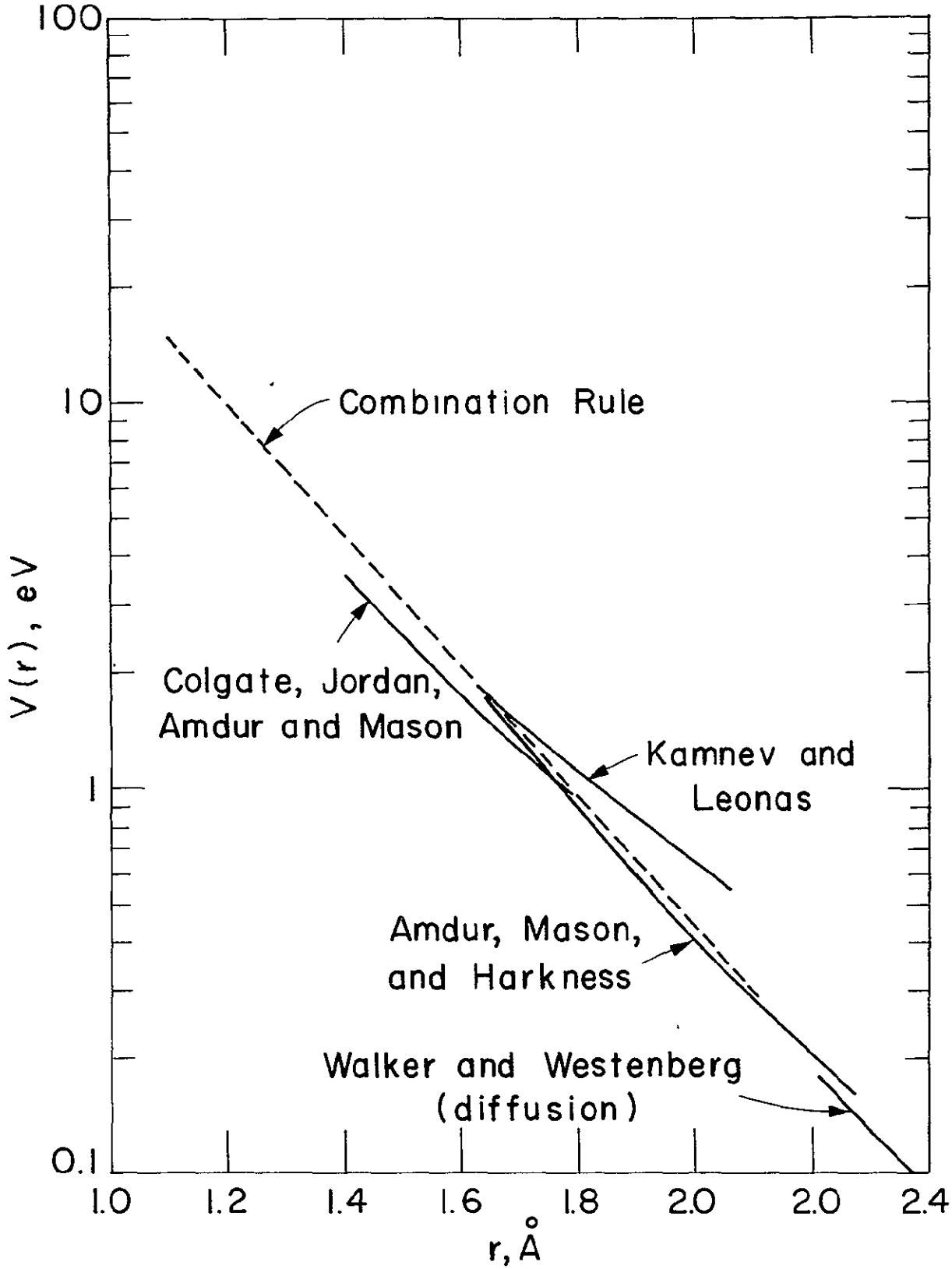
100
10
1
0.1
V(r), eV
Combination Rule
Colgate, Jordan,
Amdur and Mason
Kamnev and
Leonas
Amdur, Mason,
and Harkness
Walker and Westenberg
(diffusion)
1.0
1.2
1.4
1.6
1.8
2.0
2.0
2.4
r, Å

Figure 11

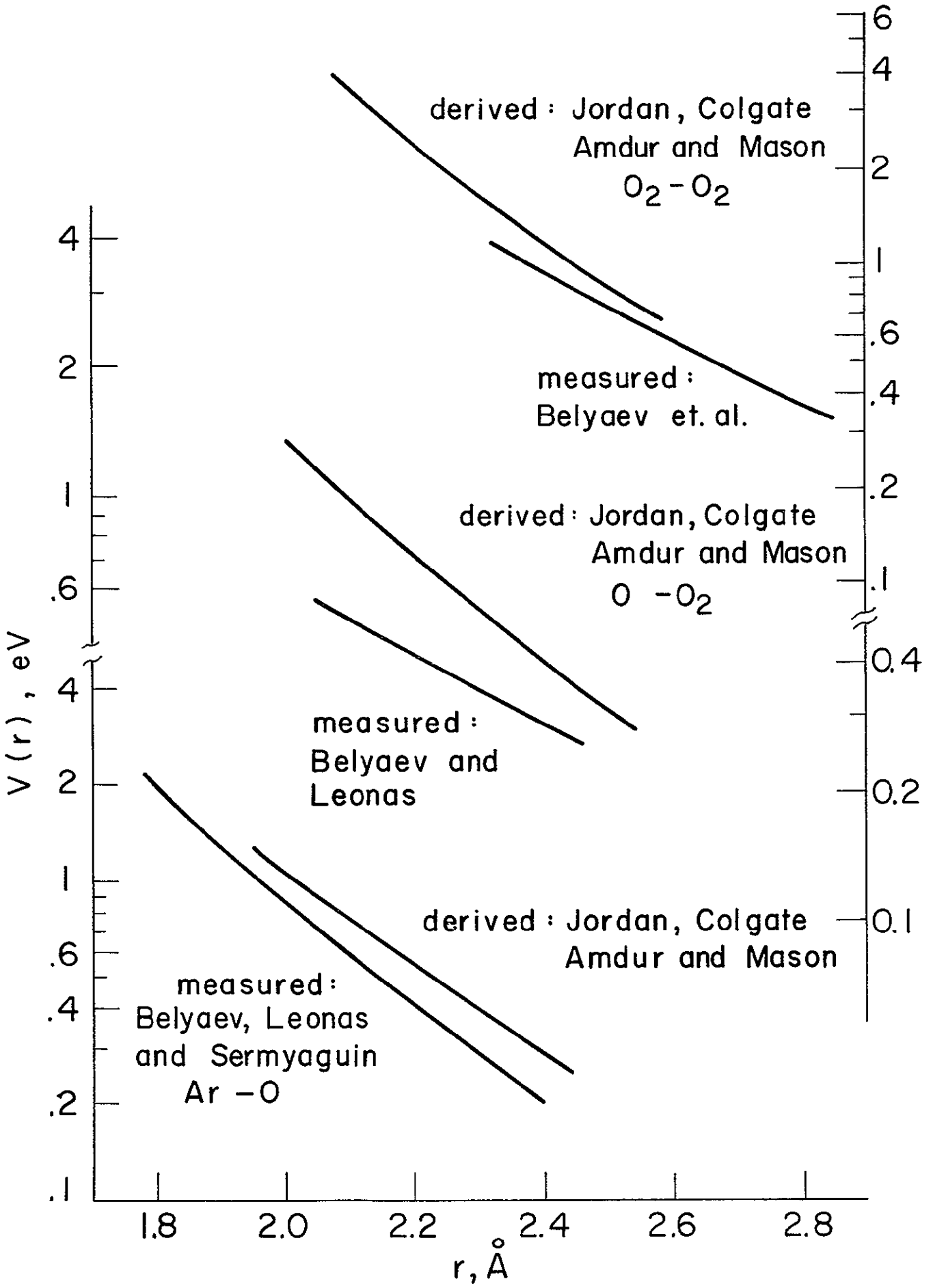
derived : Jordan, Colgate
Amdur and Mason
$O_2 - O_2$
measured :
Belyaev et. al.
derived : Jordan, Colgate
Amdur and Mason
$O - O_2$
measured :
Belyaev and
Leonas
derived : Jordan, Colgate
Amdur and Mason
measured :
Belyaev, Leonas
and Sermyaguin
Ar - O
V(r), eV
r, Å
1.8
2.0
2.2
2.4
2.6
2.8
6
4
2
1
.6
.4
.2
.1
0.4
0.2
0.1

Figure 12

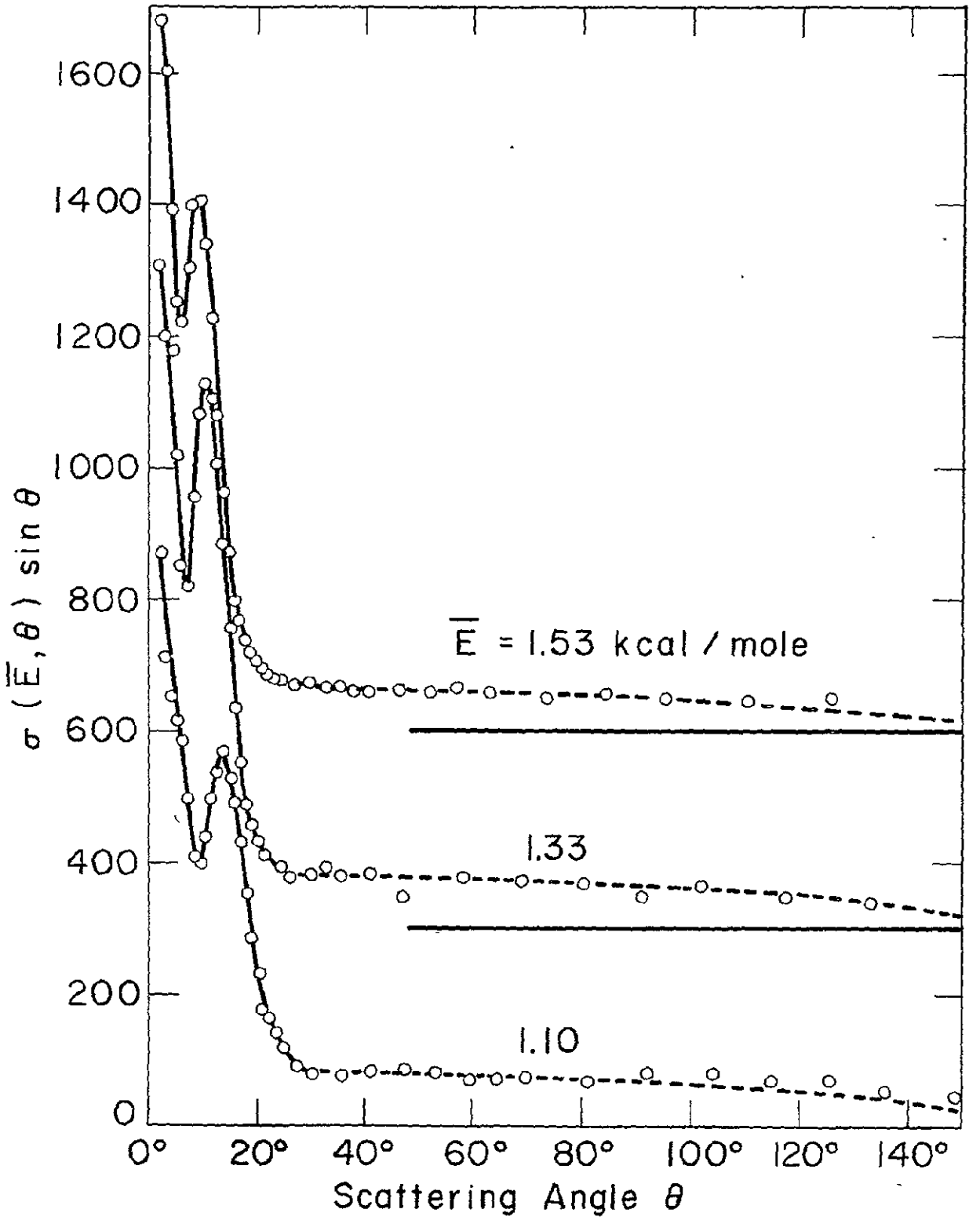
1600
1400
1200
1000
800
600
400
200
0
σ (Ē, θ) sin θ
Ē = 1.53 kcal / mole
1.33
1.10
0°
20°
40°
60°
80°
100°
120°
140°
Scattering Angle θ

Figure 13

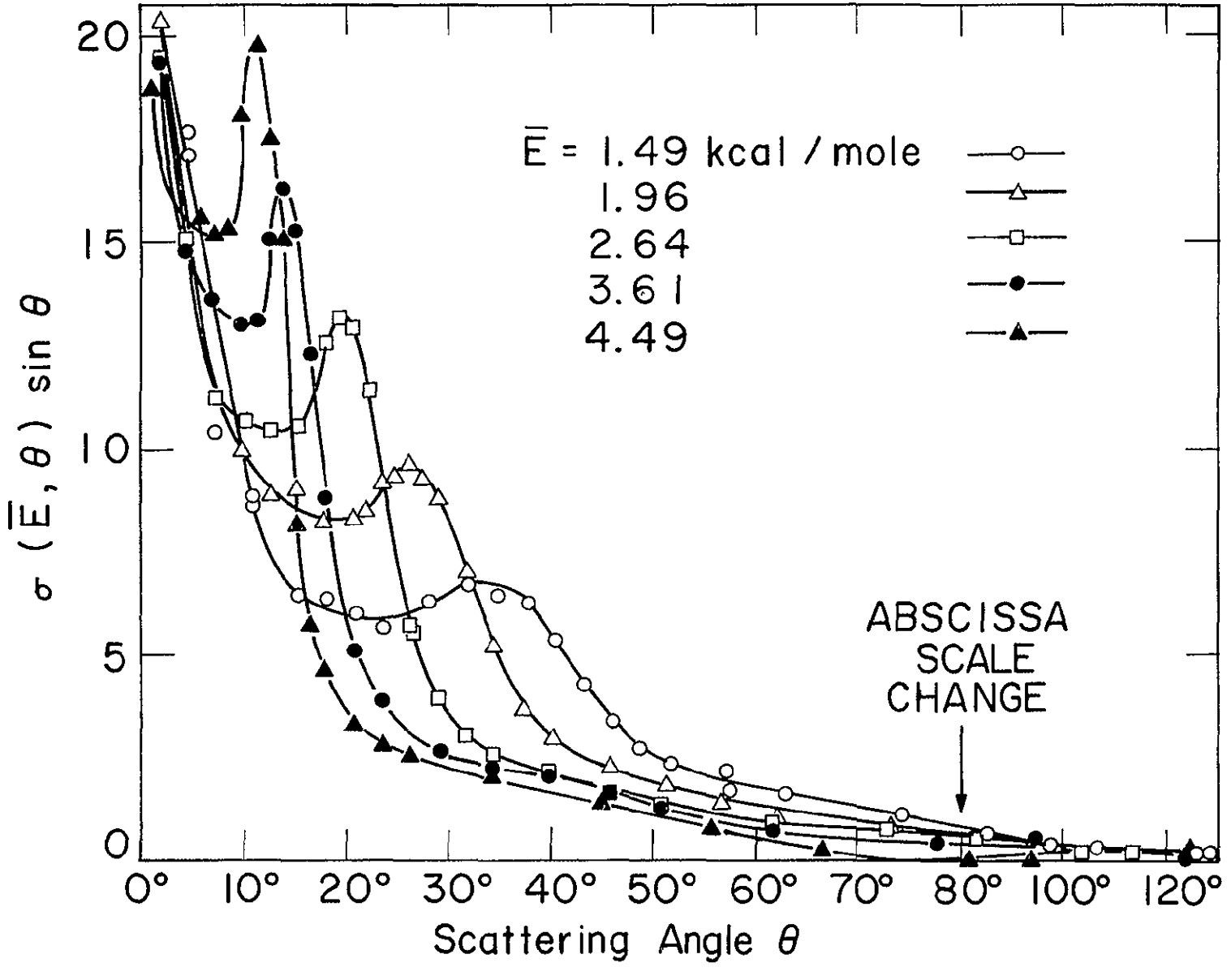
20
15
10
5
0
σ (Ē, θ) sin θ
Ē = 1.49 kcal / mole
1.96
2.64
3.61
4.49
ABSCISSA
SCALE
CHANGE
0°
10°
20°
30°
40°
50°
60°
70°
80°
100°
120°
Scattering Angle θ

Figure 14

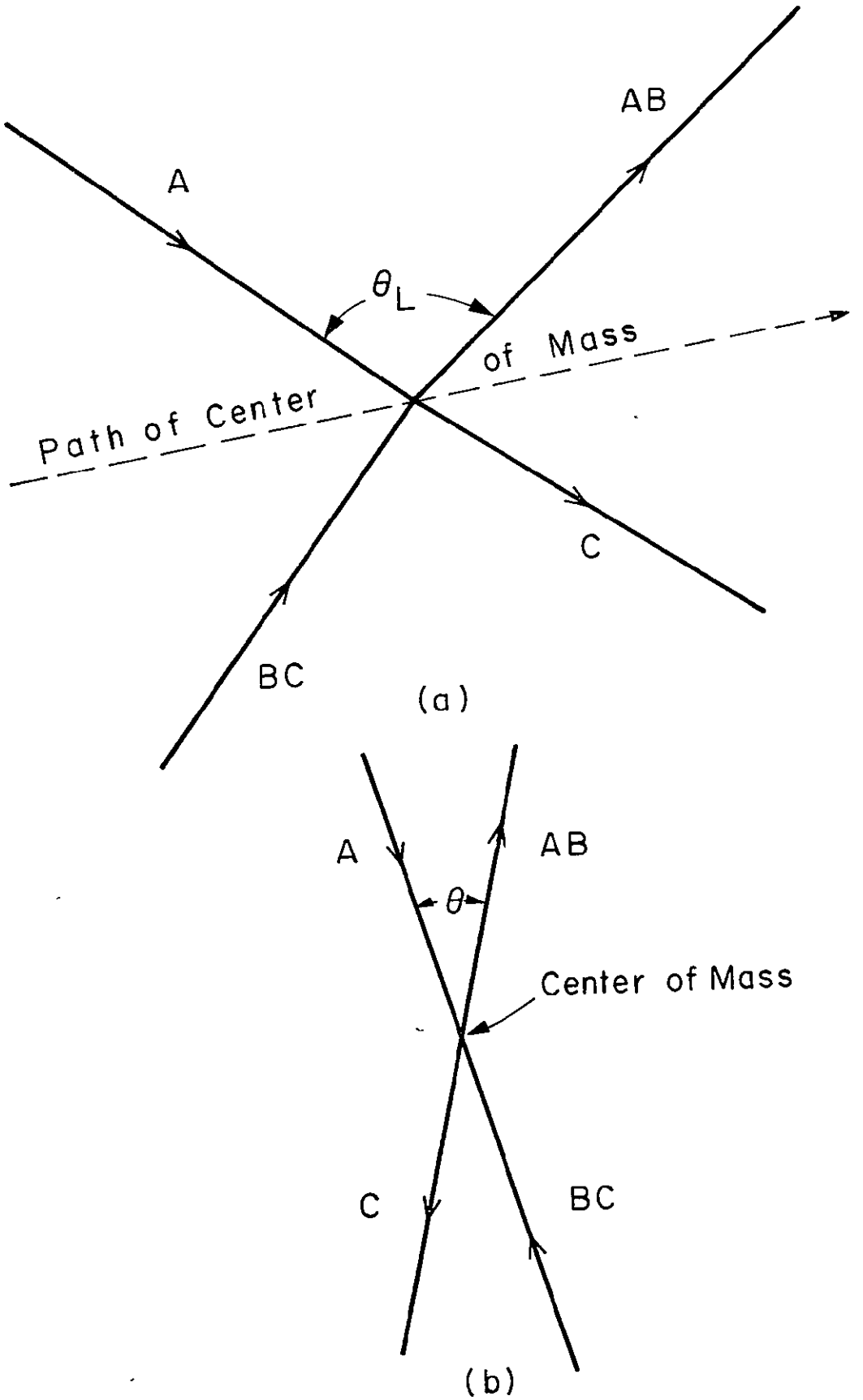
AB
A
θ_L
of Mass
Path of Center
C
BC
(a)
A
AB
θ
Center of Mass
C
BC
(b)

Figure 15

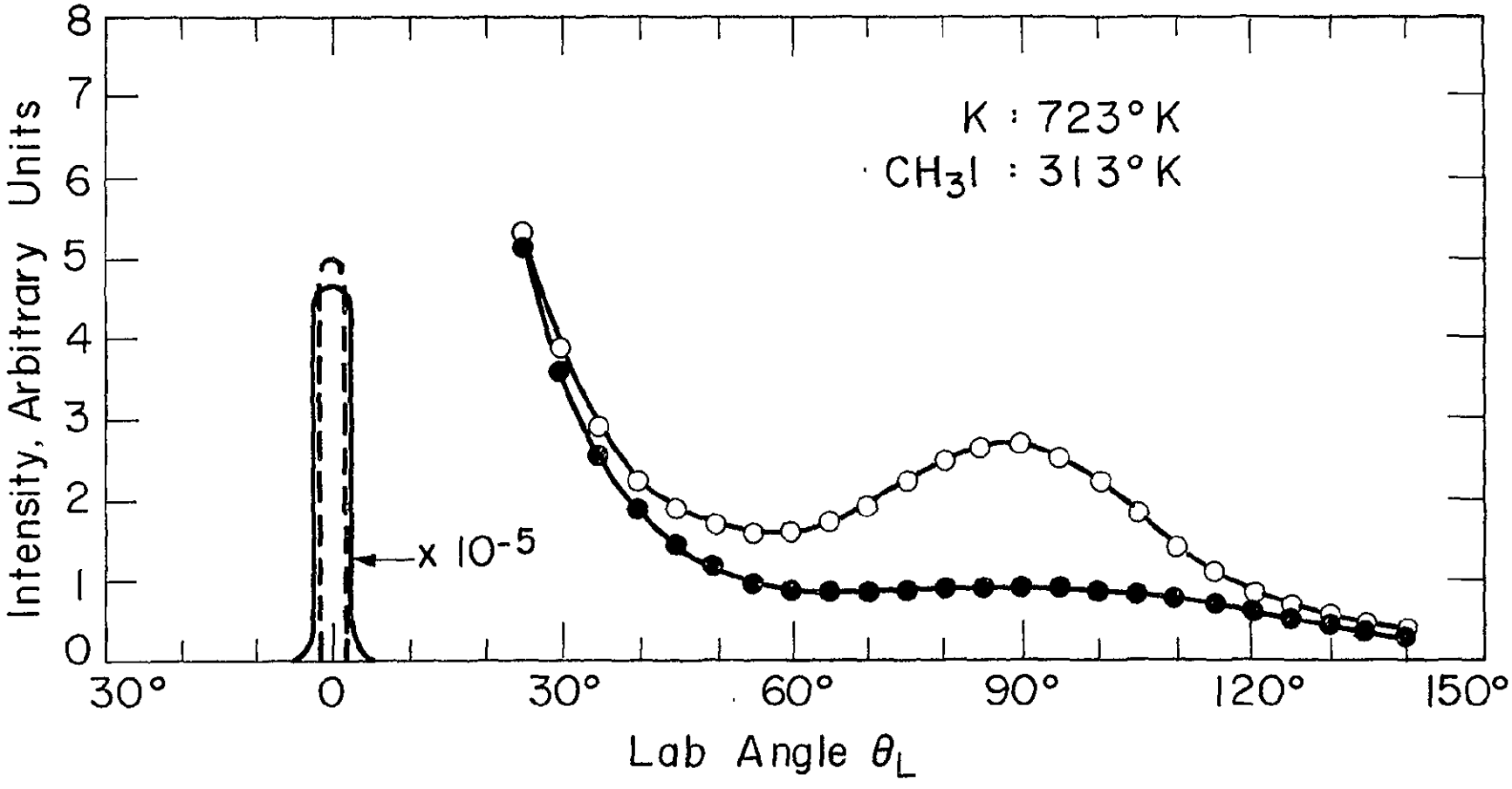
K : 723°K
CH3I : 313°K
x 10-5
Intensity, Arbitrary Units
Lab Angle θL
0
1
2
3
4
5
6
7
8
30°
0
30°
60°
90°
120°
150°

Figure 16

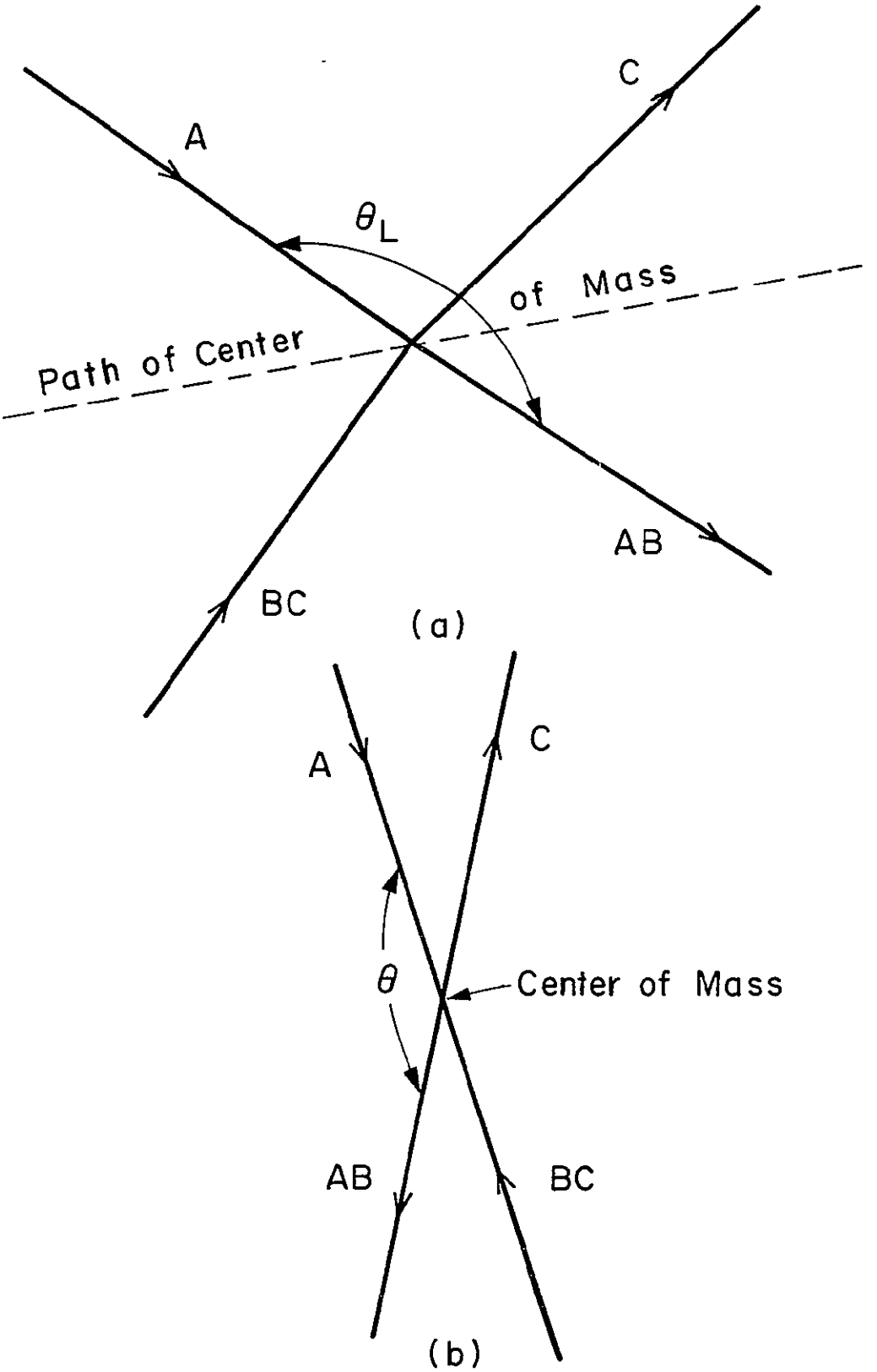
A
C
θ_L
Path of Center
of Mass
AB
BC
(a)
A
C
θ
Center of Mass
AB
BC
(b)

Figure 17

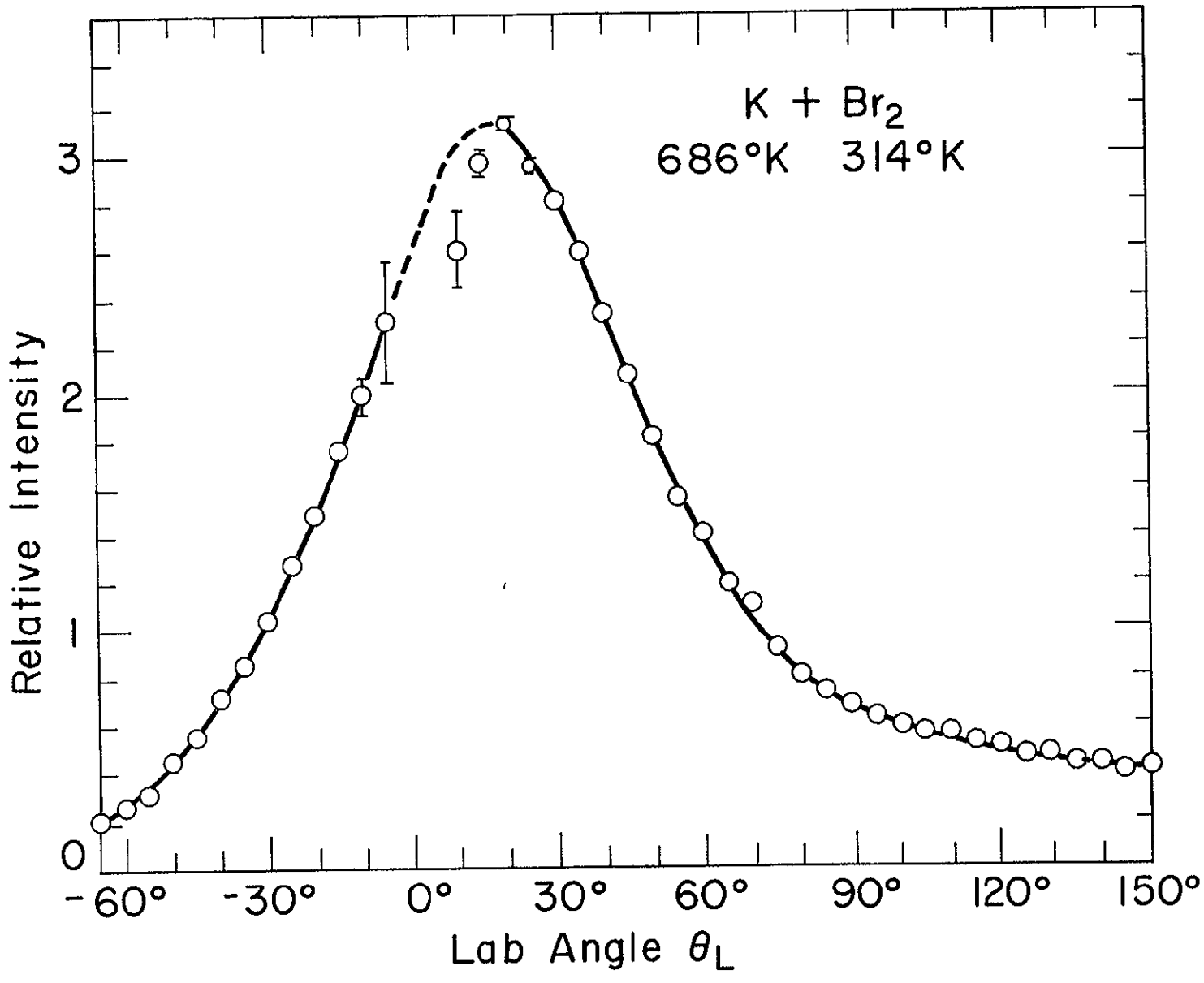
K + Br2
686°K 314°K
Relative Intensity
0
1
2
3
-60°
-30°
0°
30°
60°
90°
120°
150°
Lab Angle θL

Figure 18

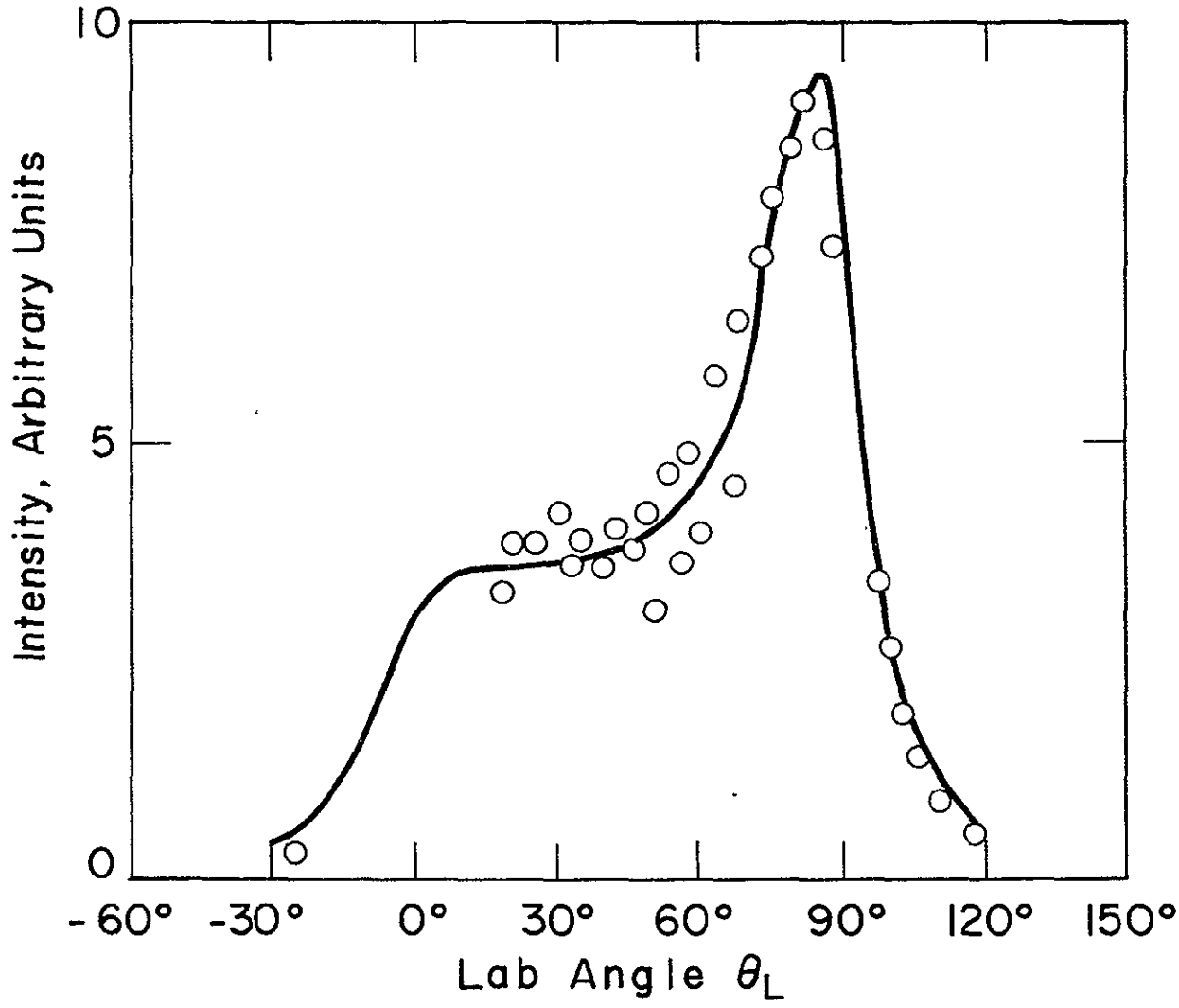
10
5
0
Intensity, Arbitrary Units
-60°
-30°
0°
30°
60°
90°
120°
150°
Lab Angle θ_L

Figure 19